NASA/TM—2018-219937 AIAA–2017–5272

Robust Exploration and Commercial Missions to the Moon Using Nuclear Thermal Rocket Propulsion and In Situ Propellants Derived From Lunar Polar Ice Deposits

Stanley K. Borowski, Stephen W. Ryan, and Laura M. Burke
Glenn Research Center, Cleveland, Ohio

David R. McCurdy and James E. Fittje
Vantage Partners, LLC, Brook Park, Ohio

Claude R. Joyner
Aerojet Rocketdyne, West Palm Beach, Florida

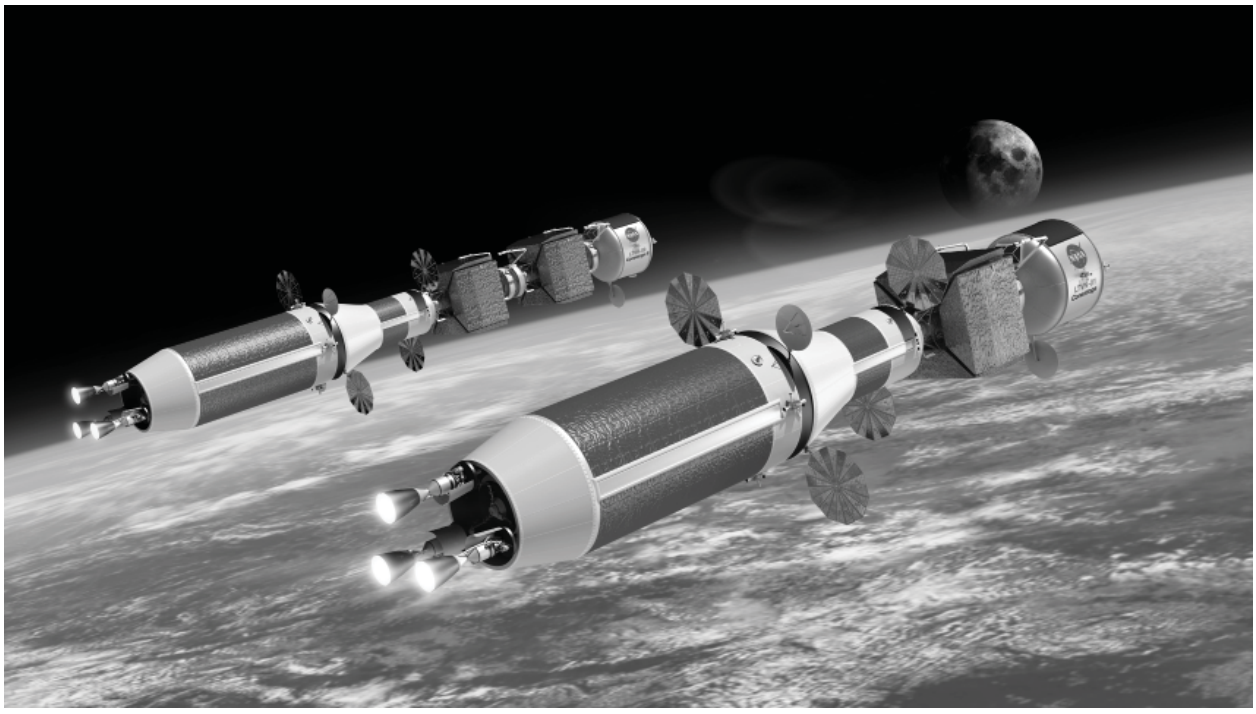

November 2018

NASA STI Program . . . in Profile

Since its founding, NASA has been dedicated to the advancement of aeronautics and space science. The NASA Scientific and Technical Information (STI) Program plays a key part in helping NASA maintain this important role.

The NASA STI Program operates under the auspices of the Agency Chief Information Officer. It collects, organizes, provides for archiving, and disseminates NASA's STI. The NASA STI Program provides access to the NASA Technical Report Server—Registered (NTRS Reg) and NASA Technical Report Server—Public (NTRS) thus providing one of the largest collections of aeronautical and space science STI in the world. Results are published in both non-NASA channels and by NASA in the NASA STI Report Series, which includes the following report types:

- TECHNICAL PUBLICATION. Reports of completed research or a major significant phase of research that present the results of NASA programs and include extensive data or theoretical analysis. Includes compilations of significant scientific and technical data and information deemed to be of continuing reference value. NASA counter-part of peer-reviewed formal professional papers, but has less stringent limitations on manuscript length and extent of graphic presentations.

- TECHNICAL MEMORANDUM. Scientific and technical findings that are preliminary or of specialized interest, e.g., "quick-release" reports, working papers, and bibliographies that contain minimal annotation. Does not contain extensive analysis.

- CONTRACTOR REPORT. Scientific and technical findings by NASA-sponsored contractors and grantees.

- CONFERENCE PUBLICATION. Collected papers from scientific and technical conferences, symposia, seminars, or other meetings sponsored or co-sponsored by NASA.

- SPECIAL PUBLICATION. Scientific, technical, or historical information from NASA programs, projects, and missions, often concerned with subjects having substantial public interest.

- TECHNICAL TRANSLATION. English-language translations of foreign scientific and technical material pertinent to NASA's mission.

For more information about the NASA STI program, see the following:

- Access the NASA STI program home page at http://www.sti.nasa.gov

- E-mail your question to help@sti.nasa.gov

- Fax your question to the NASA STI Information Desk at 757-864-6500

- Telephone the NASA STI Information Desk at 757-864-9658

- Write to:
  NASA STI Program
  Mail Stop 148
  NASA Langley Research Center
  Hampton, VA 23681-2199

NASA/TM—2018-219937 AIAA–2017–5272

Robust Exploration and Commercial Missions to the Moon Using Nuclear Thermal Rocket Propulsion and In Situ Propellants Derived From Lunar Polar Ice Deposits

Stanley K. Borowski, Stephen W. Ryan, and Laura M. Burke
Glenn Research Center, Cleveland, Ohio

David R. McCurdy and James E. Fittje
Vantage Partners, LLC, Brook Park, Ohio

Claude R. Joyner
Aerojet Rocketdyne, West Palm Beach, Florida

Prepared for the
Space 2017 Forum and Exposition
sponsored by the American Institute for Aeronautics and Astronautics
Orlando, Florida, September 12–14, 2017

National Aeronautics and
Space Administration

Glenn Research Center
Cleveland, Ohio 44135

November 2018

Acknowledgments

The author (SKB) acknowledges the NTP Project, the Nuclear Power and Propulsion Technical Discipline Team (NTDT), and Mark Klem (GRC Branch Chief) for their support of this work. Informative exchanges with Carlton Allen, Leslie Gertsch, and Jerry Sanders are also acknowledged. The author also expresses his thanks to two outstanding space artists—Bob Sauls (bob.sauls@xp4d.com) and Pat Rawlings (pat@patrawlings.com) with whom he has had the pleasure of working with over the course of his 29-year career at NASA. Their work has helped bring the vehicle designs and missions developed and proposed by the author to life. The NASA-funded images produced by Pat include Figures 1(a) and (b), 15(a) and (b), 23(a) and (b), 24(c), 28(a), and 33, and those by Bob include Figures 1(c) to (e), 5, 10 to 14, 18 to 22, 24(a), (b) and (d), 25, 26, and 28(b).

Level of Review: This material has been technically reviewed by technical management.

Available from

NASA STI Program
Mail Stop 148
NASA Langley Research Center
Hampton, VA 23681-2199

National Technical Information Service
5285 Port Royal Road
Springfield, VA 22161
703-605-6000

This report is available in electronic form at http://www.sti.nasa.gov/ and http://ntrs.nasa.gov/

Robust Exploration and Commercial Missions to the Moon Using Nuclear Thermal Rocket Propulsion and In Situ Propellants Derived From Lunar Polar Ice Deposits

Stanley K. Borowski, Stephen W. Ryan, and Laura M. Burke
National Aeronautics and Space Administration
Glenn Research Center
Cleveland, Ohio 44135

David R. McCurdy and James E. Fittje
Vantage Partners, LLC
Brook Park, Ohio 44142

Claude R. Joyner
Aerojet Rocketdyne
West Palm Beach, Florida 33410

Summary

The nuclear thermal rocket (NTR) has frequently been identified as a key space asset required for the human exploration of Mars. This proven technology can also provide the affordable "access through cislunar space" necessary for commercial development and sustained human presence on the Moon. It is a demonstrated technology capable of generating both high thrust and high specific impulse (I_{sp} ~900 s)—twice that of today's best chemical rockets. Nuclear lunar transfer vehicles—consisting of a propulsion stage using three ~16.5-klb$_f$ small nuclear rocket engines (SNREs), an in-line propellant tank, plus the payload—can enable a variety of reusable lunar missions. These include cargo delivery and crewed lunar landing missions. Even weeklong "tourism" missions carrying passengers into lunar orbit for a day of sightseeing and picture taking are possible. The NTR can play an important role in the next phase of lunar exploration and development by providing a robust in-space lunar transportation system (LTS) that can allow initial outposts to evolve into settlements supported by a variety of commercial activities such as in situ propellant production used to supply strategically located propellant depots and transportation nodes. The processing of lunar polar ice (LPI) deposits (estimated to be ~2 billion metric tons) for propellant production—specifically liquid oxygen (LO_2) and hydrogen (LH_2)—can significantly reduce the launch mass requirements from Earth and can enable reusable, surface-based lunar landing vehicles (LLVs) using LO_2/LH_2 chemical rocket engines. Afterwards, LO_2/LH_2 propellant depots can be established in lunar polar and equatorial orbits to supply the LTS. At this point a modified version of the conventional NTR called the LO_2-augmented NTR, or LANTR, would be introduced into the LTS, allowing bipropellant operation and leveraging the mission benefits of refueling with lunar-derived propellants (LDPs) for Earth return. The bipropellant LANTR engine utilizes the large divergent section of its nozzle as an "afterburner" into which oxygen is injected and supersonically combusted with nuclear preheated hydrogen emerging from the engine's choked sonic throat—essentially "scramjet propulsion in reverse." By varying the oxygen-to-hydrogen mixture ratio, LANTR engines can operate over a range of thrust and I_{sp} values while the reactor core power level remains relatively constant. A LANTR-based LTS offers unique mission capabilities including short transit time crewed cargo transports. Even a "commuter" shuttle service may be possible, allowing "one-way" trip times to and from the Moon on the order of 36 hr or less. If only 1% of the postulated trapped water ice were available for use in lunar orbit, such a supply could support routine commuter flights to the Moon for many thousands of years. This report outlines an evolving LTS architecture that uses propellants derived from LPI and examines a variety of mission types and transfer vehicle designs along with their operating characteristics and increasing

demands on LDP production as mission complexity and velocity change ΔV requirements increase. A comparison of the LDP production and mining requirements using LPI and volcanic glass to produce lunar-derived liquid oxygen (LUNOX) via the hydrogen reduction process is included, and the synergy with an evolving helium-3 mining industry is also discussed.

1.0 Introduction and Background

Over the past decade there has been considerable discussion within NASA, the Congress, and industry regarding the future direction and focus of the United States' human space program. According to NASA, the direction and focus is a "Journey to Mars" (Ref. 1) sometime around the mid-to-late 2030s. However, there is another destination of interest to the worldwide space community: the Moon. Located just 3 days from Earth, the Moon is an entire world awaiting exploration, future settlement, and potential commercialization. It has abundant resources and is an ideal location to test and demonstrate key technologies and systems (e.g., surface habitation, long-range pressurized rovers, surface power, and resource extraction systems) that will allow people to explore, work, and live self-sufficiently on another planetary surface.

Despite NASA's past "been there, done that" attitude towards the Moon, a human lunar return mission has strong appeal to many others who would like to see humans again walk on its surface. With the upcoming 50th anniversaries of the Apollo 8 orbital mission of the Moon (on Dec. 24 and 25, 1968) and the Apollo 11 landing mission (on July 20 and 21, 1969) fast approaching, lunar missions have been the topic of considerable discussion both in and outside the United States. Plans for human surface missions and even settlements on the Moon in the 2025 to 2030 timeframe are being openly discussed by Europe, China, and Russia (Refs. 2 to 4). A number of private companies in the United States—Bigelow Aerospace (BA) (Ref. 5), SpaceX (Ref. 6), Shackleton Energy Company (SEC) (Ref. 7), United Launch Alliance (ULA) (Ref. 8), and Blue Origin (Ref. 9)—are also discussing commercial ventures to the Moon, along with possible public-private partnerships with NASA.

In early March 2017, BA announced its plans (Ref. 5) to launch a private space station into low Earth orbit (LEO) by 2020 using ULA's Atlas V launch vehicle. The station would use the BA–330 habitat module, which possesses ~330 m^3 of internal volume once inflated. The company went on to say that a variant of the BA–330 module could also be placed in low lunar orbit (LLO) to serve as a transportation node and/or refueling depot for astronauts and spacecraft making their way to and from the Moon and the lunar surface (LS). This renewed interest in the Moon by U.S. industry and international rivals has prompted the Trump Administration to implement Space Policy Directive-1 (Ref. 10) directing NASA to "return American astronauts to the Moon for the first time since 1972 for long term exploration and use."

Lunar-derived propellant (LDP) production—specifically lunar liquid oxygen and hydrogen (LLO_2 and LLH_2)—has been identified as a key technology offering significant mission leverage (Ref. 11), and it figures prominently in both SEC's and ULA's plans (Refs. 7 and 8, respectively) for commercial lunar development. Samples returned from different sites on the Moon during the Apollo missions have shown that the lunar regolith has significant oxygen content. The iron-oxide- (FeO-) rich volcanic glass beads returned on the final Apollo (17) mission have turned out to be a particularly attractive source material for oxygen extraction based on hydrogen reduction experiments conducted by Allen et al. (Ref. 12). Post-Apollo lunar probe missions have also provided orbital data indicating the possible existence of large quantities of water ice trapped in deep permanently shadowed craters (PSCs) located at the Moon's poles (Ref. 13). These data have generated considerable excitement and speculation, including plans for a commercial venture by SEC (Ref. 7) that proposes to mine lunar polar ice (LPI), convert it to rocket propellant, and then sell it at propellant depots located in LEO.

Besides providing an ideal location for testing surface systems and in situ resource utilization equipment, lunar missions also provide a unique proving ground to demonstrate an important in-space technology: nuclear thermal propulsion (NTP). With its high thrust and high specific impulse (I_{sp} ~900 s)—twice that of today's best chemical rockets—the NTR can play an important role in returning humans to the Moon to stay by enabling a reusable in-space lunar transportation system (LTS)

that provides the affordable access through cislunar space necessary for initial lunar outposts to evolve into thriving settlements engaged in a variety of commercial activities.

Over the past three decades, engineers at Glenn Research Center have analyzed NTP's use for lunar missions, quantified its benefits, and developed vehicle concept designs for a variety of exploration and commercial mission applications (Refs. 14 to 17). A sampling of these vehicle concepts and mission applications is shown in Figure 1. Also shown is a transition away from vehicles using a single high-thrust engine (Fig. 1(a)) to vehicles using clustered lower thrust engines (Figs. 1(b) to (e)) to help reduce development costs and increase mission safety and reliability by providing an "engine out" capability.

The nuclear thermal rocket (NTR) achieves its high I_{sp} by using LH_2 to maintain the reactor fuel elements at their required operating temperature and then exhausting the heated hydrogen gas exiting the reactor out the engine's nozzle to generate thrust. Because the NTR is a monopropellant engine,

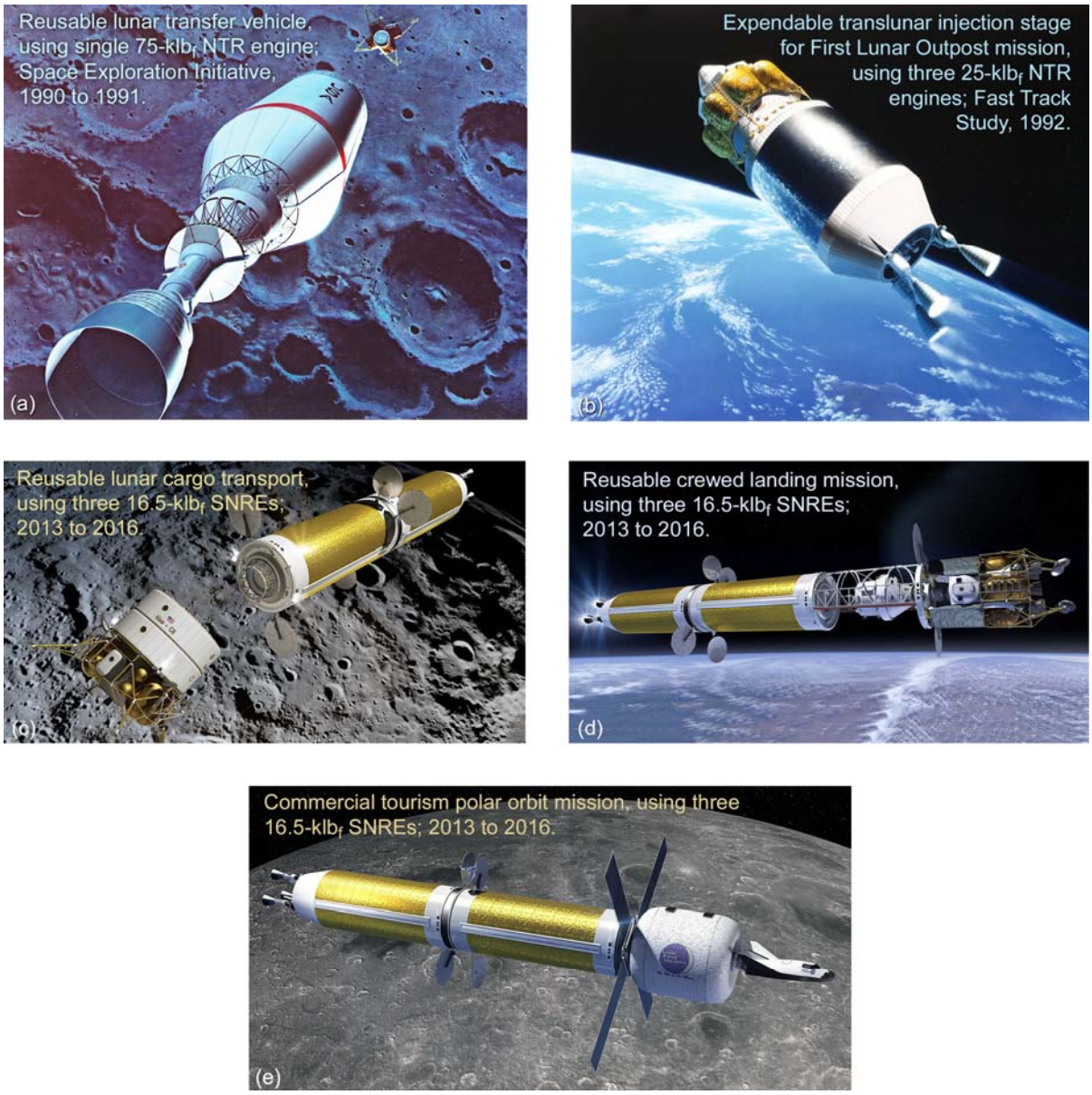

Figure 1.—Past and recent examples of crewed, cargo, and commercial lunar transfer vehicles designed by NASA Glenn Research Center showing transition away from single large to multiple smaller engines.

a key question emerges: “How can the high performance of the NTR and the leverage potential of LDP best be exploited?” The answer is “the LO_2-augmented NTR (or LANTR),” a LH_2-cooled NTR outfitted with an O_2 “afterburner nozzle” and feed system (Refs. 18 to 20). Combining NTR and supersonic combustion ramjet engine technologies, LANTR is a versatile, high-performance engine that can enable a robust nuclear LTS with unique capabilities and can take full advantage of the mission leverage provided with using LDPs by allowing bipropellant operation.

In light of the current interest being expressed in LDPs (Refs. 8 and 9), Glenn engineers have been re-examining the impact of infusing LANTR propulsion into a nuclear-powered LTS that utilizes LDPs. The author (Borowski) presented a paper on this topic 20 years ago at the 33rd Joint Propulsion Conference in Seattle, Washington (Ref. 18). In that work, the primary LDP and feedstock material considered was LLO_2, also referred to as “lunar-derived liquid oxygen (LUNOX),” and FeO-rich volcanic glass beads, respectively; however, only Earth-supplied LH_2 (ELH_2) was used in the LANTR LTS. The decision to use LUNOX back then was based on an extensive set of hydrogen reduction experiments (Refs. 21 and 22) that established ground truth for oxygen release from samples of lunar soil and volcanic glass beads returned by the Apollo missions. The highest yields—in the range of 4 to 5 wt%—were obtained from the iron-rich volcanic glass samples (Refs. 21 and 22) collected during the Apollo 17 mission to Taurus-Littrow (Fig. 2). Another important consideration was the identification of a significant number of large pyroclastic dark mantle deposits (DMDs) containing this glassy material on the lunar nearside just north of the “equatorial corridor” (Refs. 23 and 24).

This same degree of certainty cannot be claimed for LPI. While considerable enthusiasm has been expressed about mining and processing LPI for rocket propellant, and using it to create a space-faring cislunar economy (Ref. 25), the ground truth about LPI must first be established before this enthusiasm is warranted. Robotic surface missions will be required to quantify the physical state of the water ice, its vertical thickness and areal extent, and the levels of soil contamination. Also, the permanently shadowed craters, where LPI is thought to exist, are deep and extremely cold, posing major challenges for mining and processing any cold, ice-bearing regolith that might be uncovered (Ref. 26). These conditions may negate the apparent advantage that LPI has over volcanic glass as a feedstock material: namely, the ability to provide a source of LLH_2 as well as LLO_2.

There are many scientifically interesting sites on the Moon that are far from the lunar poles. For example, the Aristarchus Plateau (~27° N, 52° W) is located in the midst of a vast DMD that can supply the feedstock material needed to produce LUNOX. Access to this nearside, near-equatorial site should also be relatively easy. If a decision were made to locate a research station or base there, producing oxygen locally would probably make more sense rather than incurring the added complexity and cost of transporting it from the poles. Finally, oxygen extraction from iron-rich mare soil or volcanic glass has an additional benefit: it also produces useful metals (iron and titanium), which using LPI feedstock does not.

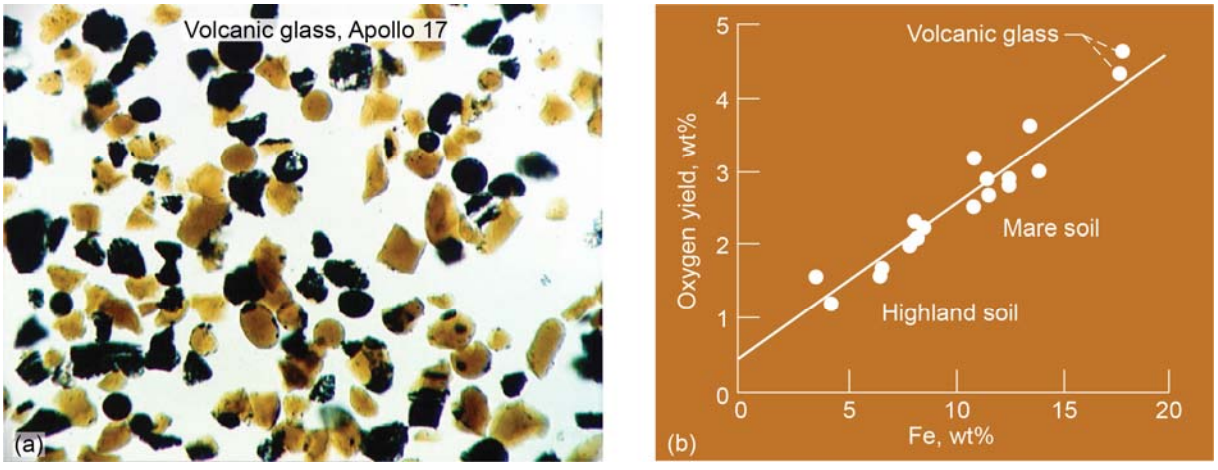

Figure 2.—Volcanic glass beads from Apollo 17 mission and oxygen yields from full range of Apollo samples (Ref. 22).

Despite the uncertainties regarding LPI mentioned above, this report examines the potential mission impact of using LPI-derived LLO_2 and LLH_2 together with LANTR propulsion in an evolving LTS. The report provides a summary of ongoing analysis results to date and includes the following topics. First, the benefits and options for using LDPs are discussed, including the use of LUNOX. Then the scientific data supporting the possible existence of water ice trapped within deep PSCs at the Moon's poles are reviewed, and proposed concepts for its mining are discussed. Next, a system description of the NTR and the LANTR concept is presented along with performance projections for the engine as a function of the oxygen-to-hydrogen mixture ratio (O/H MR) used in the afterburner nozzle. The mission and transportation system ground rules and assumptions used in the analysis are then provided and used in an evolutionary mission architecture that illustrates the benefits of using LANTR and LDP, quantifying them in terms of reduced vehicle size, launch mass, and required engine burn times. The potential for a robust, reusable LTS that includes short-transit-time crewed cargo transports and commuter shuttles is discussed next along with the refueling needs to support these more demanding and higher velocity change ΔV missions. A comparison of the LDP production and mining requirements for LPI and the volcanic glass that is used to produce LUNOX via the hydrogen reduction process (Ref. 27) follows, and the synergy with an evolving helium-3 mining industry is also discussed. The report ends with some concluding remarks and thoughts on the possibilities for future human expansion into the solar system using LANTR propulsion and sources of locally produced extraterrestrial propellant.

Acronyms and symbols used in this report are listed in the appendix to aid the reader.

2.0 Benefits of Using and Options for Producing Lunar-Derived Propellants

Previous studies conducted by NASA and its contractors (Refs. 28 and 29) have indicated a substantial benefit from using LDPs—specifically LLO_2 in the lunar space transportation system. In a LTS using LO_2/LH_2 chemical rockets, ~6 kg of mass in LEO is required to place 1 kg of payload on the LS. Of this 6 kg, ~70% (4.2 kg) is propellant, of which ~85.7% of this mass (3.6 kg) is oxygen, assuming the engines operate with an O/H MR of 6:1. Since the cost of placing a kilogram of mass on the LS is ~6 times the cost of delivering it to LEO (Ref. 11), the ability to produce and utilize LLO_2 from processed lunar volcanic glass or regolith, or LLO_2 and LLH_2 from the electrolysis of LPI, can provide a significant mission benefit. By providing a local source of oxygen and hydrogen for use in life support systems, fuel cells, and the chemical rocket engines used on lunar landing vehicles (LLVs), the initial mass in low Earth orbit (IMLEO), launch costs, and LTS size and complexity can all be reduced. Greater quantities of higher value cargo (e.g., people, propellant processing equipment, and scientific instruments) can also be transported to LEO and on to the Moon instead of bulk propellant mass, further reducing LTS costs.

2.1 Pyroclastic Deposits of Volcanic Glass: The Lunar "Persian Gulf" for Future LUNOX Production?

As mentioned in the Introduction to this report, samples brought back on the Apollo missions have shown that nearly half the mass (~43%) of the Moon's surface material is oxygen (Ref. 11), and at least 20 different techniques (Refs. 30 and 31) have been identified for its extraction. The FeO-rich volcanic glass beads returned on the final Apollo (17) mission have turned out to be a particularly attractive source material for oxygen extraction using the hydrogen reduction process. The two-step process produces iron and water, which is then electrolyzed to obtain oxygen and hydrogen. A portion of the hydrogen is recycled back as the catalyst, and the oxygen is liquefied and stored.

Reduction experiments conducted by Allen et al. (Refs. 22 and 32) have shown the glassy (orange) and crystalline (black) beads to be an attractive feedstock producing oxygen yields of ~4.3 and 4.7 wt%, respectively (Fig. 2(b))—the highest obtained from all of the Apollo samples tested. These glassy and crystalline beads are unconsolidated and fine grained (Fig. 2(a)), and can be fed directly into a LLO_2 production plant with little or no processing prior to reduction.

More importantly, a significant number of large pyroclastic deposits, thought to be the result of continuous, Hawaiian-style, fire-fountain eruptions from large vents, have been identified on the lunar nearside by Gaddis et al., (Ref. 24). These deposits are of regional extent and are composed largely of crystallized black beads, orange glass beads, or a mixture of the two. Noteworthy large deposits located just north of the lunar equator include (1) the Aristarchus Plateau (~49,015 km^2), (2) Southern Sinus Aestuum (~10,360 km^2), (3) Rima Bode (~6620 km^2), (4) Sulpicius Gallus (~4320 km^2), (5) Southern Mare Vaporum (~4130 km^2), and (6) Taurus Littrow (~2940 km^2). At the smallest of these deposits, Taurus Littrow, located at the southeastern edge of Mare Serenitatis, the largely black crystalline beads found there are thought to be tens of meters thick and could produce well in excess of a billion metric tons of LUNOX using the hydrogen reduction process, assuming a 4.5-wt% oxygen yield and a 5-m mining depth.

2.2 LPI: Its Possible Location and Estimated Quantities

Watson, Murray, and Brown first conjectured about the existence of water ice at the lunar poles in 1961 (Ref. 33). Later in 1979, Arnold (Ref. 34) estimated the mass of water deposited in PSCs at the lunar poles over the last 2 billion years at ~10 to 100 billion metric tons and concluded that the Moon's poles might provide an abundant water resource for future exploitation. The sources for this water were attributed to micrometeoroids, solar wind proton reduction of lunar regolith, and comets.

Recently, the Clementine (Ref. 35), Lunar Prospector (Ref. 36), Chandrayaan-1 (Ref. 37), Lunar Reconnaissance Orbiter (LRO) (Ref. 38), and Lunar CRater Observation and Sensing Satellite (LCROSS) (Ref. 39) lunar probe and impact missions have provided data indicating the possible existence of large quantities of water ice (estimated at hundreds of millions to billions of metric tons) trapped within a number of deep perpetually dark craters found near the Moon's poles.

The first spacecraft to observe the lunar poles in detail was Clementine, a joint Department of Defense and NASA probe launched in 1994. Using an onboard transmitter, Clementine beamed radio waves into the dark regions of the Moon's south polar region (Fig. 3(a)), including the Shackleton crater (Fig. 3(b)). Echoes of these waves were subsequently detected back on Earth using the large dish antennas of the Deep Space Network. The polarization characteristics of the echoes from this "bistatic radar experiment" (Ref. 35) were interpreted as evidence of possible water ice.

Four years later in 1998, the Lunar Prospector probe was launched. It carried a neutron spectrometer to measure the amount of hydrogen in the lunar regolith near the polar regions. The Lunar Prospector science team found enhanced hydrogen concentrations at the north and south poles that were interpreted

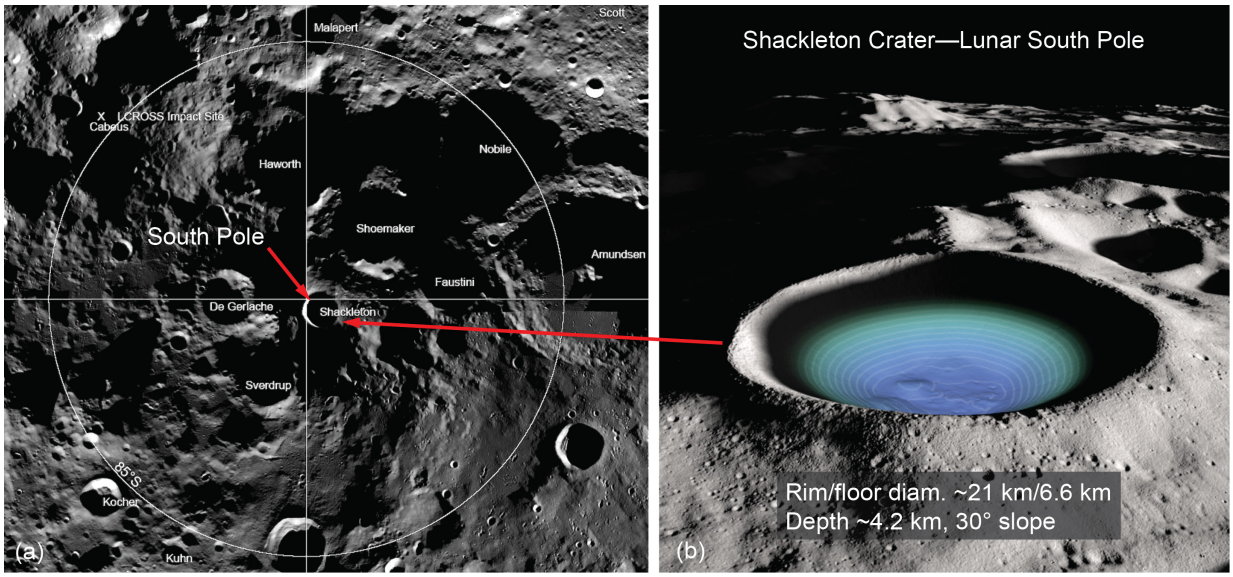

Figure 3.—Lunar south polar region. (a) Overview. (b) Features of Shackleton crater.

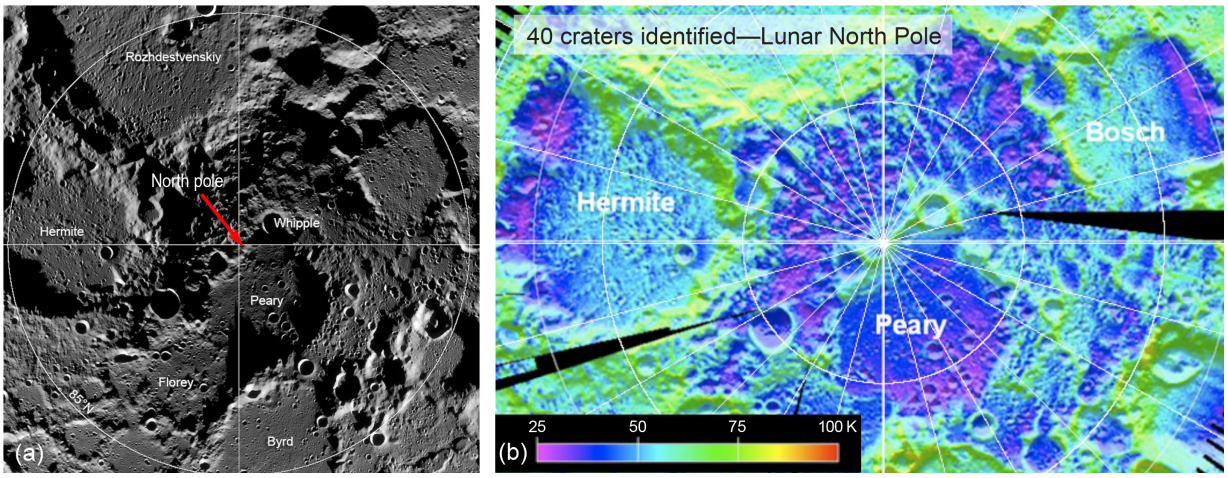

Figure 4.—Lunar north polar region. (a) Overview. (b) Measured temperatures in nearby craters.

as indications of significant amounts of water ice (~1.5±0.8 wt% in the regolith) contained within a number of these polar "cold traps." Based on estimates of the shadowed crater areas, the total quantities of water ice were estimated by Feldman et al. (Ref. 36) to be ~135 to 240 million metric tons in the south polar region and ~62 million metric tons in the north. If all of the enhanced hydrogen inventory measured by *Lunar Prospector's* neutron spectrometer were in the form of water ice crystals, Feldman et al. estimated the total amount of water at both poles to be ~2 billion metric tons.

In October 2008, India's first lunar probe, Chandrayaan-1, was launched, carrying with it NASA's Mini-SAR (synthetic aperture radar). From February to April 2009, Mini-SAR mapped more than 95% of the Moon's polar regions, extending from 80° latitude to the poles (Ref. 40). On March 1, 2010, NASA announced that the Mini-SAR had discovered more than 40 permanently shadowed, super-cold craters located within 10° of the Moon's north pole (Fig. 4(a)). The craters ranged in size from 2 to 15 km in diameter, and the amount of water ice they might contain was estimated to be ~600 million metric tons (Ref. 37).

The search for LPI continued with NASA's LRO/LCROSS mission launched in June 2009. Onboard LRO was the Miniature Radio Frequency (Mini-RF) instrument specifically designed to map the Moon's polar regions, including the permanently shadowed "cold trap" areas, and analyze the scattering properties of the RF signal in an effort to characterize the physical nature of the deposits that exist there (Ref. 38). A key parameter obtained from this scattered RF signal is the circular polarization ratio (CPR). High values of CPR not only indicate the presence of water ice, but they can also be attributed to the surface roughness of a crater. Using LRO's Mini-RF imaging radar system, Spudis et al. (Ref. 38) identified a large number of "anomalous" polar craters that exhibited high CPR values only in their interiors, which are permanently dark and very cold (<100 K). According to Spudis, these anomalously high-CPR deposits exhibit behavior consistent with the presence of water ice. If this interpretation is correct, Spudis estimated that several hundred million metric tons of relatively "clean" water ice may exist in the upper 2 to 3 m of the LS at both poles (Ref. 38).

Additional data on the existence and quantity of polar ice were obtained by LRO's companion satellite, LCROSS. On Oct. 9, 2009, the Centaur upper stage of the Atlas V launch vehicle was directed to impact the south polar crater, Cabeus, shown in the upper left corner of Figure 3(a). Shortly after impact, the LCROSS spacecraft flew through the ejecta plume and attempted to detect the presence of water vapor in the debris cloud. Analysis of spectrometry data indicated the spectral signature of water, and a later definitive analysis by Colaprete et al. (Ref. 39) determined the concentration of water ice in the regolith at the impact site to be ~5.6±2.9 wt%. On the basis of the data provided from the above lunar probe missions, it therefore appears that the concentration of water ice in the polar regolith can vary anywhere from ~0.7 to 8.5 wt%, and total quantities of LPI at both poles can range from ~600 million to ~2 billion metric tons.

2.3 Environmental Conditions and Proposed Concepts for Mining Lunar Polar Ice

LPI deposits are a potential important resource because the recovered water can be electrolyzed to supply both oxygen and hydrogen (at a ratio of 8:1), assuming the deposits can be economically accessed, mined, processed, and stored for their desired use. Higher ΔV budgets are also required to access lunar polar orbit sites and the candidate craters are deep (Fig. 3(b)), extremely cold (Fig. 4(b)), and exist in a state of perpetual darkness, posing major challenges for mining and processing these cold ice-bearing materials.

To put the operating temperature conditions into perspective, the world's 10 coldest mines are located in Russia, and all but one of these are located in Russia's Sakha Republic—a region in the country's extreme north that contains vast diamond, coal, and gold resources (Ref. 41). At the coldest of these mines, Sarylakh, the temperatures can drop to nearly –50 °C (~223 K). By contrast, the temperatures inside the polar craters, where LPI is thought to exist, are ~30 to 50 K: more than 5 times colder than the coldest mines on Earth. In fact, the coldest temperature in the solar system measured by a spacecraft was on the floor of the crater Hermite, located near the Moon's north pole (Ref. 42): a temperature of ~26 K (–247 °C) was recorded by LRO along the southwestern edge of Hermite in 2009, using its Diviner temperature instrument. Extremely cold temperatures similar to those found in Hermite were also found in the nearby craters Peary and Bosch (Fig. 4(b)) as well as at the bottoms of several PSCs located in the Moon's south polar region. All are candidates for LPI deposits and potential mining.

In addition to working in dark, extremely cold surroundings where metals can become brittle, mining equipment must also be designed to operate in a hard vacuum, on electricity rather than petrol, and in gravity that is one-sixth that of Earth. It must also be able to tolerate an increased radiation environment, and the abrasive nature of the lunar dust, which can cause increased rubbing friction, wreaks havoc on machinery and has a tendency to adhere to everything it touches (Ref. 43). On Earth, surface mining is the most common approach to mineral extraction, and a variety of systems developed for terrestrial application have also been examined for mining lunar regolith (Refs. 44 and 45). The mining process itself involves the following operations: fragmentation, excavation, loading, hauling, and resource separation.

Mechanical mining methods frequently combine multiple operations into a single machine. For example, a mechanical excavator can be designed to break up, or fragment, the ice-bearing regolith, then excavate and transport it to the water extraction plant. A notional design for a combined excavator-hauler is shown in Figure 5. It features a bucket wheel excavator and conveyor system that digs and lifts the ice-bearing regolith to an upper dump bed until it is filled (shown in Fig. 5(a)). Articulated legs on the excavator-hauler allow it to walk over to the water extraction plant where the regolith is deposited. While one excavator-hauler empties its load, another returns to the mining site to begin the cycle again (shown in Fig. 5(b)). Multiple units would be used consistent with the desired production rate. Whereas legged

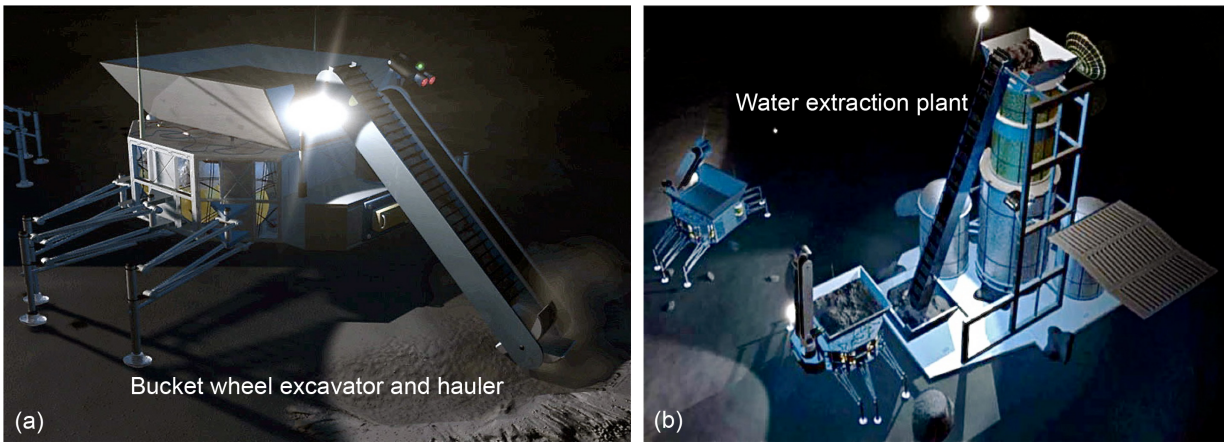

Figure 5.—Notional combination excavator and hauler for water extraction and subsequent propellant production on Moon. (a) Bucket wheel excavator-hauler. (b) Transporting ice-rich regolith to water-processing plant.

Figure 6.—Combination REL and supporting HV for production-class LPI mining operations.

vehicles have certain advantages operating on rocky ground, wheeled vehicles are more versatile and can provide faster movements on relatively smooth terrain. Wheeled vehicles are also more adaptable to teleoperations and automation than legged vehicles, which have more complex movements.

During the early 1990s under NASA sponsorship, the Department of Interior's Bureau of Mines conducted a LS mining equipment study and proposed two pieces of mining equipment potentially compatible with previously established design criteria, basic mining principles, and the lunar environment (Refs. 45 and 46). The ripper-excavator-loader (REL) and its companion hauler vehicle (HV), shown in Figure 6, were conceptualized to be a multipurpose, production-class mining equipment, and were designed for teleoperation. The REL is equipped with a ripper on its back end that would be used to loosen compacted or ice-cemented regolith, and its front bucket scoop would be used to excavate, self-load, and transport regolith. The HV has a rear-dump bed and is optimized for regolith hauling and higher ground speeds. Introduced as production rates increase, the HV would transport feedstock material from the mine to the processing plant and tailings from the plant back to the planned dumpsite.

Both vehicles use cleated, conical wheels to provide an efficient traction interface with the lunar soil and to avoid the problems of abrasive wear that tracked vehicles would encounter with their many moving parts. Each wheel is driven by a separate electric motor and a hydrogen/oxygen fuel cell system provided power to each vehicle. The onboard hydrogen and oxygen tanks would be refilled, and the leftover water reprocessed, at an electrolysis station powered by a surface nuclear power plant.

Although lacking specific quantitative details, Gustafson and Rice (Ref. 47) outlined three basic approaches for extracting lunar ice. The first involves in situ heating of the ice-regolith mixture without excavation using a mobile rover with a microwave generator aimed at the soil. As the regolith is heated from within and the ice turns to vapor and is collected on cold plates located within a domed cover placed over the area being processed. The refrozen ice is then removed from the cold plates and transported out of the shadowed crater in storage tanks that are mounted on a fuel-cell-powered rover. Although a number of design issues must be considered (e.g., the choice of frequency, the dielectric properties of the regolith, and the electrical-to-microwave energy conversion efficiency), the microwave extraction process (Ref. 48) is envisioned to be simpler, less disruptive, and more "environmentally friendly" to the surrounding LS.

In the second approach, the ice-regolith mixture is mechanically excavated and processed within the cold trap using a water extraction furnace that uses nuclear or solar energy as the heat source. The liquid or gaseous water is then transported to a collection site outside of the shadowed crater for filtration, purification, and storage. The third option excavates the fragmented ice-rich regolith using a dragline bucket (Ref. 44) that transports it from the cold trap to a sunlit area outside the crater for processing. Each of these concepts has its advantages and disadvantages.

Before detailed mining and water extraction systems can be designed and evaluated, the material characteristics of the ice-regolith mixture (e.g., physical properties, the form, concentration, and spatial resolution of ice within the regolith) needs to be determined. NASA's Resource Prospector (RP) mission

(Ref. 49), originally set to launch in 2022 but unexpectedly cancelled in late April, had planned on using onboard neutron and infrared spectrometers and a drill (capable of obtaining samples from a depth of ~1 m), to (1) characterize the nature and distribution of water and other volatiles in polar subsurface material, (2) demonstrate the extraction and capture of native water, and (3) demonstrate the extraction of oxygen from the lunar regolith using the hydrogen reduction process.

In the meantime, tests are being conducted and measurements are being made using simulated ice-regolith mixtures in laboratory settings here at Earth. Gertsch et al. (Refs. 50 and 51) have analyzed the effects of varying water ice content (from 0 to ~12 wt%) in a lunar regolith simulant (JSC–1) to determine the effect on the excavatability of different ice-regolith mixtures. Load-penetration tests were conducted on compacted samples cooled to 77 K (using liquid nitrogen, LN_2) to simulate conditions expected in lunar cold traps. Based on the measured values of specific penetration (used to predict material excavatability and uniaxial compressive strength) and specific energy (used to predict excavator power and production rate), Gertsch et al. matched the different ice-regolith mixtures to the following types of terrestrial mined rocks: (1) at 0 to ~0.3 wt% ice, the mixture behaves like weak coal that is easy to excavate; (2) at ~0.6 to 1.5 wt% ice (similar to that measured by Lunar Prospector), the mixture behaves like weak shale or mudstone and is readily excavatable; (3) at ~8.4 wt% ice (similar to that measured by LCROSS), the mixture behaves like moderate-strength limestone and sandstone and is excavated using mechanical excavators; and (4) at ~10 to 12 wt% ice, the mixture behaves like strong limestone and sandstone and high-strength concrete, which require massive excavators. According to Gertsch, a dual-focused program of material characterization and excavator design and testing will be required (Ref. 50) to develop a robust rotating cutterhead (Ref. 51) with the capabilities needed to mine lunar ice deposits in the future.

3.0 NTR and LANTR System Description and Performance Characteristics

The NTR uses a compact fission reactor core containing "enriched" U-235 fuel to generate hundreds of megawatts of thermal power (MW_t) required to heat the LH_2 propellant to high exhaust temperatures for rocket thrust (Ref. 52). In an "expander cycle" engine (shown in Fig. 7), high-pressure LH_2 flowing from a turbopump assembly (TPA) is split into two paths: the first cools the engine's nozzle, pressure vessel, neutron reflector, and control drums, and the second path cools the engine's core support tie tube (TT) assemblies. The flows are then merged, and the heated H_2 gas is used to drive the TPAs. The hydrogen turbine exhaust is then routed back into the reactor pressure vessel and through the internal radiation shield and upper core support plate before entering the coolant channels in the reactor's fuel elements (FEs). Here it absorbs energy produced from the fission of U-235 atoms, is superheated to high exhaust temperatures (~2700 K or more depending on the uranium fuel loading), then expanded out a high-area-ratio nozzle (~300:1) for thrust generation.

Controlling the NTR during its various operational phases (startup, full thrust, and shutdown) is accomplished by matching the TPA-supplied LH_2 flow to the reactor power level. Multiple control drums, located in the reflector region surrounding the reactor core, regulate the neutron population and reactor power level over the NTR's operational lifetime. The internal neutron and gamma radiation shield, located within the engine's pressure vessel, contains its own interior coolant channels. It is placed between the reactor core and key engine components to prevent excessive radiation heating and material damage.

Recent studies showing the benefits of NTP for a variety of exploration and commercial lunar missions (Refs. 16 and 17) have used a common NTP stage (NTPS) employing a cluster of three small nuclear rocket engines (SNREs). The engine's reactor core is composed of hexagonal-shaped FEs and core support TTs developed and tested during the Rover/NERVA (Nuclear Engine for Rocket Vehicle Applications) program (Ref. 52). Each FE was fabricated using a graphite matrix material that contained the U-235 fuel in the form of either coated particles of uranium carbide (UC_2) or as a dispersion of uranium and zirconium carbide (UC-ZrC) referred to as "graphite composite" (GC) fuel (Fig. 8).

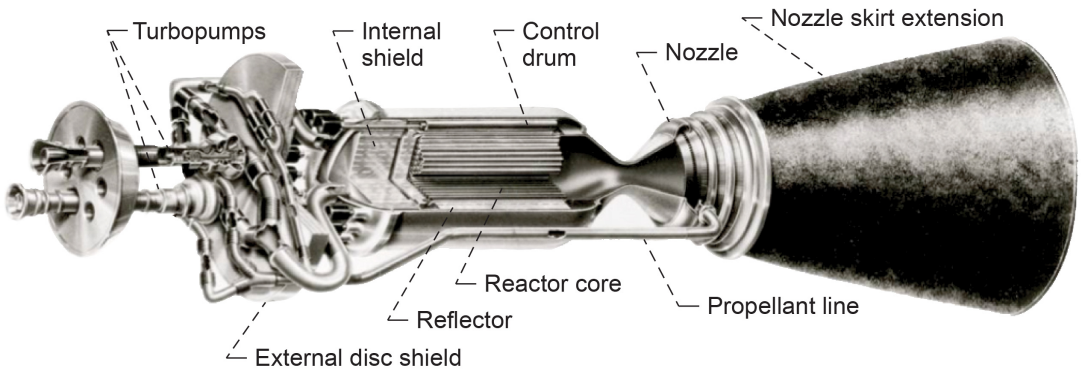

Figure 7.—Expander cycle NTR engine with dual LH_2 turbopumps.

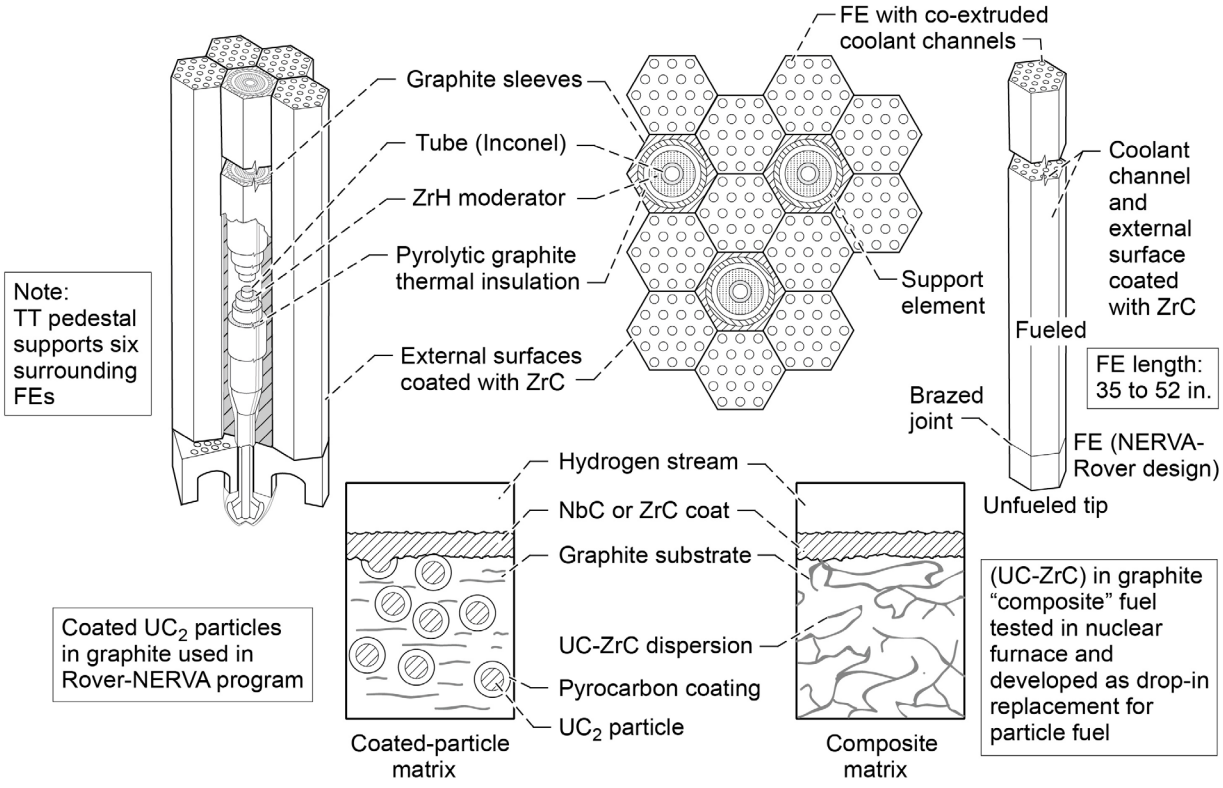

Figure 8.—Coated-particle and graphite composite SNRE fuel element (FE) and tie tube (TT) arrangement.

This higher performance GC fuel was developed as a "drop-in replacement" for the coated-particle fuel and was tested in the Nuclear Furnace 1 (NF–1) FE test reactor (Ref. 52) near the end of the Rover program. The GC elements achieved a peak power density of ~5 MW_t per liter (~5000 MW_t/m^3) and a peak fuel temperature of ~2700 K. The GC elements also demonstrated better corrosion resistance than the standard coated-particle FEs used in the previous Rover/NERVA reactor tests. This improved resistance of the GC fuel was attributed to its higher coefficient of thermal expansion that more closely matched that of the protective ZrC coating, thereby helping to reduce coating cracking. Electrical-heated composite FEs were also tested by Westinghouse in hot hydrogen at 2700 K for ~600 min—equivalent to ten 1-hr cycles.

Heritage Rover/NERVA FEs had a hexagonal cross section (~0.75 in. across the flats) and 19 axial coolant channels (Fig. 8) that were coated with niobium carbide (NbC) initially, then with zirconium carbide (ZrC) using a chemical vapor deposition process. This protective coating, applied to the FE's exterior surfaces as well, helped to reduce coating cracking, hydrogen penetration, and subsequent erosion of the graphite matrix material. Individual elements were 1.32 m (52 in.) in length and produced ~1 MW_t during steady-state, full-power operation. Also included in the engine's reactor core were hexagonal-shaped TTs that provided structural support for six surrounding FEs (Fig. 8). A coaxial Inconel tube inside the TT carries hydrogen coolant that is then used to supply a source of heated hydrogen for turbine drive power in the SNRE's expander cycle engine design. A sleeve of zirconium hydride (ZrH) moderator material is also incorporated into each TT (Fig. 8) to help increase core reactivity and allow construction of smaller, lower thrust engine systems like the SNRE developed by Los Alamos National Laboratory near the end of the Rover/NERVA program (Ref. 52).

Although it was not built, the SNRE incorporated all of the lessons learned from the program's 20 previous reactor designs and test results. The FE had the same hexagonal cross section and coolant channel number, but was 35 inches long, used GC fuel, and produced ~0.65 MW_t. To help increase core reactivity, the "SNRE" FE-TT pattern increased the number of TTs so that each FE had three TTs and three FEs surrounding it (Fig. 8). With the SNRE pattern, the FE-to-TT ratio is ~2 to 1, with each TT providing redundant mechanical support for six surrounding FEs.

The baseline SNRE used in this study has a nominal power output of ~365 MW_t, an average power density of ~3.44 MW_t/L, and produces ~16.5 klb_f (1 klb_f = 1000 pounds force) of thrust. The reactor core has 564 FEs and 241 TTs and is surrounded by a 14.7-cm-thick perimeter neutron reflector resulting in a pressure vessel outer diameter (OD) of ~98.5 cm. With a fuel loading of ~0.6 g/cm^3, the SNRE's FEs contain ~60 kg of 93% enriched U-235. The GC fuel operates at a peak temperature of ~2860 K, and the corresponding hydrogen exhaust temperature is ~2734 K. With a chamber pressure of 1000 psia, a hydrogen flow rate of ~8.30 kg/s and a nozzle area ratio of ~300:1, the engine's I_{sp} is ~900 s. The total engine length is ~5.8 m with the ~1.8-m-long radiation-cooled retractable nozzle section fully extended. The nozzle exit diameter is ~1.53 m and the engine's thrust-to-weight ratio is ~3.02.

3.1 LANTR: An Enhanced NTR With "Bipropellant" Operational Capability

In order to take full advantage of LLO_2 once it becomes available in lunar orbit, the LTS transitions over to LO_2-augmented NTR (LANTR) operation, with each SNRE outfitted with an O_2 afterburner nozzle containing O_2 injectors and an O_2 feed system. The oxygen is stored as a cryogenic liquid at low pressure and must be pressurized and gasified prior to its injection into the nozzle. This is accomplished by diverting a small fraction of the engine's hydrogen flow (~3%) to an oxidizer-rich gas generator that drives a LO_2 TPA used to deliver the gasified LO_2 to injectors positioned inside the afterburner nozzle downstream of the throat (Refs. 18 to 20). A simplified schematic of LANTR engine operation is illustrated in Figure 9(a). Here it mixes with the hot H_2 and undergoes supersonic combustion adding both mass and chemical energy to the rocket exhaust—essentially scramjet propulsion in reverse.

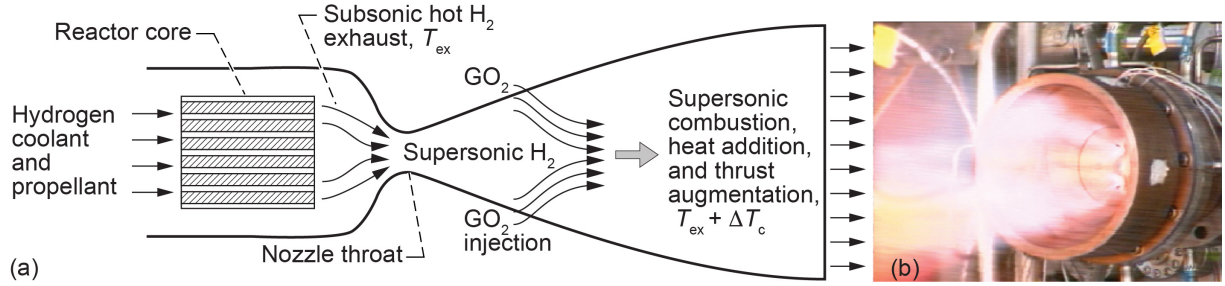

Figure 9.—LANTR concept (Ref. 53). (a) Simplified schematic. (b) Proof-of-concept test article.

Downstream nozzle injection in the LANTR isolates the reactor core from oxygen's damaging effects, provided the throat retains choked flow. This operating condition can be satisfied using a "cascade" scramjet injector developed by Aerojet (now Aerojet Rocketdyne) (Ref. 20). A three-zone staged injection approach (Ref. 20) is envisioned using multiple cascade injectors to control the oxygen addition and heat release within the nozzle while keeping the flow supersonic. This approach also increases penetration, mixing, and combustion of the injected oxygen within the hydrogen flow while minimizing shock losses and the formation of high heat flux regions, thereby maximizing engine performance and life. A high reactor outlet pressure is also desirable since it allows the use of a high-area-ratio nozzle—important for increasing combustion efficiency—at reasonable size and mass.

Also shown in Figure 9(b) is a photograph of a nonnuclear, "proof-of-concept" demonstration test of a LANTR nozzle that used a fuel-rich 2100-lb_f chemical rocket engine operating at an O/H MR <2 to simulate a NTR. The water-cooled, copper test nozzle had a nozzle area ratio of 25:1 and used three wedge-shaped injectors (two of which are visible in Fig. 9(b)) (Ref. 53). These tests and follow-on tests with a 50:1 nozzle indicated that up to 73% of the injected oxygen burned within these short nozzles, resulting in an augmented thrust level of ~53% as measured on the engine thrust stand (Ref. 20).

The LANTR concept has the potential to be an extremely versatile propulsion system. By varying the O/H MR, the LANTR engine can operate over a wide range of thrust and I_{sp} values (Table I) while the reactor core produces a relatively constant power output. As the MR varies from 0 to 5, the engine thrust level for the SNRE increases from 16.5 to ~56.8 klb_f (over 344%) while the I_{sp} decreases from 900 to 516 s (~57%), which is still 54 s higher than that achieved by today's best LO_2/LH_2 chemical engine, the RL10B–2 (Ref. 54). This thrust augmentation feature means that large-engine performance can be obtained using smaller, more affordable LH_2-cooled NTR engines that are easier to build and less costly to test on the ground. The engines can then be operated in space in the augmented high-thrust mode to shorten burn times (thereby extending engine life) and reduce gravity losses (thereby eliminating the need for and concern over using a multiple-perigee-burn Earth departure maneuver). Lastly, the increased use of high-density LO_2 in place of low-density LH_2, and the ability to resupply or reoxidize LANTR vehicles with LLO_2 prior to Earth return, are expected to significantly reduce vehicle size and mass while increasing delivered payload.

TABLE I.—SNRE AND LANTR PERFORMANCE CHARACTERISTICS AS FUNCTION OF O/H MIXTURE RATIO[a]

O/H mixture ratio	Specific impulse,[b] I_{sp}, s	Thrust augmentation factor	Thrust, lb_f	Engine mass, lb_m	Engine thrust/weight
0	900	1.0	16,500	5462	3.02
1	725	1.611	26,587	5677	4.68
2	637	2.123	35,026	5834	6.00
3	588	2.616	43,165	5987	7.21
4	552	3.066	50,587	6139	8.24
5	516	3.441	56,779	6295	9.02

[a]Acronyms are defined within report and in appendix.
[b]Fuel exit and hydrogen exhaust temperature = 2734 K, chamber pressure = 1000 psia, and nozzle area ratio = 300:1.

4.0 Mission, Payload, and Transportation System Ground Rules and Assumptions

Specific mission and payload (PL) ground rules and assumptions used in this report are summarized in Table II, which provides information about the different lunar mission scenarios, along with the assumed parking orbits at Earth and the Moon. Specific trajectory details and ΔV budgets for the different missions examined are provided within the appropriate sections of the report. In addition to the large ΔV requirements for the primary propulsion maneuvers like translunar injection (TLI), lunar orbit capture (LOC), trans-Earth injection (TEI), and Earth orbit capture (EOC), smaller ΔV maneuvers are needed for propellant settling; vehicle midcourse correction maneuvers; orbital operations in lunar polar orbit (LPO), including rendezvous and docking (R&D) of the lunar transfer vehicle (LTV) with surface-based LLVs or with the lunar propellant depot; and lastly, LTV-depot separation and station keeping.

TABLE II.—MISSION AND PAYLOAD GROUND RULES AND ASSUMPTIONS[a]

• Crewed lunar landing using NTR (3-day transits to and from Moon with 3 to 14 days on surface) • Crewed cargo transport using LANTR (1.5- to 3-day transits to and from Moon with 3 days in LPO) • LANTR commuter shuttle carries passenger transport module (PTM) (one-way transit of 36 hr or less)	• Reusable LTV carries *Orion* MPCV, reusable LLV and surface payload to LPO; returns MPCV and spent LLV to elliptical Earth orbit (EEO); *Orion* capsule used for crew recovery at mission end • Reusable, LANTR LTV transports habitat module, crew, and varying amounts of cargo, depending on the transit times to and from LPO; LTV refuels with LDP at a LPO depot before returning to Earth • Reusable, LANTR LTV transports a PTM to LPO for subsequent delivery to the lunar surface by LLV; LTV refuels with LDP at LPO depot before returning to Earth with another PTM
• NTR and LANTR missions depart from LEO, then capture and depart from LPO • NTR missions return to EEO, and LANTR missions return to LEO	• LEO: 407 km circular • LPO: 300 km circular • 2.81-hr EEO: 500 by 7072 km • 24-hr EEO: 407 by 71,310 km
• Primary mission velocity change increment ΔV maneuvers: NTR or LANTR engines used • Additional ΔV requirements: AMBR RCS thrusters used to perform nonprimary propulsion maneuvers as well as primary burn maneuvers under 100 m/s	• ΔV budgets for different missions discussed in relevant sections • Propellant settling burn: ~1 m/s • Midcourse correction: ~10 m/s • Lunar orbit rendezvous and docking and maintenance: ~40 m/s • Depot separation and station keeping: ~10 m/s
• Crewed landing mission payload masses: Reusable NTR LTV delivers *Orion* MPCV and single-stage LO_2/LH_2 LDAV to LPO; LDAV carries four crew and 5 t of payload to lunar surface; LTV with *Orion* MPCV, LDAV, and surface samples returned to 24-hr EEO	• *Orion* MPCV: 13.5 t • Saddle truss assembly (STA): 7.2 t • LDAV crew cab and dry mass: 8.6 t • Crew (4) and extravehicular activity (EVA) suits: 0.8 t • LDAV propellant load: 20.9 to 22.4 t • LDAV surface payload: 5.0 t • Returned samples: 0.1 t
• Crewed cargo transport payload masses: Reusable LANTR LTV delivers a habitat module, crew, and cargo (10 to 20 t, depending on transit time) from LEO to LPO, then returns to LEO	• Habitat module: 9.9 t • Single star truss with RMS: 5.29 t • Outbound payload (4 to 8 cargo pallets): 2.5 t each • Crew (4) and EVA suits: 0.80 t • Returned samples: 0.25 t
• Commuter shuttle payload mass: Reusable LANTR LTV delivers PTM from LEO to LPO then back again	• PTM: 15 t (includes 2 crew and 18 passengers)

[a]Acronyms are defined within report and in appendix.

A variety of different PLs are also considered. On initial "all LH_2" NTR crewed landing missions, a forward-mounted saddle truss is used to connect the payload elements to the transfer vehicle's in-line tank. The truss is open on its underside, and its forward adaptor ring provides a docking interface between the multipurpose crew vehicle (MPCV) and the single-stage LO_2/LH_2 lunar descent and ascent vehicle (LDAV) shown in Figure 10(a). The LDAV is a heritage design (Ref. 55) analyzed in considerable detail during NASA's earlier Space Exploration Initiative studies. It carries a crew of four plus 5 t of surface PL stored in two 2.5-t PL pallets mounted on each side of the crew cab. The LDAV mass breakdown including the propellant loading and landed payload is shown in Table II. On the lunar landing mission analyzed here, the crew collects and returns ~100 kg of samples.

Delivered to LPO by a NTR-powered cargo transport, a 36-t "wet" LLV (without a crewed PL and ascent stage) is capable of delivering ~28 t to the LS. Assuming it can be configured to fit within the upgraded Space Launch System (SLS–1B) PL shroud, the landed PL can take the form of a fully functional habitat lander, a LPI processing plant, or various pieces of heavy mining equipment such as the notional rotating bucket-wheel excavator shown in Figure 10(b). Without any attached PL, the NTR cargo transport can also function as a propellant "tanker," delivering just under 29 t of ELH_2 to a LPO depot on each roundtrip mission.

For the reusable, space-based crewed cargo transport (CCT) missions using LANTR propulsion and LDP on the Earth return mission leg, the LTV carries a habitat module that supports a crew of four. Two crewmembers operate the vehicle and manage the unloading of the PL. The other two represent rotating crewmembers on assignment at the lunar base or the LPO propellant depot. Connecting the habitat module to the rest of the LANTR LTV is a "star truss" that has four concave sides to accommodate four PL pallets (shown in Fig. 10(c)). The forward circular truss ring also has a remote manipulator system (RMS) with twin arms attached to it. Using the habitat module's rear viewing window, the crew uses these arms to unload and attach the transport's cargo to the depot or to a co-orbiting LLV that is transferring crew and awaiting cargo delivery.

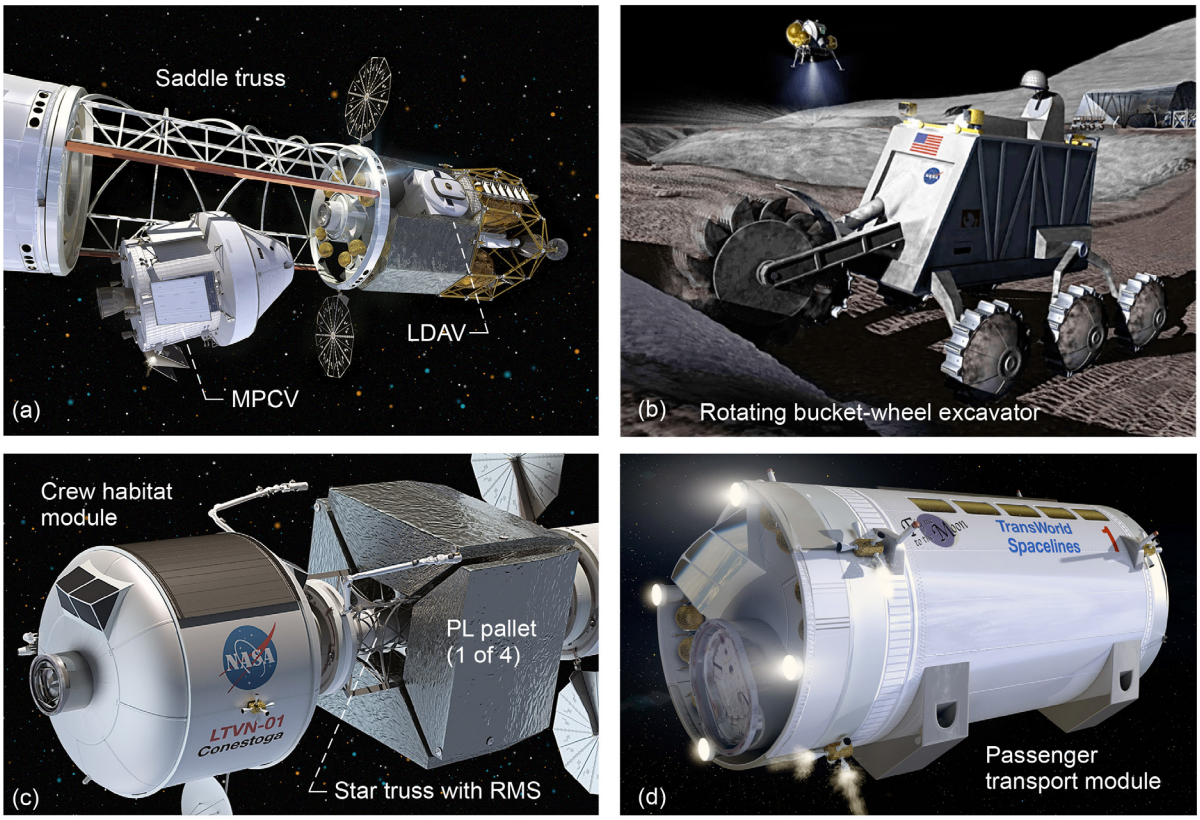

Figure 10.—Payload elements carried by NTR and LANTR lunar transfer vehicles.

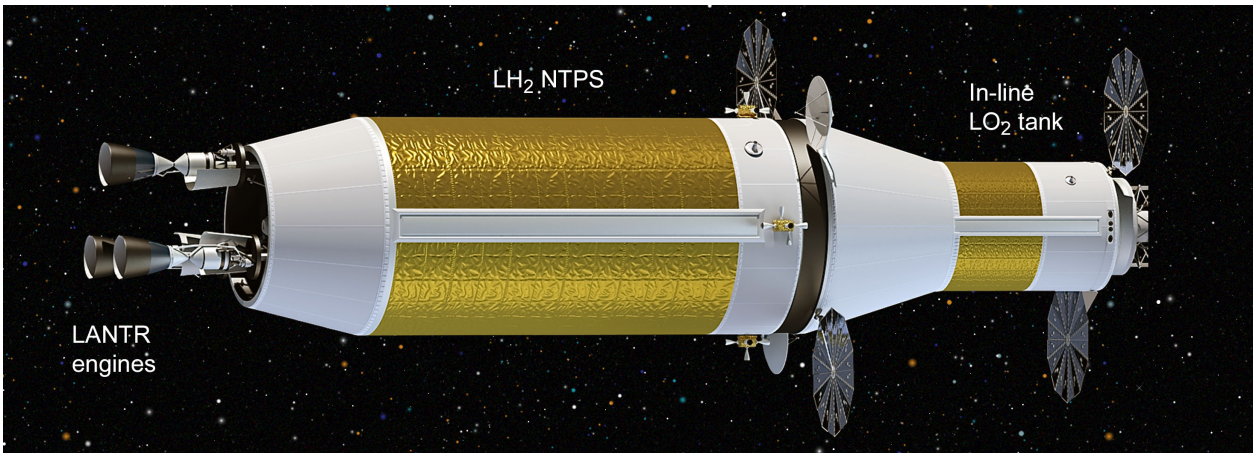

Figure 11.—Key elements of LANTR lunar transfer vehicle system: LH_2 NTPS and in-line LO_2 tank.

Using the same LANTR LTV system elements shown in Figure 11, routine commuter flights to and from the Moon can also be considered. For the commuter shuttle application, the cargo transport's habitat module, star truss, and PL pallets are removed and replaced with a passenger transport module (PTM) (Fig. 10(d)) that carries 18 passengers and 2 crewmembers.

Table III lists the key ground rules and assumptions used in the NTR and LANTR transportation system elements. The NTPS carries only LH_2 and uses a three-engine cluster of SNRE-class engines initially before transitioning over to LANTR operation. The smaller diameter in-line tank located in front of the NTPS carries only LO_2. It is assumed the LANTR LTVs operating out of LPO refuel with primarily LLO_2 but are also able to "top off" their NTPS for Earth return using the excess LLH_2 produced at the LPO depot during the H_2O electrolysis process. Details on the NTR and LANTR engine design and performance are provided in Section 3.0 and summarized in Table III. The total mission LH_2 and LO_2 propellant loadings consist of the usable propellant plus performance reserve and tank-trapped residuals. Additional LH_2 is also provided for engine cooldown after each major propulsive maneuver.

For the smaller auxiliary and primary propulsion maneuvers under ~100 m/s, a storable bipropellant reaction control system (RCS) with Advanced Material Bipropellant Rocket (AMBR) thrusters is used (details in Table III). The LANTR LTV utilizes a split RCS with approximately half the AMBR thrusters and bipropellant mass located on the NTPS and the other half located at the front end of the in-line LO_2 tank just behind the mission-specific PL.

The LH_2 propellant carried in the NTPS is stored in the same "state-of-the-art" Al/Li LH_2 propellant tank being developed for the SLS and its upgrade to support future human exploration missions. Sizing of the LH_2 tank assumes a 30-psi ullage pressure, 5g axial and 2.5g lateral launch loads, a safety factor of 1.5, and a 3% ullage factor. The in-line LO_2 tank with its rear conical adaptor section uses the same sizing and launch load assumptions. All tanks use a combination spray-on foam insulation (SOFI) and multilayer insulation (MLI) system for passive thermal protection. A zero boil-off (ZBO) "reverse turbo-Brayton" cryocooler system is used on the NTPS to eliminate LH_2 boil-off from the NTPS during the course of the mission. A passive thermal protection system is used on the in-line LO_2 tank since it is drained after the LOC burn and is subsequently refueled with LLO_2 before the trip back to LEO. The heat load on the NTPS hydrogen tank is the highest in LEO and determines the size of the ZBO cryocooler system. Two sets of circular solar photovoltaic arrays (PVAs)—each producing ~14 kW_e—are baselined with one set supplying the primary electrical power needed for all key LTV subsystems and the second set providing power for the different mission PLs considered here.

Table III also provides the assumed dry weight contingency (DWC) factors, along with the requirements for delivered mass to LEO and the shroud cylindrical payload envelope for the SLS and its upgrade. A 30% DWC is used on the NTR and LANTR systems and advanced composite structures (e.g., stage adaptors and trusses); 15% is used on heritage systems (e.g., Al/Li tanks, RCS, etc.). The NTPS mass (~70 t) and size (~7.6-m OD and ~26.5-m length (L)) determines the required lift capability and the usable shroud PL volume for the upgraded SLS. The combined saddle truss (~13.7-m L) and LDAV (~9.6-mL) carried on the crewed landing mission (shown in Fig. 12(b)) has this same approximate length. On the CCT mission discussed in Section 7.0, the habitat module (~6.5-m OD by ~8.5-m L) and star truss (~11-m L) can be launched together, or the truss can be launched together with the in-line LO_2 tank and its conical adaptor (~11.5-m L).

TABLE III.—NTR AND LANTR TRANSPORTATION SYSTEM GROUND RULES AND ASSUMPTIONS[a]

NTR and LANTR characteristics	• Engine (fuel type): NERVA-derived (UC-ZrC composite) • Propellants: LH_2 (NTR), LH_2 and LO_2 (LANTR) • Thrust level: 16.5 klb_f (SNRE-class engine using only LH_2) 26.5 to 56.8 klb_f (LANTR, O/H MR = 1 to 5) • Fuel element length: 0.89 m (SNRE baseline) • Exhaust temperature: ~2734 K (with 2860 K peak temperature) • Chamber pressure: ~1000 psi • Nozzle area ratio: ~300:1 • Specific impulse range: I_{sp} = 900 to 516 s with LANTR (MR = 0 to 5)
Propellant margins	• Cooldown: 3% of usable LH_2 propellant • Performance reserve: 1% on ΔV • Tank trapped residuals: 2% of total tank capacity
RCS (used for propellant settling, midcourse correction burns, lunar orbit operations, and primary maneuvers under ~100 m/s)	• Propulsion type: AMBR 200-lb_f thrusters • Propellant: nitrogen tetroxide (N_2O_4) and hydrazine (N_2H_2) • Nominal I_{sp}: 335 s
LH_2 cryogenic tanks and passive thermal protection system	• Material: Aluminum-lithium (Al/Li) • Tank – Outer diameter (OD): 7.6 m (LH_2); 7.6 m and 4.6 m (LO_2) – Length (L): 15.65 m (core NTPS tank) 20.15 m (in-line LH_2 tank) 5.23 to 7.95 m (in-line LO_2 tank) • Geometry: Cylindrical with √2/2 ellipsoidal domes • Insulation: 1-in. SOFI (~0.78 kg/m^2) 60 layers of MLI (~0.90 kg/m^2)
Active cryofluid management and zero boil-off (ZBO) LH_2 propellant system	• Reverse turbo-Brayton ZBO cryocooler system powered by photovoltaic arrays (PVAs) • ZBO system mass and power requirements driven by core stage size; ~760 kg and ~5.26 kW_e (for 7.6-m OD tank)
PVA primary power system	• Circular PVA sized for ~7 kW_e at 1 A.U., two arrays provide power for ZBO cryocoolers on core stage, PVA mass is ~566 kg for two ~25-m^2 arrays, second set of arrays provides power to mission PLs • "Keep-alive" power supplied by lithium-ion battery system
Dry weight contingency factors	• 30% on NTR system and composite structures (e.g., saddle and star trusses) • 15% on established propulsion, propellant tanks, and spacecraft systems
SLS and SLS upgrade launch requirements: – Usable PL delivered to LEO – Cylindrical PL envelope	• ~70 t (SLS) and 105 to 110 t (SLS–1B) • 7.6 m OD by ~26.5 m L

[a]Acronyms and symbols are defined within report and in appendix.

5.0 Performance Impact of Integrating LANTR and LDP Into the LTS Architecture

As previously mentioned, the author presented a paper on the enhanced mission capability resulting from the combined use of LANTR propulsion and LUNOX 20 years ago at the 33rd Joint Propulsion Conference in Seattle, Washington (Ref. 18). In that paper, an evolutionary LTS architecture was analyzed that began with a LTS using high-performance NTP to maximize delivered surface payload on each mission. The increased PL was dedicated to installing modular LUNOX production units with the intent of using this LDP to supply surfaced-based LLVs initially, then in-space LTVs using LANTR propulsion at the earliest possible opportunity. This section re-examines this evolutionary LTS architecture to see how recent nuclear-powered LTV (NLTV) designs and missions (Refs. 16 and 17) are impacted by the introduction of LANTR and the ability to refuel with LLO_2 and LLH_2 provided by a LPO depot.

The NTPS, with its three 16.5-klb_f SNREs, is the "workhorse" element of the cargo and crewed NLTVs shown in Figures 12(a) and (b), respectively. It has a 7.6-m-OD by ~15.7-m-L Al-Li tank that carries ~39.8 t of LH_2 propellant. Housed within and mounted on the forward cylindrical adaptor section of the NTPS are the RCS, avionics, batteries, two deployable circular PVAs, a docking system, and a reverse turbo-Brayton cryocooler system for ZBO LH_2 storage. The cryocooler system mass and power requirements increase with tank diameter and are sized to remove ~42 W of heat penetrating the 60-layer MLI system while the stage is in LEO, where the highest tank heat flux occurs. To remove this heat load, the two-stage cryocooler system requires ~5.3 kW_e for operation.

The second major element is an in-line Al-Li LH_2 tank that connects the NTPS to the forward PL element. It has the same diameter but a longer length (~20.2 m) than that used in the NTPS and supplies an additional ~52.8 t of LH_2 propellant used during the single-burn TLI maneuver. The in-line tank element also includes forward and aft cylindrical adaptor sections that house quick-connect propellant feed lines, electrical connections, a RCS along with docking and payload adaptors. A ZBO cryocooler system is not used on the in-line LH_2 tank since it is drained during the TLI maneuver. The total length of the in-line element is ~25.2 m.

5.1 Reusable Lunar Cargo Delivery and Propellant Tanker Missions

Using the NTPS and in-line tank discussed above, the NTR cargo transport can deliver ~63.8 t of cargo to LPO then return to Earth for refueling and reuse. Three SLS–1B launches deliver the vehicle and PL elements to LEO where assembly occurs via autonomous R&D. The cargo transport then departs from LEO (ΔV_{TLI} ~3.442 km/s including g-losses of ~354 m/s) and arrives at the Moon ~72 hr later. It then begins a three-burn LOC maneuver that places it into a 300-km circular LPO (total ΔV_{LOC} ~1.142 km/s with g-losses). The first LOC burn captures the cargo transport into a highly elliptical orbit around the Moon with a perigee altitude of 300 km, the same as the final parking orbit. The second burn is performed

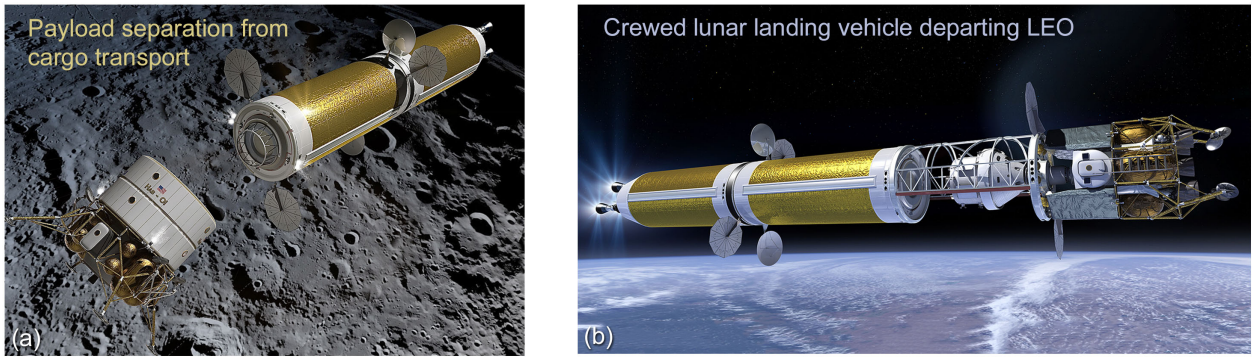

Figure 12.—Reusable NTR cargo delivery and crewed lunar landing vehicles.

at apogee to change the plane of the orbit to match the inclination of the desired parking orbit: in this case 90° for LPO. The third and final burn is performed near perigee to lower the orbit's apogee resulting in the final 300-km circular LPO. The duration of the LOC maneuver can range from several hours to a day to complete. A short 2.5-hr duration is baselined here, but it requires a larger total ΔV_{LOC}.

Once in orbit, the PL with its LLV separates from the cargo transport (shown in Figure 12(a)) and descends to the surface, landing autonomously at a predetermined location near one of the lunar poles. As mentioned in the previous section, the usable PL that can be delivered by LLV is on the order of ~28 t and—assuming it can be configured to fit within the SLS–1B PL shroud—can take the form of a fully functional habitat lander, a processing plant for LPI, or various pieces of heavy mining equipment. Without any attached PL, the NTR cargo transport can also function as a propellant "tanker" delivering ~28.8 t of ELH_2 to a LPO depot on each roundtrip mission.

After PL separation and a day or so in LPO, the cargo transport performs the TEI maneuver (total ΔV_{TEI} ~913 m/s including g-losses). Like the capture maneuver, TEI requires three burns and 2.5 hr to complete. The first burn raises the apogee of the orbit, resulting in a highly elliptical orbit around the Moon. The second burn is a plane change burn performed near apogee that adjusts and aligns the plane of the elliptical orbit from 90° to that needed for departure. The third and final burn is again performed near perigee, and after it is completed, the NLTV has escaped the Moon and is on a 3-day trajectory back to Earth.

On final approach, the cargo transport performs the EOC burn (ΔV_{EOC} ~356 m/s) and captures into a 24-hr elliptical Earth orbit (EEO) with a 407-km perigee by 71,310-km apogee. Postburn engine cooldown thrust is then used to assist in orbit lowering. Afterwards, an auxiliary tanker vehicle operating from a LEO propellant depot rendezvous and docks with the cargo vehicle and supplies it with the additional LH_2 propellant needed for the final orbit lowering and rendezvous with the LEO transportation node, where it is refurbished and resupplied before its next mission.

The cargo NLTV has an IMLEO of ~202 t consisting of the NTPS (~68.7 t), the in-line tank element (~67 t), plus the PL element (~63.8 t) with its connecting structure (2.5 t). The mission requires six primary burns by the three SNRE engines and uses ~88 t of LH_2 propellant. With ~49.5 klb_f of total thrust and I_{sp} ~900 s, the total engine burn time is ~58.8 min. For the propellant tanker mission, the IMLEO is ~136.9 t, and the total engine burn time is just over 40 min.

5.2 Reusable Crewed Lunar Landing Mission

On the crewed landing mission, the NLTV (Fig. 13(a)) carries a forward-mounted saddle truss assembly (STA) that connects the payload elements to the transfer vehicle's in-line tank. The truss is open on its underside, and its forward adaptor ring provides a docking interface between the *Orion* MPCV and the single-stage LO_2/LH_2 LDAV as shown in Figure 12(b). The LDAV carries a crew of four plus 5 t of surface PL stored in two "swing-down" pallets mounted on each side of the crew cab (Fig. 13(b)).

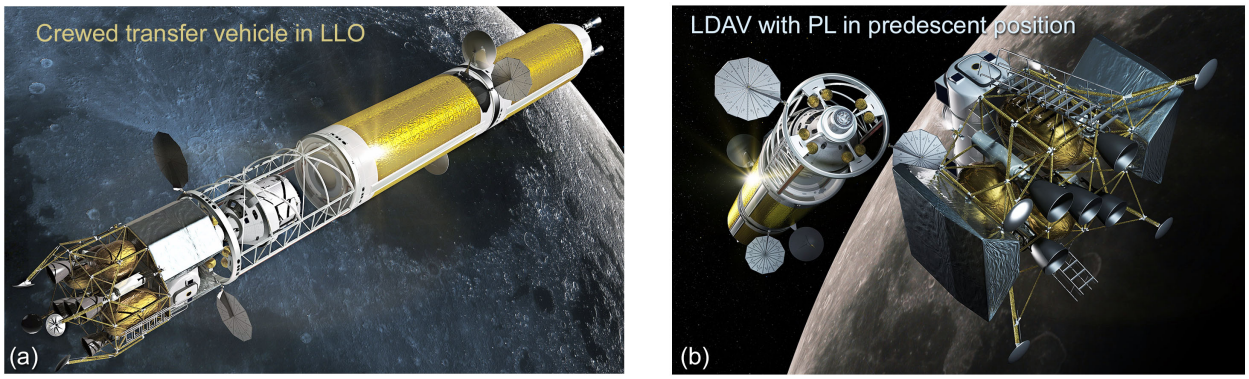

Figure 13.—Crewed lunar landing mission. (a) Transfer vehicle capture into LPO. LDAV landing preparation.

Three SLS–1B launches are used to deliver the two NTR vehicle elements and the PL element to LEO for assembly via autonomous R&D. The PL element includes the connecting STA plus the LDAV with its surface cargo containers. In addition to front and rear docking capabilities, the STA's forward adaptor ring also carries twin PVAs and a RCS. Once assembled, the *Orion* MPCV and crew are launched and rendezvous with the NLTV positioning itself inside the STA and docking with the LDAV using the docking port and transfer tunnel mounted to the STA's forward adaptor ring (Fig. 10(a)).

After the single-burn TLI maneuver (ΔV_{TLI} ~3.417 km/s including a g-loss of ~330 m/s), the crew begins its 3-day coast to the Moon. Because the crewed NLTV carries a significant amount of payload mass (the STA, MPCV, and "spent" LDAV) back from the Moon, it uses an ~20.2-m-long in-line tank to supply the required amount of LH_2 propellant needed for this reusable mission. After its 72-hr transit, the NLTV begins the LOC maneuvers (ΔV_{LOC} ~1.142 km/s including g-loss) required to insert itself and its payload into LPO. Like the cargo transport, the crewed NLTV uses the same 2.5-hr-long three-burn orbital insertion sequence described above.

Once in LPO, the crew enters the LDAV and separates from the transfer vehicle. After separation, the LDAV's two PL pallets are rotated 180° and lowered into their landing position in preparation for descent to the LS (Fig. 13(b)). The ΔV budget used in the Martin Marietta LDAV design (Ref. 55) is ΔV_{des} ~2.115 km/s and ΔV_{asc} ~1.985 km/s for descent and ascent, respectively. The LDAV uses five RL10A–4 engines operating with a I_{sp}~450 s and ~13.5 t of LO_2/LH_2 propellant is expended during the descent to the surface.

After completing the surface mission, the crew returns to LPO in the LDAV carrying 100 kg of lunar samples. At liftoff, the LDAV mass is ~15.1 t, and ~5.5 t of propellant is used during the ascent to LPO. The LDAV then rendezvous with the transfer vehicle, and preparations for the TEI maneuver begin. After completing the three-burn departure sequence (total ΔV_{TEI} ~913 m/s with g-loss), the crew spends the next 3 days in transit readying their vehicle for the final phase of the mission: capture into a 24-hr EEO (ΔV_{EOC} ~356 m/s). Afterwards, the crew re-enters and lands using the *Orion* capsule.

The crewed lunar landing mission has an IMLEO of ~193 t that includes the NTPS (~69.2 t), the in-line tank assembly (~67.6 t), the STA (~7.3 t), the wet LDAV (~29.5 t) with its surface PL (~5 t), the *Orion* MPCV (~13.5 t), consumables (~0.1 t), and four crewmembers (~0.8 t includes suits for lunar extravehicular activity (EVA)). At departure, the LH_2 propellant loading in the NTPS and the in-line tank are at their maximum capacity of ~39.8 and ~52.8 t, respectively. The overall length of the crewed NLTV is ~77.5 m. Like the cargo mission, the crewed landing mission requires six primary burns by the NTPS using ~88 t of LH_2 propellant, and the total engine burn time is again ~58.8 min.

5.3 Impact of Using LDP to Refuel Surface-Based LDAVs and In-Space NLTVs

Figure 14 shows the variation in NLTV size, IMLEO, increased mission capability, and engine burn time resulting from the development and utilization of LPI-derived LLO_2 and LLH_2. Figure 14(a) shows the reusable, crewed NLTV discussed above. It departs from LEO and captures into a 300-km LPO. At the end of the mission, the NLTV returns to Earth with the spent LLV and captures into a 24-hr EEO because it has a much lower ΔV requirement. In order to return to LEO, the NLTV would need an additional ~138 t of LH_2 propellant requiring the insertion of a star truss with four attached drop tanks between the vehicle's in-line tank and forward payload. The additional mass of the extra truss, propellant and tanks increases the vehicle's IMLEO to ~371.5 t.

The first significant step in LDP production occurs when polar outpost assets and production levels of LLO_2 and LLH_2 become sufficient to support a LS-based LDAV. By not having to transport a wet LDAV to LPO on each flight, the crewed NLTV now has a lower starting mass in LEO (~163.2 t) plus sufficient onboard propellant to return to a lower, higher energy ~2.81-hr EEO (407-km perigee by 7072-km apogee with ΔV_{EOC} ~1.914 km/s including g-losses) as shown in Figure 14(b).

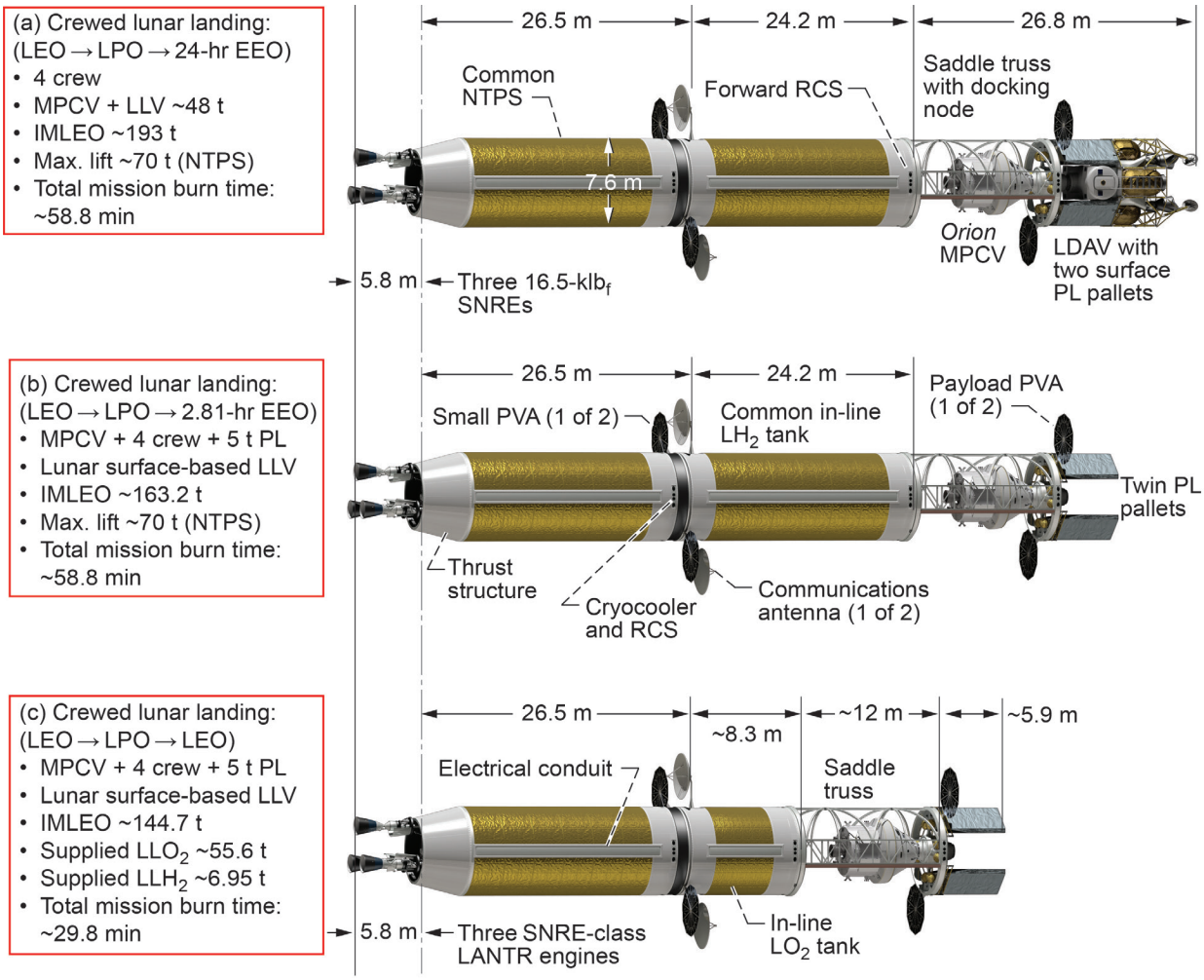

Figure 14.—Variation in NLTV size, IMLEO, mission capability and engine burn time resulting from the development and utilization of LDP and the transition to LANTR operation.

After entering orbit, a surface-based LDAV, operated autonomously from the LS during liftoff, R&Ds with the crewed NLTV to pick up the crew and cargo. The cargo, consisting of two 2.5-t PL pallets, is positioned at the front end of the saddle truss ring so that the pallets readily attach on both sides of the crew cab and can subsequently be lowered into the "saddlebag" position for descent as shown in Figure 13(b). At liftoff the LDAV carries up to 22.4 t of LLO_2/LLH_2 propellant. It uses ~13 t to achieve LPO and another 9 t returning to the LS after picking up the crew and cargo. Operating at an O/H MR of ~6, the LDAV's chemical rocket engines use ~3.2 t of LLH_2 and ~19.2 t of LLO_2 propellant during its roundtrip mission to LPO and back. Because of this O/H MR and the 8:1 stoichiometry of H_2O, it will be necessary to extract and electrolyze ~28.8 t of water and overproduce LLO_2 by ~6.4 t to obtain the required amount of LLH_2 needed to support LDAV operation between the LS and LPO and back again.

As LPI mining and LDP production levels increase further, a propellant depot would be established in LPO and routinely supplied with water transported from the LS by specialized tanker LLVs. At the depot, the water is electrolyzed and the LDPs are stored for subsequent use. Periodically, the depot could also receive additional ELH_2 delivered by a NTR tanker vehicle operating between LEO and LPO. At this point, the NLTV's SNREs are refitted with afterburner nozzles and LO_2 feed systems, and the large in-line LH_2 tank used in the two previous vehicles is replaced by a smaller LO_2 tank (shown in Fig. 14(c)). The LO_2 tank, consisting of two $\sqrt{2}/2$ ellipsoidal domes, is ~5.23 m long and has a 7.6 m OD that is compatible with the saddle truss diameter.

In the analysis results presented in this report, it is assumed that the LANTR LTVs operating out of LPO refuel with LLO_2 primarily but are also able to top off their NTP stages for Earth return using the excess LLH_2 produced from the H_2O electrolysis process. By refueling with ~55.6 t of LLO_2 and ~6.95 t of LLH_2 (at a ratio of 8:1), a smaller, more capable crewed NLTV is possible. It is ~18.5 t lighter than the vehicle shown in Figure 14(b) and can now return back to LEO as well—a significant advance in performance capability. It is also important to note that with LO_2 augmentation and refueling with LDPs, the total engine burn time is cut in half to just under 30 min.

The LANTR engines used in this study are sized with the appropriate hardware mass (pumps, controls, lines, etc.) for the maximum MR operation to allow the full range of O/H MRs from 0 to 5 to be accessible during the mission. A multidisciplinary analysis and mission assessment code (MAMA) with optimization capability (Ref. 56) is used to determine the propellant requirements for the various missions examined. By giving the optimizer control over the O/H MRs used for the individual mission burns, initial propellant loading and refueling amounts, one can find the minimum propellant requirements needed to complete the mission. Depending on the specified mission objective, the optimizer can be used to minimize the total propellant, Earth-supplied propellant, or lunar-supplied propellant usage. Alternatively, one can explore other possibilities by giving the optimizer control over cargo mass or transit times. Using this capability, one can determine the maximum cargo that can be delivered for a given mission scenario and vehicle configuration, along with the propellant and refueling requirements. Access to both LPI-derived LO_2 and LH_2 in LPO opens up the mission trade space, and the addition of LLH_2 can be leveraged to reduce the IMLEO and total propellant requirements for various mission types despite the larger ΔV needed to access LPO.

6.0 Growth Mission Possibilities Using Depots and LDP Refueling

Over time we envision the development of a totally space-based LTS with different types of NLTVs operating between transportation nodes and/or propellant depots located in LEO (Fig. 15(a)) and LPO. Because abundant deposits of volcanic glass are located at a number of sites just north of the lunar equator, a depot established in equatorial low lunar orbit (LLO) (Fig. 15(b)) would also be a good idea. These depots would be routinely supplied with LUNOX or H_2O from tanker LLVs operating between the LS and either LLO or LPO. Orbiting lunar depots could also evolve into key transportation nodes, providing convenient staging locations where NTR tankers, CCTs, and commuter shuttles can drop off ELH_2, cargo, and passengers that would then be picked up by LLVs for transport to the LS.

Initially, one-way transit times to and from the Moon on the order of ~72 hr would be normal. Eventually, however, as lunar outposts grow into permanent settlements staffed by visiting scientists, engineers, and administrative personnel representing both government and private ventures, more frequent flights of shorter duration could become commonplace. As shown in Figure 16, cutting the Earth-Moon transit time in half to ~36 hr requires increasing the total mission ΔV budget by ~30% (from ~8.7 to 11.3 km/s). As a result, versatile LANTR engines with adequate supplies of LLO_2 and LLH_2 for refueling will be key to ensuring LTVs of reasonable size.

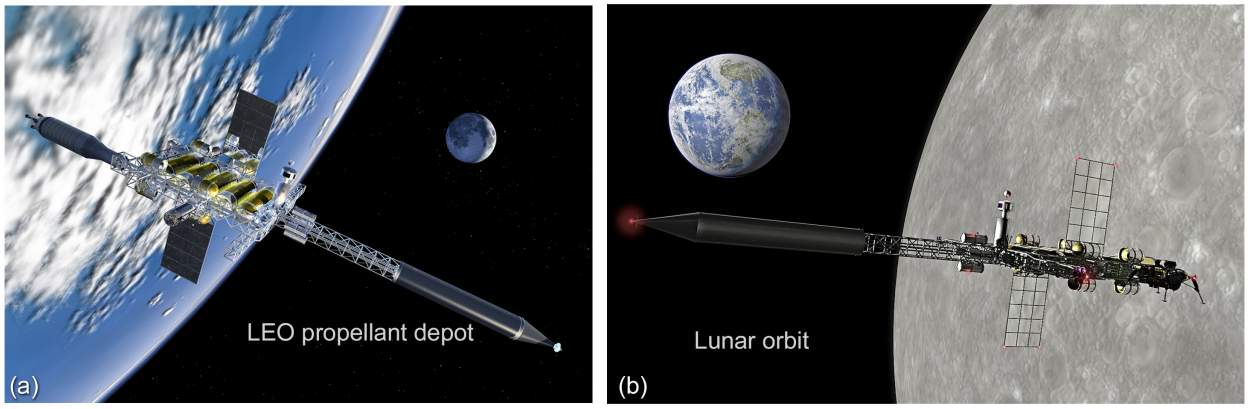

Figure 15.—Propellant depots in LEO and lunar orbit: critical elements for a robust lunar transportation system.

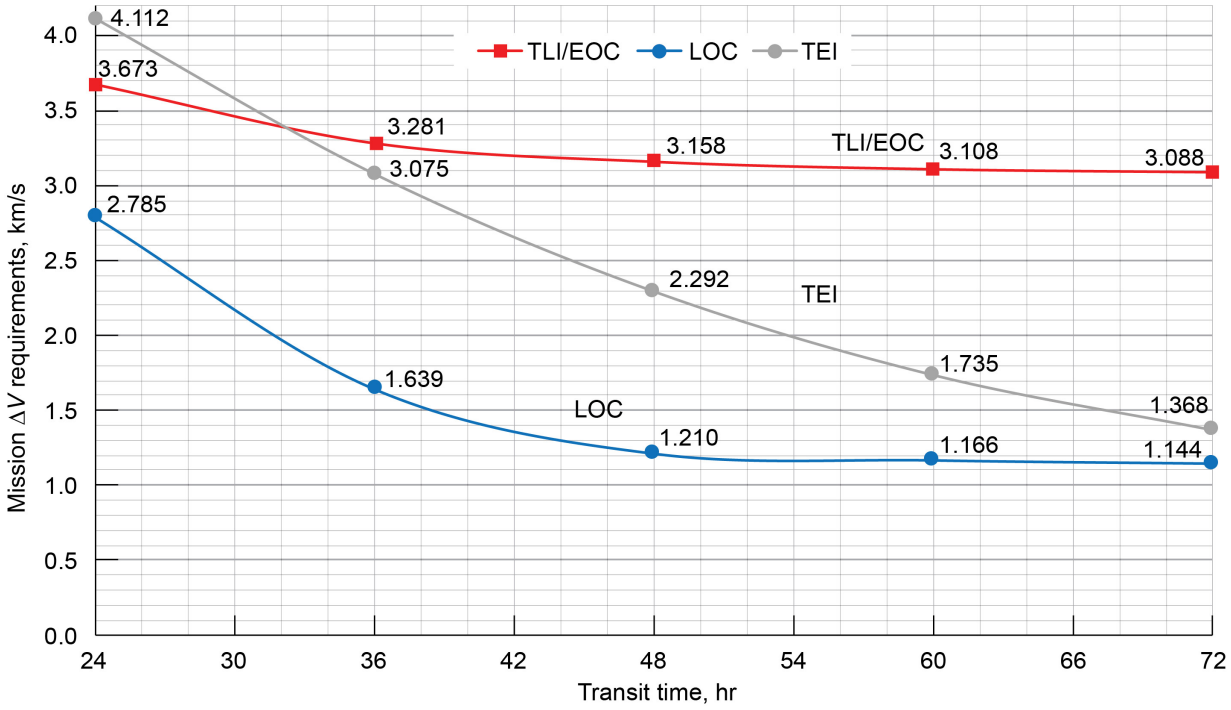

Figure 16.—Variation of primary-maneuver ΔV values with flight time. Note: transit times shown do not include the additional 2.5 hr needed for capture and departure, plane change, and circularization burns needed to access LPO.

7.0 *Conestoga*—A Reusable, Space-Based Crewed Cargo Transport

The original Conestoga wagon was a freight wagon developed in Lancaster County, Pennsylvania, in the early 1700s (Ref. 57) and used extensively in Pennsylvania and the nearby states of Maryland, Ohio, and Virginia for more than 150 years. It was designed for hauling heavy loads—up to 6 t—and had a distinctive bed that was curved upward at both ends to prevent the wagon's contents from shifting or falling out while traveling over rough roads. A white canvas cover protected the wagon's contents from inclement weather, and a team of four to six strong horses pulled the wagon some 12 to 14 miles each day (Fig. 17).

Named after its earlier ancestor, the *Conestoga* CCT shown in Figure 18 is a space-based, reusable LTV that uses LANTR propulsion and refuels with LDP. *Conestoga* has its own dedicated habitat module that supports a crew of four and has a mass of ~10 t. Two crewmembers operate the vehicle and manage the unloading of the PL. The other two represent rotating crewmembers on assignment at the lunar base or the LPO propellant depot. Connecting the habitat module to the rest of the LANTR LTV is a four-sided star truss that has four PL pallets attached to it, each weighing up to ~2.5 t. To accommodate the wedge-shaped geometry of the cargo pallets, the sides of the star truss are concave—a feature similar to the upward curving ends of the Conestoga wagon's bed, although not for the same design reason. Attached to the star truss's forward circular ring is a RMS with twin arms that are free to move around the ring's outer perimeter (Fig. 18). Using the habitat module's rear viewing window, the crew uses these manipulator arms to unload and attach the *Conestoga's* cargo to either the depot or to a co-orbiting LDAV transferring crew and awaiting cargo delivery. Key features and dimensions of the *Conestoga* are shown in Figure 19, and major mission activities are shown in Figure 20.

Figure 17.—Conestoga wagons, the "ships of inland commerce," were used from 1700s to early 1900s to transport settlers, farm produce, and freight across Pennsylvania and neighboring states (image ca. 1910). Courtesy of Landis Valley Village & Farm Museum, Pennsylvania Historical Museum Commission.

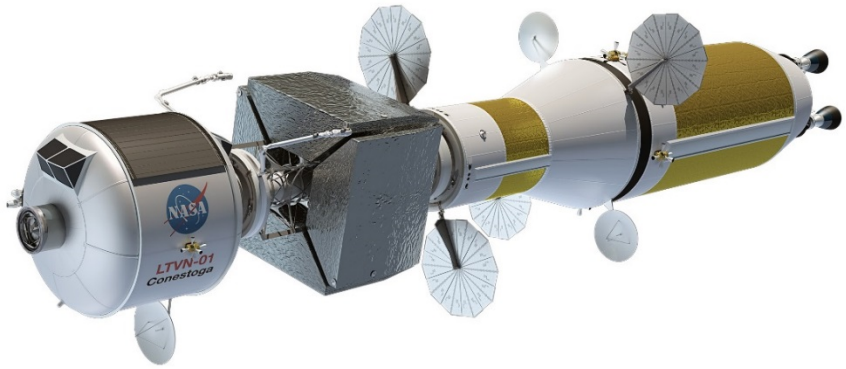

Figure 18.—*Conestoga*: space-based crewed cargo transport, using common NTPS and in-line LO_2 tank.

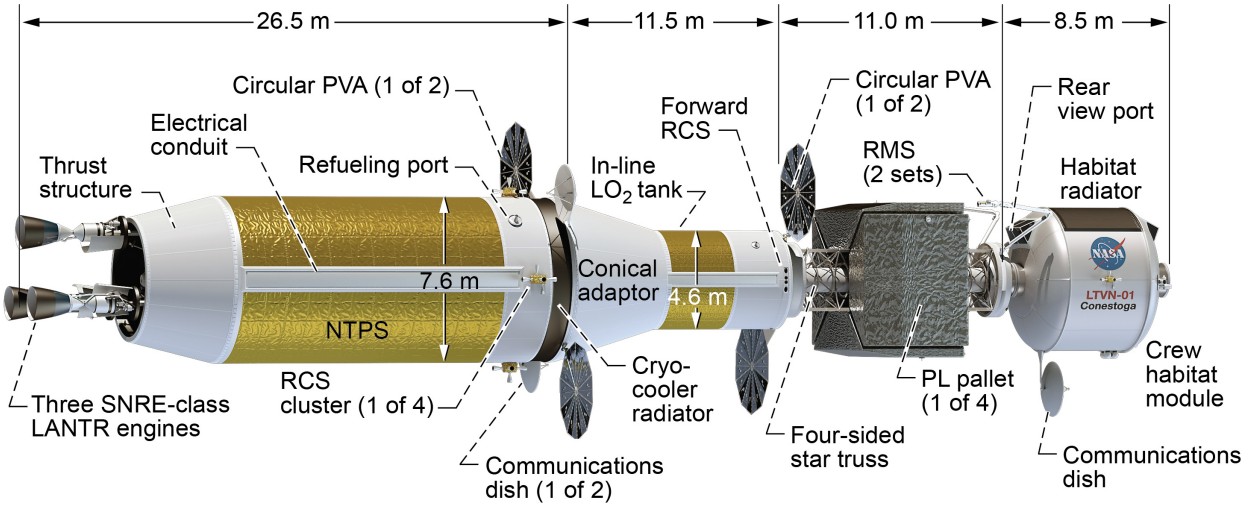

Figure 19.—Key features and dimensions of *Conestoga* crewed cargo transport.

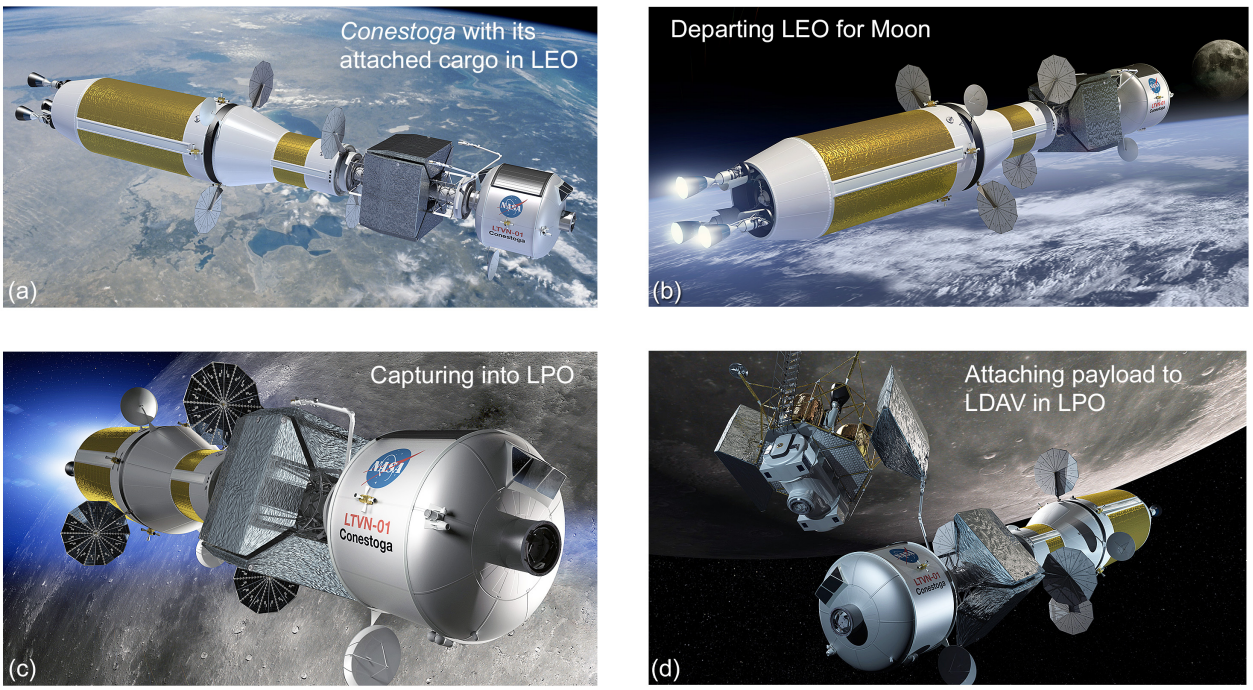

Figure 20.—*Conestoga* crewed cargo transport mission: LEO, outbound, and LPO operations.

The *Conestoga* CCT is a versatile vehicle that can deliver varying amounts of cargo (from 10 to 40 t) to lunar orbit depending on the transit times out and back. Once loaded with cargo and propellant from the LEO transportation node and depot (Fig. 20(a)), the *Conestoga* leaves orbit for the Moon (Fig. 20(b)). After LOC (Fig. 20(c)) and maneuvering into LPO, the *Conestoga* unloads its cargo at the depot or can attach it directly to a waiting LDAV using the vehicle's RMS (Fig. 20(d)). Outfitted with refueling appendages, the *Conestoga* can also function as a tanker capable of transferring some of the LH_2 from its NTPS to the depot or supplying it directly to the LDAV. Refueling ports and twin PVAs are located at the forward ends of both the NTPS and in-line LO_2 tank assembly for refueling in LEO and lunar orbit and for powering the NTPS and forward PL element as shown in Figure 19.

In this study, *Conestoga's* NTPS is limited to a launch mass of ~70 t, which includes ~39.8 t of LH_2 propellant. In a previous study (Ref. 27), the LANTR-based LTVs operated out of equatorial LLO and used only LUNOX for refueling. *Conestoga's* LH_2 propellant loading was fixed so the outbound and return O/H MRs used by the LANTR engines were optimized to achieve the desired propulsion performance required to satisfy the particular mission objectives. Here, however, Conestoga's NTPS can top off its propellant tank with the excess LH_2 produced during the water electrolysis process. This ability to refuel with both LLO_2 and LLH_2 (albeit limited to an 8:1 ratio) provides an added degree of operational and mission flexibility that is not available to LANTR-based LTVs using LUNOX alone.

Table IV provides a comparison of crewed cargo missions to LLO and LPO with different delivered payloads and trip times along with the associated IMLEO and LDP refueling requirements. All the cases shown use the same common NTPS and in-line LO_2 tank assembly as that shown in Figures 19 and 20. Case 1 shows the performance and refueling requirements for the baseline *Conestoga* CCT discussed in a previous study (Ref. 27). Operating between LEO and equatorial LLO, *Conestoga* was configured to deliver twice the PL (10 t) to LLO in half the time (36 hr instead of 72 hr). To meet these demanding mission objectives with a fixed LH_2 propellant loading in the NTPS of ~39.8 t, *Conestoga's* in-line LO_2 tank (~4.6-m OD and 7.95-m L) is sized to hold ~111.2 t of LO_2 at mission start, and its LANTR engines are operated "O_2 rich" on both the outbound mission leg (O/H MR ~5, I_{sp} ~516 s for TLI; MR ~4.1, I_{sp} ~550 s for LOC) and return mission leg (MR ~5, I_{sp} ~516 s for both the TEI and EOC burns).

After dropping off its cargo and picking up 250 kg of lunar samples, *Conestoga* refuels with ~74.9 t of LLO_2 for the trip back to LEO. For this mission, *Conestoga* has an IMLEO of ~214.3 t consisting of the NTPS (~71 t), the in-line LO_2 tank and conical adaptor (~117.2 t), the star truss assembly with its RMS (~5.3 t) and attached PL (10 t), the habitat module (9.9 t), consumables (~0.1 t) plus the two crew and two passengers with their EVA suits (~0.8 t). The total mission ΔV to go from LEO to LLO and back again is ~9.92 km/s, including g-losses. With the augmented thrust levels provided by the LANTR engines (~56.8 klb_f per engine at MR ~5), the burn times for the individual maneuvers are ~11.5 min (TLI), ~3.8 min (LOC), ~4.4 min (TEI), and ~5.6 min (EOC), totaling ~25.3 min. This total burn time is essentially fixed by the available amount of LH_2 in the NTPS and the LH_2 flow rate for each engine of ~8.3 kg/s. What varies in this case (as well as in Cases 4 and 7) is the amount of LO_2 supplied in LEO and LLO and the different MRs used by the LANTR engines to achieve the specified mission objectives.

Case 2 shows the impact on *Conestoga* performance and refueling when operating out of LPO instead of LLO. Despite access to ~11.4 t of top-off LLH_2, *Conestoga's* refueling requirements for the same mission scenario are increased by ~27.7 t (102.7 t of LLO_2 and LLH_2 versus ~75 t of LLO_2 (LUNOX) when operating out of LLO and using only ELH_2). The LANTR engines operate at O/H MRs of 5.0 (TLI), 5.0 to 3.5 (LOC and TEI), and 2.6 (EOC). The IMLEO for this mission is ~216.4 t, and the total mission ΔV increases to ~11.428 km/s, which is attributed to the higher ΔV values required for the shorter 2.5-hr LOC and TEI maneuvers. The total engine burn time for Case 2 also increases to ~32.7 min, 7.4 min longer than in Case 1 since the LANTR engines now have to provide a larger ΔV increment to the *Conestoga* and have additional refuel LH_2 available to use.

As the mining and processing of LPI for propellant production increases, one might choose to minimize the total propellant requirements for the mission (both in LEO and LPO) by relying more heavily on LDPs especially if LEO launch costs remain high. Using this strategy, Case 3 illustrates that it is possible to reduce the amount of LEO-supplied LO_2 required for the same cargo delivery and mission trip time by ~31.8%—from ~111.2 to ~75.8 t—by leveraging the greater availability of LLO_2 and LLH_2, which in this case is ~121.9 t at an 8:1 ratio. For this case, the *Conestoga's* LANTR engines run at low O/H MRs on the outbound mission leg and O_2 rich on the inbound leg. The IMLEO for Case 3 drops by ~35.5 to ~180.9 t, but the total mission burn time increases to ~34.1 min, which is again due to the availability of additional LH_2 for the LANTR engines to use.

TABLE IV.—LANTR CREWED CARGO MISSIONS, TRAJECTORY AND ΔV BUDGETS, AND LDP REFUELING NEEDS[a]

Case description[b]	Objective	Trajectory and orbits[c]	In-line LO_2 tank	Results
1. LANTR crewed cargo transport (CCT) •9.9-t habitat module •11-m star truss •Carry 10 t cargo to LLO	Determine LLO_2 refueling needed to deliver 10 t cargo to LLO, cutting transit times to 36 hr	36-hr one-way transit times LEO → LLO → LEO ΔV ~9.920 km/s	4.6-m OD by ~7.95-m L (~111.2 t LO_2)	IMLEO ~214.3 t ~111.2 t LO_2 supplied in LEO ~74.9 t LLO_2 refueling in LLO
2. LANTR CCT •9.9-t habitat module •11-m star truss •Carry 10 t cargo to LPO	Determine LLO_2 and LLH_2 refueling needed to deliver 10 t cargo to LPO, cutting transit times to 36 hr	36-hr one-way transit times LEO → LPO → LEO ΔV ~11.428 km/s	4.6-m OD by ~7.95-m L (~111.2 t LO_2)	IMLEO ~216.4 t ~111.2 t LO_2 supplied in LEO ~91.3 t LLO_2 refueling in LPO ~11.4 t LLH_2 refueling in LPO
3. LANTR CCT •9.9-t habitat module •11-m star truss •Carry 10 t cargo to LPO	Minimize LEO LO_2 and LLO_2 refueling needed to deliver 10 t cargo to LPO, cutting transit times to 36 hr	36-hr one-way transit times LEO → LPO → LEO ΔV ~11.421 km/s	4.6-m OD by ~7.95-m L (~111.2 t LO_2)	IMLEO ~180.9 t ~75.8 t LO_2 supplied in LEO ~108.4 t LLO_2 refueling in LPO ~13.5 t LLH_2 refueling in LPO
4. LANTR CCT •9.9-t habitat module •Two 11-m star trusses •Carry 20 t cargo to LLO	Determine LLO_2 refueling needed to deliver 20 t cargo to LLO with transit times of 72 hr	72-hr one-way transit times LEO → LLO → LEO ΔV ~8.057 km/s	4.6-m OD by ~7.95-m L (~111.2 t LO_2)	IMLEO ~189.6 t ~71.0 t LO_2 supplied in LEO ~52.1 t LLO_2 refueling in LLO
5. LANTR CCT •9.9-t habitat module •Two 11-m star trusses •Carry 20 t cargo to LPO	Determine LLO_2 and LLH_2 refueling needed to deliver 20 t cargo to LPO with transit times of 72 hr	72-hr one-way transit times LEO → LPO → LEO ΔV ~8.393 km/s	4.6-m OD by ~7.95-m L (~111.2 t LO_2)	IMLEO ~233 t ~111.2 t LO_2 supplied in LEO ~31.6 t LLO_2 refueling in LPO ~3.95 t LLH_2 refueling in LPO
6. LANTR CCT •9.9-t habitat module •Two 11-m star trusses •Carry 20 t cargo to LPO	Minimize LEO LO_2 and LLO_2 refueling needed to deliver 20 t cargo to LPO with transit times of 72 hr	~72-hr one-way transit times LEO → LPO → LEO ΔV ~8.381 km/s	4.6-m OD by ~7.95-m L (~111.2 t LO_2)	IMLEO ~178.5 t ~56.4 t LO_2 supplied in LEO ~54.4 t LLO_2 refueling in LPO ~6.80 t LLH_2 refueling in LPO
7. LANTR CCT •9.9-t habitat module •Two 11-m star trusses •Carry 40 t cargo to LLO	Determine LLO_2 refueling needed to deliver 40 t cargo to LLO with transit times of 72 hr	72-hr one-way transit times LEO → LLO → LEO ΔV ~8.064 km/s	4.6-m OD by ~7.95-m L (~111.2 t LO_2)	IMLEO ~250.7 t ~109.8 t LO_2 supplied in LEO ~60.3 t LLO_2 refueling in LLO
8. LANTR CCT •9.9-t habitat module •Two 11-m star trusses •Carry 40 t cargo to LPO	Determine LLO_2 and LLH_2 refueling needed to deliver 40 t cargo to LPO with transit times of 72 hr	72-hr one-way transit times LEO → LPO → LEO ΔV ~8.393 km/s	4.6-m OD by ~7.95-m L (~111.2 t LO_2)	IMLEO ~255.6 t ~111.2 t LO_2 supplied in LEO ~47.8 t LLO_2 refueling in LPO ~5.98 t LLH_2 refueling in LPO
9. LANTR CCT •9.9-t habitat module •Two 11-m star trusses •Carry 40 t cargo to LPO	Minimize LEO LO_2 and LLO_2 refueling needed to deliver 40 t cargo to LPO with transit times of 72 hr	~72-hr one-way transit times LEO → LPO → LEO ΔV ~8.381 km/s	4.6-m OD by ~7.95-m L (~111.2 t LO_2)	IMLEO ~238 t ~93.5 t LO_2 supplied in LEO ~57.1 t LLO_2 refueling in LPO ~7.14 t LLH_2 refueling in LPO

[a]Acronyms and symbols are defined within report and in appendix.

[b]Cases use common LH_2 NTPS (7.6-m OD by ~15.7-m L). Propellant depots are assumed in LEO, LPO, and LLO. LANTR engines use optimized O/H MRs out and back.

[c]Altitude: 407 km (LEO) and 300 km (LPO and LLO, equatorial). Total round-trip mission ΔV values shown include 2.5-hr LPO insertion maneuvers plus g-losses.

By extending one-way transit times to 72 hr, Case 4 shows that a *Conestoga*-class vehicle can double the amount of cargo delivered to equatorial LLO from 10 to 20 t. The *Conestoga-II*, shown in Figure 21, is a heavy CCT that adds a second 11-m-long star truss and RMS and four more 2.5-t PL pallets to the baseline vehicle configuration. This addition results in an increase in the vehicle's overall length from ~57.5 to ~68.5 m. Departing LEO with 71 t of LO_2, *Conestoga-II's* LANTR engines are run at an O/H MR of ~3.4 and I_{sp} of ~573 s. During LOC, the engines operate at a low MR of ~0.9 and I_{sp} of ~737 s. Once in orbit, the crew unloads the forward PL pallets first. This allows an unobstructed view of the rear PL section from the habitat module's rear viewing port during the unloading process. After picking up samples, the *Conestoga-II's* LO_2 tank is refueled with ~52.1 t of LLO_2. On the return leg of the mission, the engines operate at MR ~4.7 and I_{sp} ~527 s during the TEI maneuver. For EOC, the engines operate at MR ~3.8 and I_{sp} ~558 s. The total mission ΔV is ~8.06 km/s, and the total burn time on the engines is ~25.3 min, again determined by the available amount of LH_2 in *Conestoga-II's* NTPS.

In Cases 5 and 6, the *Conestoga-II* operates out of LPO and is able to refuel with both LLO_2 and LLH_2. Case 5 minimizes LDP usage (~35.6 t) at the expense of an increased LEO LO_2 loading (~111.2 t) and IMLEO (~233 t). In Case 6, LDP usage is increased, and the *Conestoga-II's* LANTR engines operate with low MR values outbound and higher values inbound. The result is a reduction in the amount of LEO-supplied LO_2 down to ~56.4 t and a decrease in the vehicle IMLEO to ~178.5 t. The amount of refuel LLO_2 and LLH_2 is ~61.2 t, again supplied at an 8:1 ratio.

Case 7 pushes the *Conestoga-II's* cargo delivery capability to LLO to its limit for the amount of LH_2 and LO_2 propellant available in the NTPS and in-line LO_2 tank. Assuming 72-hr transit times, this limit is ~40 t (eight 5-t PL pallets). For this mission, the LO_2 loading at LEO departure is ~109.8 t (~98.5% of the tank's maximum capacity), and the LANTR engines are operated at O/H MR ~4.4, I_{sp} ~536 s (TLI) and MR ~3.3, I_{sp} ~578 s (LOC). On the return leg, the *Conestoga-II* is refueled with ~60.3 t of LLO_2, and its engines are operated at MR ~5, I_{sp} ~536 s (TEI) and MR ~4.8, I_{sp} ~522 s (LOC). These MR conditions were selected by the optimizer to deliver the specified PL while also minimizing the total LO_2 requirement for the mission. The IMLEO for Case 7 is ~250.7 t, and the total mission ΔV and engine burn time are ~8.06 km/s and ~25.3 min, respectively.

In Cases 8 and 9, the *Conestoga-II* delivers its 40 t PL to LPO and then refuels with both LLO_2 and LLH_2. Case 8 minimizes LDP usage (~53.8 t) at the expense of increased LEO LO_2 loading (~111.2 t) and IMLEO (~255.6 t). In Case 9, LDP usage is again increased leading to a reduction in LEO-supplied LO_2 down to ~93.5 t and a decrease in the vehicle IMLEO to ~238 t. The amount of refuel LLO_2 and LLH_2 used on the return mission leg is ~64.3 t, and the total engine burn time is just short of 30 min.

The *Conestoga*-class CCTs shown in Figure 22 departing LEO for the Moon can provide the basis for a robust and flexible LTS that offers a wide range of cargo delivery capability and transit times made possible through the use of LANTR propulsion and supplies of LDP provided at transportation nodes and/or propellant depots located in lunar orbit. Today, "time is money" for the long-distance freight haulers traveling our highways, oceans, and skies. In the future, *Conestoga*-class vehicles could play the same important role in establishing cislunar trade and commerce as the Conestoga wagons of old did for more than a century throughout Pennsylvania and its neighboring states.

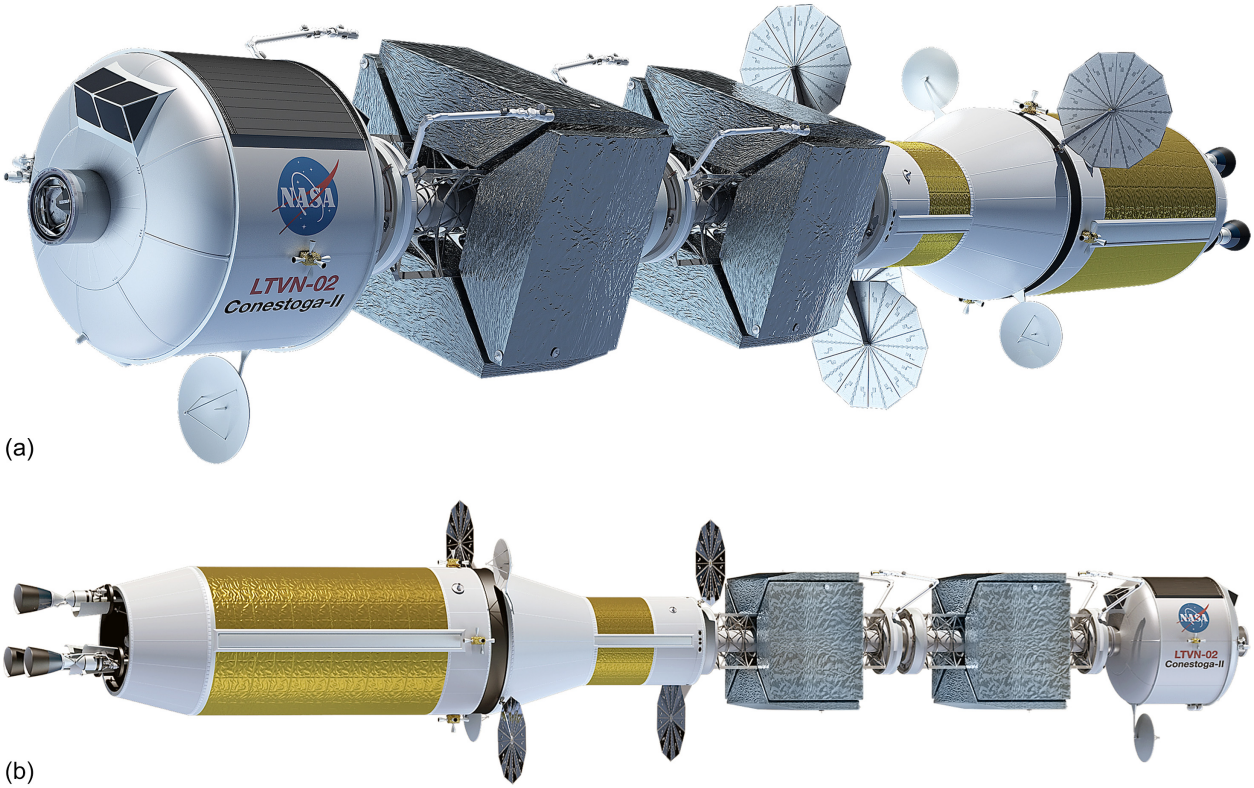

Figure 21.—*Conestoga-II* heavy crewed cargo transport isometric and elevation views.

Figure 22.—*Conestoga*-class crewed cargo transports departing LEO for Moon.

8.0 Feasibility of Commuter Shuttle Missions to the Moon

In the movie "2001: A Space Odyssey," released by MGM in 1968 (Ref. 58), Dr. Heywood Floyd departs from a huge artificial gravity space station orbiting Earth bound for the Moon. He arrives there 24 hr later (Ref. 59) aboard a large spherical-shaped LTV called *Ares*, which touches down on a landing pad that subsequently descends to a large sprawling lunar settlement located underground. Today, 50 years later, the images portrayed in Stanley Kubrick and Arthur C. Clarke's film remain well beyond our capabilities and "2100: A Space Odyssey" seems a more appropriate title for the movie. In this section, the feasibility and requirements for commuter flights to the Moon using LANTR propulsion and LDPs are evaluated to see if the operational capabilities presented in "2001: A Space Odyssey" can be achieved, albeit on a more "Spartan" scale.

A 24-hr commuter flight to the Moon is a daunting challenge. This is about the time it now takes to fly from Washington, DC, to Melbourne, Australia, with a 3-hr layover in San Francisco. As Figure 16 shows, decreasing the Earth-to-Moon transit time from 72 to 24 hr increases the outbound ΔV requirement from ~4.2 to 6.5 km/s and the total roundtrip ΔV requirement by ~5.6 km/s. Increasing the flight time from 24 to 36 hr each way decreases this additional ΔV requirement by ~3 km/s, down to ~2.6 km/s. Also, at these higher velocities free-return trajectories are no longer available, so multiple engines will be required to improve reliability and increase passenger safety.

How might a typical commuter flight to the Moon proceed? A possible scenario starts with passengers boarding a future Earth-to-orbit shuttle for a flight to a future commercial artificial gravity station (AGS) shown in Figure 23(a). There they would enter a PTM containing its own life support, power, instrumentation and control systems, and RCS. The PTM provides the "brains" for the LANTR-powered shuttle and is home to the 18 passengers and 2 crewmembers operating it while on route to the Moon. After departing the AGS (Fig. 23(b)), the PTM docks with the fueled LANTR shuttle awaiting it a safe distance away (Fig. 24(a)). At the appropriate moment, the LANTR engines are powered up, and the shuttle climbs rapidly away from Earth (Fig. 24(b)). For a 36-hr flight to the Moon, the acceleration experienced by the passengers during Earth departure will range from ~0.37g at the start of the burn to ~0.66g near the end of the TLI burn.

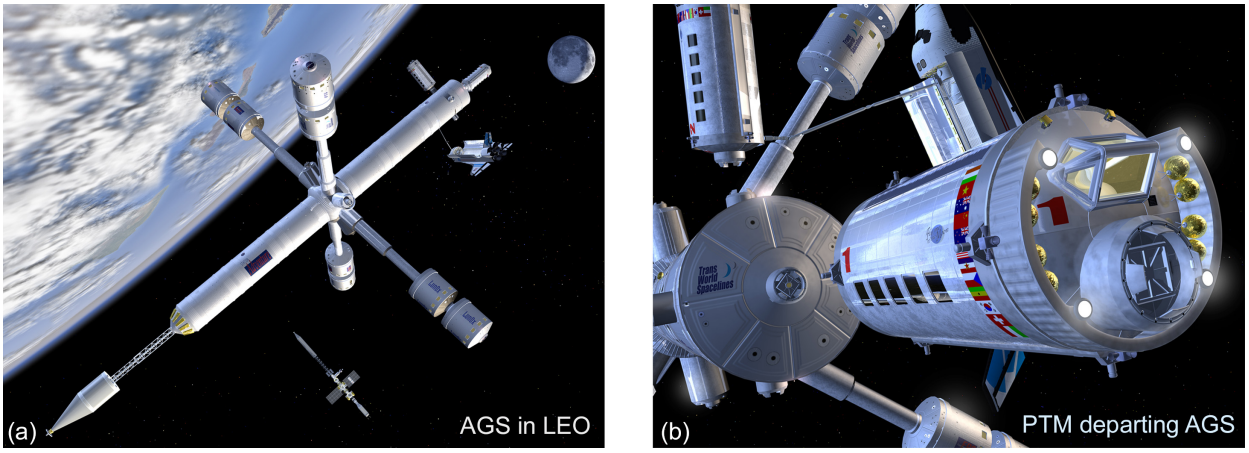

Figure 23.—Future commercial artificial gravity station (AGS) provides transportation hub for PTMs arriving and departing from LEO.

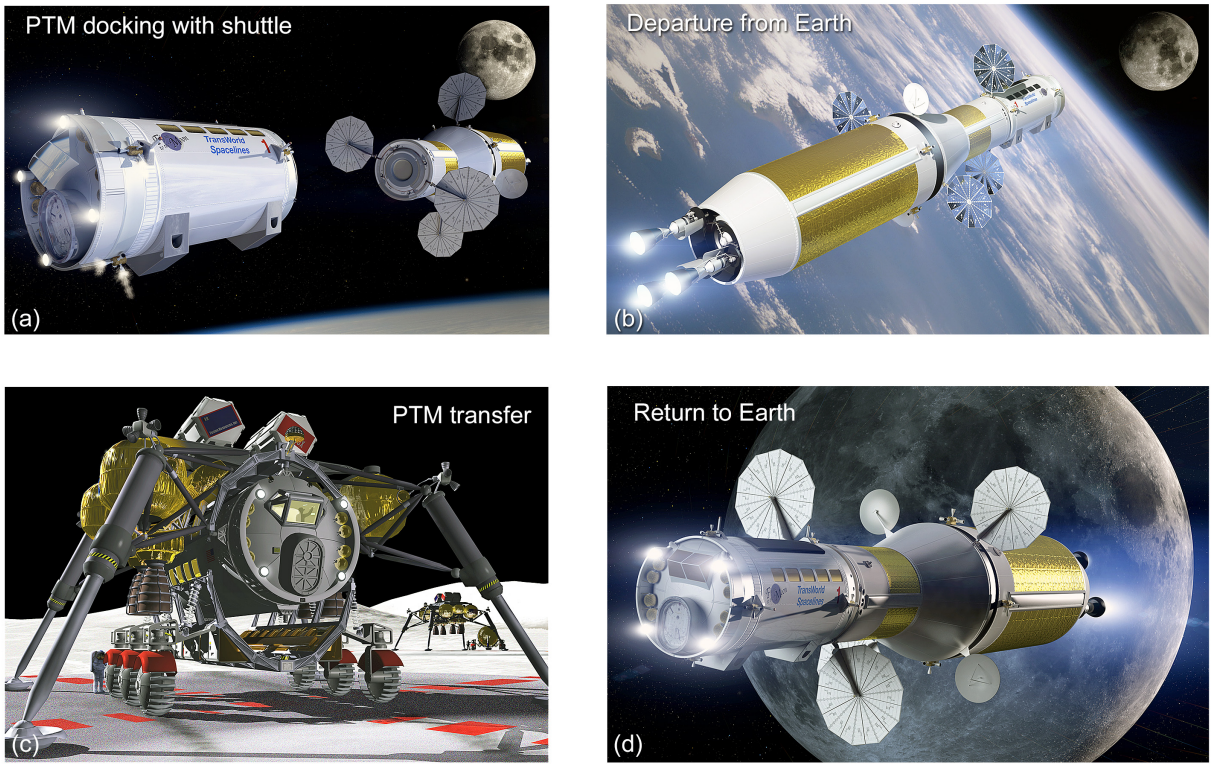

Figure 24.—Various phases of LANTR commuter shuttle mission to Moon.

Following the 36-hr transfer and additional 2.5 hr for the LANTR shuttle to maneuver into LPO, the PTM detaches and docks with a waiting Sikorsky-style LLV. A commercial propellant depot (Fig. 15(b)) provides a convenient staging node for lunar orbit operations supplying the LANTR shuttle with LDP for Earth return and the LLV with supplemental ELH_2 needed to deliver the PTM to the LS. From here the PTM is lowered to a flatbed surface vehicle (Fig. 24(c)) and electronically engaged, providing the PTM with surface mobility. The PTM then drives itself to the lunar base airlock for docking and passenger unloading. This scenario is reversed on return trip to Earth (Fig. 24(d)). At the end of the flight, the passengers will also experience a bit of excitement as the deceleration force builds from ~0.68g initially to ~1.25g at the end of the LEO capture burn.

The commercial commuter shuttle envisioned here utilizes the same NTPS, LANTR engines, and in-line LO_2 tank assembly used on the *Conestoga* CCT shown in Figure 19. For the commuter shuttle application, the CCT's habitat module, star truss, and PL pallets are removed and replaced with a 20-person PTM (shown in Fig. 25). The fully loaded PTM has an estimated mass of ~15 t, and its OD and length are ~4.6 and ~8 m, respectively.

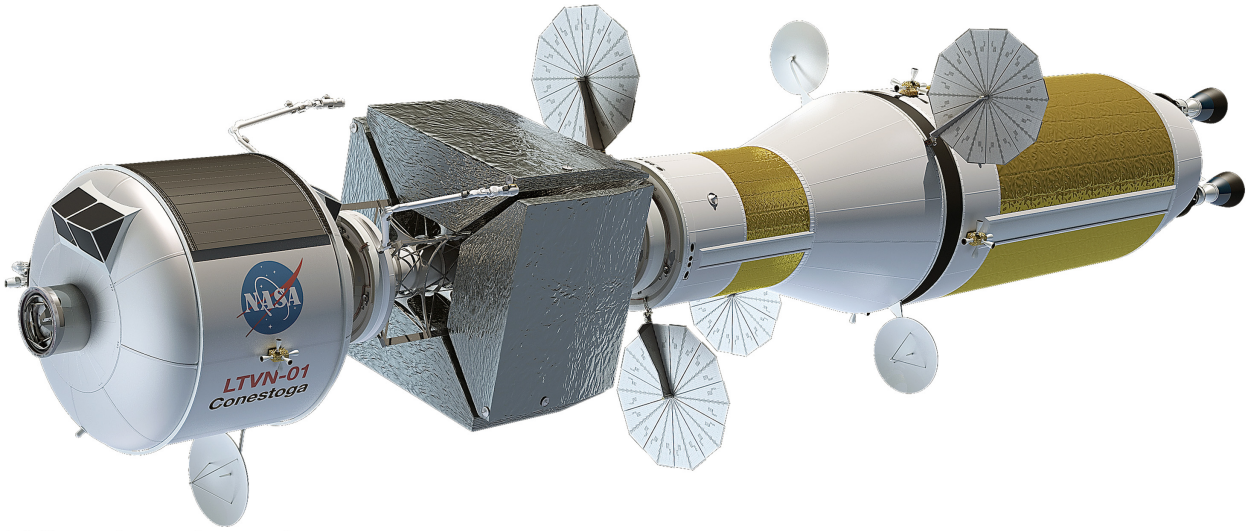

(a) Crewed cargo transport.

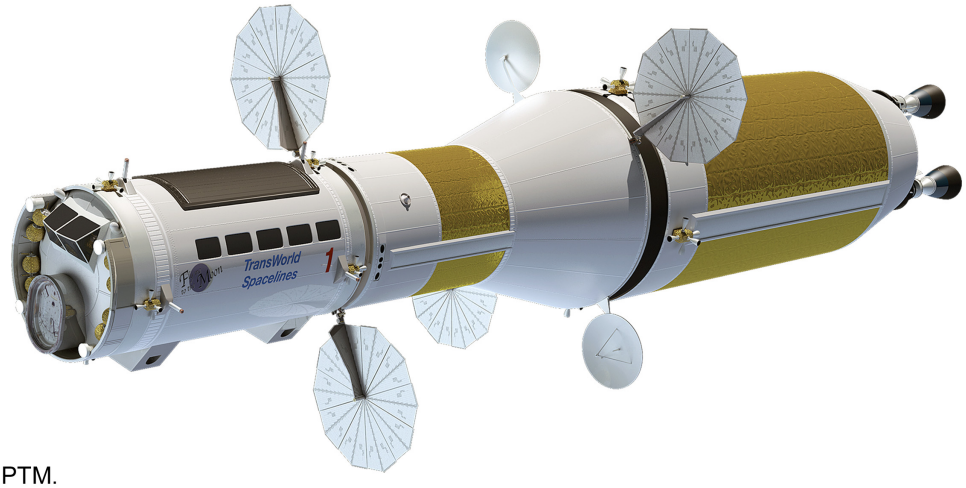

(b) Commuter shuttle with PTM.

Figure 25.—Relative sizes of *Conestoga* CCT and commuter shuttle using same NTPS and in-line LO_2 tank assembly.

Table V provides a sampling of the different LANTR shuttle missions to LLO and LPO considered in this study. These missions looked at transit times ranging from 36 to 24 hr along with the LDP refueling requirements needed to achieve these trip times. Cases 1 through 6 use the same NTPS, clustered LANTR engines and in-line LO_2 tank assembly used on the *Conestoga*-class vehicles shown in Figure 22. In Case 1, the PTM is transported to and from LLO with one-way transit times of 36 hr. The optimization feature in the MAMA code is used to minimize the LO_2 resupply in LEO by increasing the use of LLO_2 refueling for the return to Earth. Supplied with just over 76 t of LO_2 prior to TLI, the shuttle's engines operate at low O/H MRs on the outbound leg (~3.9 for TLI and ~1.7 for LOC), requiring more LH_2 to be consumed. On the return leg, the LANTR engines operate O_2 rich (O/H MR ~5 for TEI and ~4.9 for EOC), so the LLO_2 refueling requirement is ~72.8 t. The mission IMLEO is ~168.2 t, which includes the NTPS (~71 t), the in-line LO_2 tank assembly and conical adaptor (~82.2 t), and the PTM (15 t). The total mission ΔV is ~9.914 km/s, and the total engine burn time is ~25.3 min, which includes the following individual burn times: ~10.5 min (TLI), ~5.0 min (LOC), ~4.3 min (TEI), and ~5.5 min (EOC).

TABLE V.—LANTR COMMUTER SHUTTLE OPTIONS, TRIP TIME AND ΔV BUDGETS, AND LDP REFUELING NEEDS[a]

Case description[b]	Objective	Trajectory and orbits[c]	In-line LO_2 tank	Results
1. LANTR commuter shuttle carrying 15-t passenger transport module (PTM) to LLO then back to LEO	Minimize LEO LO_2 refueling needed to deliver 15-t PTM to and from LLO with transit times of 36 hr	36-hr one-way transit times LEO → LLO → LEO ΔV ~9.914 km/s	4.6-m OD by ~7.95-m L (~111.2 t LO_2)	IMLEO ~168.2 t ~76.1 t LO_2 supplied in LEO ~72.8 t LLO_2 refueling in LLO
2. LANTR commuter shuttle carrying 15-t PTM to LPO then back to LEO	Minimize LEO LO_2 and LLO_2 refueling needed to deliver 15-t PTM to and from LPO with transit times of 36 hr	36-hr one-way transit times LEO → LPO → LEO ΔV ~11.420 km/s	4.6-m OD by ~7.95-m L (~111.2 t LO_2)	IMLEO ~147.0 t ~53.4 t LO_2 supplied in LEO ~104.0 t LLO_2 refueling in LPO ~13.0 t LLH_2 refueling in LPO
3. LANTR commuter shuttle carrying 15-t PTM to LPO then back to LEO	Minimize LEO LO_2 and LLO_2 refueling needed to deliver 15-t PTM to and from LPO with transit times of 33.5 hr	33.5-hr one-way transit times LEO → LPO → LEO ΔV ~11.807 km/s	4.6-m OD by ~7.95-m L (~111.2 t LO_2)	IMLEO ~168.9 t ~75.5 t LO_2 supplied in LEO ~104.0 t LLO_2 refueling in LPO ~13.0 t LLH_2 refueling in LPO
4. LANTR commuter shuttle carrying 15-t PTM to LLO then back to LEO	Determine LLO_2 refueling needed to deliver PTM to and from LLO with shortest transit times	32.8-hr one-way transit times LEO → LLO → LEO ΔV ~10.481 km/s	4.6-m OD by ~7.95-m L (~111.2 t LO_2)	IMLEO ~203.3 t ~111.1 t LO_2 supplied in LEO ~80.4 t LLO_2 refueling in LLO
5. LANTR commuter shuttle carrying 15-t PTM to LPO then back to LEO	Determine LLO_2 and LLH_2 refueling needed to deliver PTM to and from LPO with shortest transit times	30.6-hr one-way transit times LEO → LPO → LEO ΔV ~12.423 km/s	4.6-m OD by ~7.95-m L (~111.2 t LO_2)	IMLEO ~204.5 t ~111.1 t LO_2 supplied in LEO ~109.0 t LLO_2 refueling in LPO ~13.63 t LLH_2 refueling in LPO
6. LANTR commuter shuttle carrying 15-t PTM to LPO then back to LEO	Determine LLO_2, LLH_2, and ELH_2 refueling needed to deliver PTM to and from LPO with shortest transit times	25-hr one-way transit times LEO → LPO → LEO ΔV ~13.982 km/s	4.6-m OD by ~7.95-m L (~111.2 t LO_2)	IMLEO ~206.5 t ~111.2 t LO_2 supplied in LEO ~109.0 t LLO_2 refueling in LPO ~13.63 t LLH_2 refueling in LPO ~14.62 t ELH_2 refueling in LPO

[a]Acronyms and symbols are defined within report and in appendix.
[b]Cases 1 to 6 use common LH_2 NTPS (7.6-m OD by ~15.7-m L). Propellant depots are assumed in LEO, LPO, and LLO. LANTR engines use optimized O/H MRs out and back.
[c]Altitudes: 407 km (LEO), 300 km (LPO and LLO, equatorial). Total round-trip mission ΔV values shown include 2.5-hr LPO insertion and departure maneuver ΔVs plus g-losses.

Case 2 assumes the same 36-hour transit times, but the shuttle now transports the PTM to and from LPO rather than LLO and is able to refuel with both LLO_2 and LLH_2 before returning to LEO. The optimizer also minimizes total LO_2 usage so that the amount of LEO-supplied LO_2 is reduced to ~53.4 t prior to TLI. The LANTR engines run fuel rich on the outbound leg and O_2 rich on the inbound leg, and they refuel with ~104 t of LLO_2 and ~13 t of LLH_2 prior to TEI. The mission IMLEO is ~147 t and includes the NTPS (~71.8 t), the in-line LO_2 tank assembly and conical adaptor (~60.2 t), and the PTM (15 t). With the short 2.5-hr LPO insertion and departure maneuver times used in Case 2, the total mission ΔV increases by ~1.51 km/s to ~11.420 km/s. The total engine burn time also increases by ~8.4 to ~33.7 min, with the additional top-off LLH_2 used by the LANTR engines on the return mission leg.

Case 3 provides a more direct, point-to-point comparison with Case 1 by reducing the transit times to 33.5 hr to take into account the 2.5-hr LPO insertion and departure maneuver times. For this shorter transit time, a higher O/H MR is used on the outbound mission leg so the amount of LEO-supplied LO_2 is increased to ~75.5 t. The shuttle again refuels with ~104 t of LLO_2 and ~13 t of LLH_2 and runs O_2 rich on the inbound leg. The IMLEO increases to ~168.9 t, including the NTPS (~71.7 t), the in-line LO_2 tank assembly (~82.2 t), and the PTM (15 t), and the total mission ΔV increases to ~11.807 km/s. The total engine burn time is again ~33.7 min since the LANTR engines use the same amount of LEO-supplied LH_2 and top-off LLH_2 during the mission. Although Cases 1 and 3 have comparable IMLEO values, Case 3 shows that operating out of LPO instead of LLO requires more LDP production, has a higher total mission ΔV, and requires longer engine burn times for the same point-to-point mission time.

Case 4 focuses on achieving the fastest transit times to and from LLO by taking full advantage of the extra propellant capacity that exists in the vehicle's in-line LO_2 tank. By increasing the commuter shuttle's LO_2 loading to its maximum capacity of ~111.2 t before TLI, refueling with ~80.4 t of LLO_2 before TEI, and operating the LANTR engines O_2 rich (O/H MR = 5) out and back, the shuttle can decrease its one-way transit time from 36 to 32.8 hr. The additional LO_2 loading prior to TLI increases the required IMLEO from ~168.2 t (Case 1) to ~203.3 t, which includes the NTPS (~71 t), the in-line LO_2 tank assembly and adaptor section (~117.3 t), and the PTM (15 t). The decreased transit times increase the total mission ΔV by ~0.567 km/s to ~10.5 km/s. The total mission burn time is ~25.3 min, and the individual burn times are ~11 min (TLI), ~3.5 min (LOC), ~5.1 min (TEI), and ~5.7 min (EOC).

Case 5 is also focused on achieving the fastest transit times, but to and from LPO instead of LLO. Like Case 4, the commuter shuttle's LO_2 tank is filled to near maximum capacity before TLI. It then refuels with ~109 t of LLO_2 and ~13.6 LLH_2 and operates its engines at optimum MRs out to the Moon and back, enabling the shuttle to decrease its one-way transit times from 36 to ~30.6 hr (~33.1 hr when the 2.5-hr-long LPO capture and departure maneuver times are included). The additional LO_2 loading prior to TLI and the higher total mission ΔV (~12.4 km/s) increases the shuttle's IMLEO to ~204.5 t. The extra refueling with top-off LLH_2 also increases the total burn time on the engines to just over ~34 min.

Case 6 is similar to 5 except that it also uses some of the ELH_2 reserved at the LPO depot (for use by water tanker and PTM-delivery LLVs as needed) to supplement the shuttle's NTPS before returning to Earth. By resupplying the three-engine LANTR shuttle with ~111.2 t of LO_2 before TLI; refueling it with ~109 t of LLO_2, ~13.6 t of LLH_2, and ~14.6 t of ELH_2 before TEI; and operating the shuttle's engines at optimum MRs out to the Moon and back, the fastest achievable LEO-to-LPO mission time is ~27.5 hr—close to the 24-hr trip taken by Dr. Floyd in "2001: A Space Odyssey." The IMLEO for Case 6 is ~206.5 t, which includes the NTPS (~72.6 t), the in-line LO_2 tank assembly (~118.9 t), and the PTM (15 t). The total ΔV required for this ~27.5-hr shuttle capability is ~13.982 km/s with g-losses. With the additional LH_2 supplied to the NTPS, the total engine burn time also increases to ~43.5 min, which includes burn times of ~12.8 min (TLI), ~6.6 min (LOC), ~13.1 min (TEI), and ~11.0 min (EOC).

9.0 Estimated Total LDP Mission Needs and Resulting Mining and Processing Requirements

In the last two sections of this report, two different options for obtaining and using LDPs were discussed and compared. In Option 1, LLO_2 or LUNOX is produced from vast volcanic glass deposits located on the lunar nearside and then routinely transported from the LS to a propellant depot in equatorial LLO using reusable tanker LLVs. In Option 2, the focus of this report, LPI deposits are mined and processed to produce lunar water (LH_2O) that is then transported to a LPO depot, again using reusable tanker LLVs. At the depot the LH_2O is electrolyzed to produce both LLO_2 and LLH_2 that is then stored for subsequent use by the LTS elements.

Because of water's composition (8:1 O/H mass ratio), ~1.125 t of LH_2O must be produced and electrolyzed for every ton of LLO_2 required for LTV refueling. Additional water must also be produced to supply the LDP the tanker LLVs need to deliver water to the depot. Because the LLVs use LO_2/LH_2 chemical rockets operating at an O/H MR of ~6, it will be necessary to overproduce water to supply the required amounts of LH_2 needed by the LLVs unless additional ELH_2 is supplied to the depot for their use.

To determine the range of LDP needed at both the orbiting depot and surface LPI mining and processing facility, it is necessary to look at the different LANTR mission types, their transit times, and their frequency of occurrence. The needs of the various LLVs supporting each mission type must also be taken into account. To illustrate this, a LANTR CCT mission is examined. It has an IMLEO of ~143.4 t, employs 72-hr transit times, and flies one mission per month. The CCT delivers 10 t of cargo (four 2.5 t PL pallets) to LPO where it unloads by attaching two of the pallets to a waiting LDAV (shown in Fig. 26). Two LDAV flights are needed to transport the four PL pallets to the LS. After transferring its cargo, the CCT refuels with ~48.9 t of LLO_2 and ~6.1 t of top-off LLH_2 at the depot then returns to LEO. Multiple tanker LLVs based at various polar production facilities supply the depot with the required quantities of LH_2O consistent with the return propellant needs of the CCT.

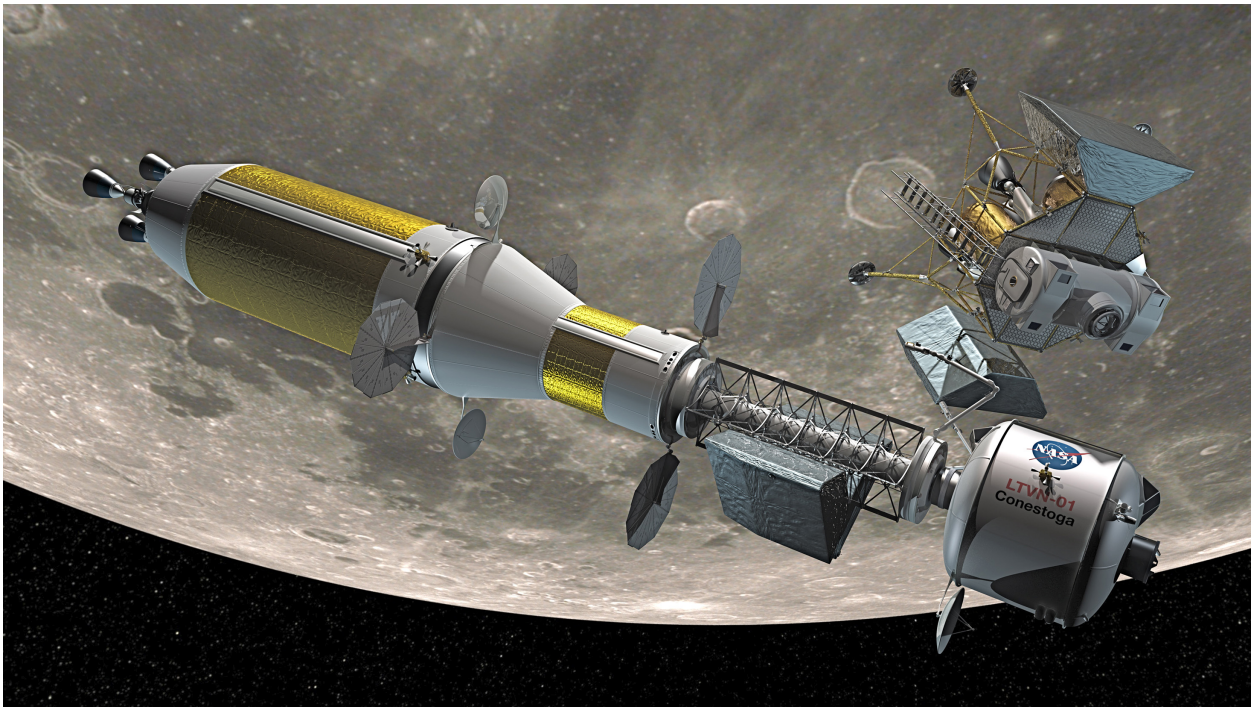

Figure 26.—CCT-to-LDAV cargo transfer operations in LPO.

Supporting monthly CCT flights between LEO and LPO will require an annual LH_2O production rate just over ~2180 t/yr (see Table VI) and the processing of ~62,285 t of polar regolith, assuming an average water ice content in the PSCs of ~3.5 wt%. Approximately 660 t of LH_2O is required by the LANTR CCT and ~519 t by the LDAVs in transporting cargo from LPO to the LS. The required LH_2 propellant for the LDAV's engines on each PL pickup and delivery flight is ~3.2 t. Electrolysis of the ~21.6 t of LH_2O, needed to produce the 19.2 t of LLO_2, however, produces only 2.4 t of excess LLH_2—a shortfall of 0.8 t per LDAV flight. This shortfall is overcome by transferring 1.6 t of ELH_2 from the CCT's NTPS to the depot on each mission for subsequent LDAV usage. This eliminates the need to overproduce on LH_2O by ~173 t/yr, which would be required if the LDAV's entire LH_2 propellant needs for the year (~76.8 t) were to come from water electrolysis alone.

Similarly, ~1002 t of LH_2O must be produced and electrolyzed on the LS for use by three second-generation Sikorsky-style LH_2O tanker LLVs, each flying nine resupply missions to the depot over the course of a year. Each LLV has a dry mass of ~10.9 t and a maximum LH_2/LO_2 propellant capacity just under 40 t. Like the LDAV flights, there is a shortfall of ~1.4 t of LH_2 per LLV flight. Two NTP tanker flights each year can supply the depot with ~57.6 t of ELH_2—more than enough to cover the shortfall for both the crewed LDAV and tanker LLV flights each year. The required electrical power on the depot needed for electrolysis is estimated to be ~0.370 MW_e, with the electrolysis power (MW_e) equal to ~0.2042 × (H_2O electrolysis rate, t/day). The corresponding power levels supporting LDAV and LLV tanker operations at the polar facilities are ~0.29 and ~0.56 MW_e, respectively.

To get an idea what the total LDP needs are for a more ambitious mission, the 36-hr LEO-to-LPO commuter shuttle mission (Case 3 in Table V) is examined. The 36-hr duration includes one-way transit times of 33.5 hr along with 2.5-hr LPO insertion and departure maneuver times. The LDP refueling requirements include ~104 t of LLO_2 and ~13 t of top-off LLH_2. Supporting weekly commuter flights to and from LPO require a dramatic increase in the annual LH_2O production rate to ~18,878 t/yr (see Table VII) and the processing of over ~539,370 t of polar regolith, again assuming an average water ice content of ~3.5 wt%. Approximately 6084 t of LH_2O must be produced, transported to, and electrolyzed at the depot annually to supply the propellant needs of the LANTR shuttles. Electrolyzing ~16.7 t of LH_2O each day will require ~3.4 MW_e from the depot's electrical power system.

On the LS, ~9887 t of LH_2O must be produced and electrolyzed to supply propellant to five Sikorsky-style LH_2O tanker LLVs flying one resupply mission to the LPO depot each week over the course of a year. Another ~2907 t of LH_2O is required to supply propellant to similar Sikorsky-style LLVs that transport arriving and departing PTMs to and from the LS.

As Table VII indicates, there is a LH_2 shortfall between what is produced during LH_2O electrolysis and what is required by the tanker and PTM transport LLVs of ~466 t. If this entire amount were produced from electrolysis of LH_2O, the required annual production rate would increase by ~22% to 23,076 t/yr. The corresponding electrolysis power on the LS would also increase by ~32.7%, from ~7.16 to ~9.5 MW_e.

An alternative to overproducing LH_2O would be to use multiple nuclear electric propulsion tanker vehicles to supply the LH_2 shortfall to the depot. Four tankers operating in a synchronized fashion are envisioned. One tanker loads LH_2 in LEO, and a second tanker unloads it at the LPO depot. During the LEO loading and depot unloading period, the third and fourth tankers would travel to and from the Moon, beginning the cycle again.

Each tanker uses hydrogen magnetoplasmadynamic (MPD) thrusters for propulsion and carries ~160 t of ELH_2 stored in five tanks, each with its own ZBO cryocooler system (see Fig. 27). The MPD thrusters consume ~40 t of LH_2 during the tanker's roundtrip mission to and from the depot. Two fission reactors each with a pair of Brayton conversion units provide multi-MW_e-class power to the tanker, and four right-triangle-shaped, double-sided radiator panels are used to reject waste heat. Separate radiator panels are used for the MPD power processing units (PPUs).

TABLE VI.—TOTAL LDPs and H_2O REQUIRED TO SUPPORT MONTHLY CCT FLIGHTS[a]
[72-hr one-way transits, delivering 10 t cargo and 1.6 t ELH_2 to LPO each flight.]

LANTR CCT	
(48.9 t LLO_2 and 6.1 t LLH_2/mission/month) × (12 months/year):	586.8 t LLO_2/yr
	+ 73.3 t LLH_2/yr
	660.1 t LH_2O/yr
CCT supplied:	(19.2 t ELH_2/yr)
LDAV[b,c]	
(19.2 t LLO_2 and 3.2 t LH_2/flight) × (2 flights/month) × (12 months/year):	460.8 t LLO_2/yr
	+ 57.6 t LLH_2/yr
	518.4 t LH_2O/yr
LH_2 shortfall:	(19.2 t LLH_2/yr)
LLV[b,d]	
(33.0 t LLO_2 and 5.5 t LH_2/flight) × (9 flights/LLV/year) × (3 LLVs):	891.0 t LLO_2/yr
	+ 111.4 t LLH_2/yr
	1002.4 t LH_2O/yr
LH_2 shortfall:	(37.1 t LLH_2/yr)
Total LH_2O production:	2180.9 t/yr
Total ELH_2 required:	37.1 t/yr

[a]Acronyms and symbols are defined within report and in appendix.
[b]O/H MR = 6 and I_{sp} = 450 s. Descent and ascent velocity changes ΔV_{desc} = 2.115 km/s and ΔV_{asc} = 1.985 km/s assumed.
[c]Two crewed LDAVs rendezvous with CCT in LPO; each returns to LS with 5 t of PL.
[d]LLV tanker transports ~25 t of LH_2O to LPO depot; returns to LS with empty 5-t tank.

TABLE VII.—TOTAL LDPs and H_2O REQUIRED TO SUPPORT WEEKLY LEO-TO LPO COMMUTER FLIGHTS[a]
[33.5-hr one-way transits, delivering 15-t, 20-person PTM to LPO each flight.]

LANTR shuttle	
(104 t LLO_2 and 13 t LLH_2/mission/week) × (52 weeks/year):	5408 t LLO_2/yr
	676 t LLH_2/yr
	6084 t LH_2O/yr
LLV[b,c]	
(33.8 t LLO_2 and 5.6 t LH_2/flight) × (1 flight/LLV/week) × (5 LLVs) × (52 weeks/year):	8788 t LLO_2/yr
	1099 t LLH_2/yr
	9887 t LH_2O/yr
LH_2 shortfall:	(357 t ELH_2/yr)
LLV[b,d]	
(49.7 t LLO_2 and 8.3 t LH_2/round-trip flight/week) × (52 weeks/year):	2584 t LLO_2/yr
	+ 323 t LLH_2/yr
	2907 t LH_2O/yr
LH_2 shortfall:	(109 t ELH_2/yr)
Total LH_2O production:	18,878 t/yr
Total ELH_2 required:	466 t/yr

[a]Acronyms and symbols are defined within report and in appendix.
[b]O/H MR = 6 and I_{sp} = 450 s. Descent and ascent velocity changes ΔV_{desc} = 2.115 km/s and ΔV_{asc} = 1.985 km/s assumed.
[c]LLV tanker transports ~25 t of LH_2O to LPO depot; returns to LS with empty 5-t tank.
[d]Total for LLV delivery of PTM from LPO to LS plus PTM return from LS to LPO.

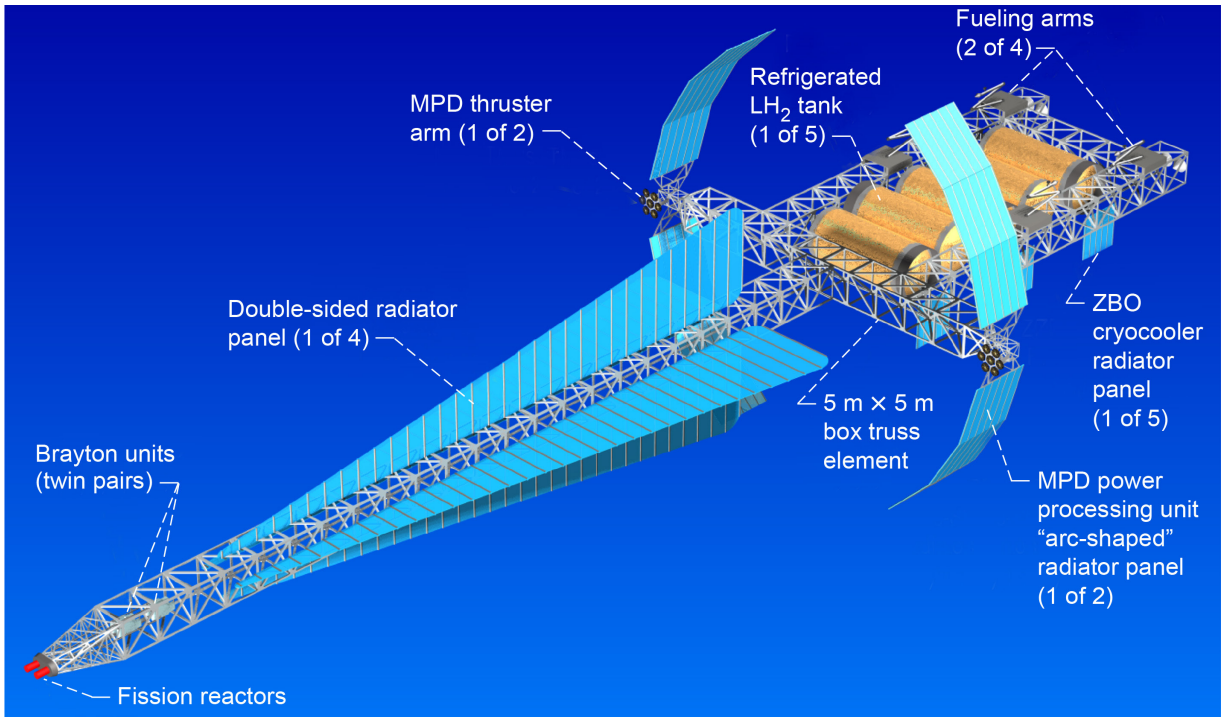

Figure 27.—Key features of conceptual nuclear electric propulsion LH_2 tanker vehicle.

9.1 Comparison of LPI and LUNOX Options

The electrolysis power levels on the LS and at the orbital depot for the missions cited above represent only a portion of what is required. An estimate of the total power demand will need to include mining, transportation of the ice-bearing regolith to the processing plant, water extraction and filtering, storage, and eventual electrolysis. As discussed in Section 2.0, there are still many unknowns and many questions that need to be answered about LPI mining and processing before total system mass and power estimates can be made. For example, what is the water content of the ice-bearing regolith? What kind of mining equipment is needed for its extraction? Can it be operated reliably in the deep, cold, permanently dark polar craters? Does the equipment need to be heated, can the polar regolith be warmed using microwaves or infrared heaters in front of the mining equipment, or will both be required? How much water is lost (escaping as vapor) during the mining process? Is the regolith processed within the crater or outside and by what means? What is the power source—nuclear fission or solar using photovoltaic arrays located around the rims of candidate craters?

By contrast, the viability of producing LUNOX from samples of ilmenite and FeO-rich volcanic glass returned on earlier Apollo missions has been demonstrated experimentally using the hydrogen reduction process (Refs. 21 and 22), and a detailed concept design study of a LUNOX production facility using this process has also been produced (Ref. 31). To illustrate the differences between the LPI and LUNOX options, Tables VIII and IX summarize the refueling requirements for comparable CCT and commuter shuttle missions that use LUNOX only. The CCT mission examined in Table VIII has an IMLEO of ~194.1 t, employs 72-hr transit times, and flies one mission per month to a LLO depot. There it delivers 10 t of cargo (four 2.5 t PL pallets) to two waiting LDAVs for transport to the LS. By operating its LANTR engines O_2 rich (with O/H MR = 5 and I_{sp} ~516 s) out to the Moon and back, the CCT can also function as a tanker, transferring ~9.6 t of ELH_2 from its NTPS to the depot (Ref. 27) for use by the LDAV and tanker LLVs as needed. The total burn time on the LANTR engines for this mission is ~19.1 min. For a 10-hr full-power lifetime on the engine fuel, a *Conestoga*-class CCT can perform just over 30 missions. Assuming a four-ship fleet and monthly trips to the Moon, each CCT would make three flights per year, resulting in a service life of ~10 years.

After unloading its payload, the CCT refuels with ~54 t of LUNOX then returns to LEO. To accommodate a monthly CCT flight rate and the LLV flights supporting it, an annual LUNOX production rate of ~2000 t/yr is required (see Table VIII). Approximately 648 t of LUNOX is used by the LANTR shuttle, ~461 t by the LDAVs transporting cargo from LLO to the LS and ~891 t by three LUNOX tanker LLVs flying nine resupply missions to the LLO depot over the course of a year. With the CCT flights supplying ~115.2 t of ELH_2 to the depot yearly, the remaining net requirement for ~110 t of ELH_2 can be supplied with four NTP tanker flights to the depot each year.

To contrast the differences between Table VII and the LUNOX option, a similar 36-hr LANTR commuter shuttle mission to LLO (Case 1 in Table V) is examined in Table IX. In this case the shuttle refuels with only ~72.8 t of LUNOX since its NTPS utilizes ELH_2 during the round trip to LLO and back. To support weekly commuter flights, annual LUNOX production levels of ~11,643 t/yr are required for the LANTR shuttles and supporting LLV flights. Approximately 3786 t of LUNOX is used by the LANTR shuttles, ~5273 t by three LUNOX tanker LLVs flying one resupply mission to the LLO depot each week over the course of a year (Fig. 28(a)), and ~2584 t is used by the same Sikorsky-style LLVs to transport arriving and departing PTMs to and from the LS (Fig. 28(b)). For these more ambitious LUNOX architectures the increasing amounts of ELH_2 required and methods of delivering it to LLO are concerns. A potential solution to the LH_2 resupply issue is discussed in more detail shortly.

TABLE VIII.—TOTAL LUNOX AND ELH_2 REQUIRED TO SUPPORT MONTHLY CCT FLIGHTS[a]
[72-hr one-way transits, delivering 10 t cargo and 9.6 t ELH_2 to LLO each flight.]

LANTR CCT		
(54 t LUNOX/mission/month) × (12 months/year):		648.0 t LUNOX/yr
	CCT supplied:	(115.2 t ELH_2/yr)
LDAV[b,c]		
(19.2 t LLO_2 and 3.2 t ELH_2/flight) × (2 flights/month) × (12 months/year):		460.8 t LUNOX/yr
		+ 76.8 t ELH_2/yr
LLV[b,d]		
(33.0 t $LUNOX_2$ and 5.5 t LH_2/flight) × (9 flights/LLV/year) × (3 LLVs):		891.0 t LUNOX/yr
		+ 148.5 t ELH_2/yr
	Total LUNOX production:	1999.8 t/yr
	Total ELH_2 required:	110.1 t/yr

[a]Acronyms and symbols are defined within report and in appendix.
[b]O/H MR = 6 and I_{sp} = 450 s. Descent and ascent velocity changes ΔV_{desc} = 2.115 km/s and ΔV_{asc} = 1.985 km/s assumed.
[c]Two crewed LDAVs rendezvous with CCT in LPO; each returns to LS with 5 t of PL.
[d]LLV tanker transports ~25 t of LH_2O to LPO depot; returns to LS with empty 5-t tank.

TABLE IX.—TOTAL LUNOX AND ELH_2 REQUIRED TO SUPPORT WEEKLY LEO-TO-LLO COMMUTER FLIGHTS[a]
[36-hr one-way transits, delivering 15-t, 20-person PTM to LLO each flight.]

LANTR shuttle		
(72.8 t LUNOX/mission/week) × (52 weeks/year)		3786 t LUNOX/yr
LLV[b,c]		
(33.8 t LUNOX and 5.6 t ELH_2/flight) × (1 flight/LLV/week) × (3 LLVs) × (52 weeks/year)		5273 t LUNOX/yr
		+ 874 t ELH_2/yr
LLV[b,d]		
(49.7 t LUNOX and 8.3 t ELH_2/round-trip flight/week) × (52 weeks/year)		2584 t LUNOX/yr
		+ 432 t ELH_2/yr
	Total LUNOX production:	11,643 t/yr
	Total ELH_2 required:	1306 t/yr

[a]Acronyms and symbols are defined within report and in appendix.
[b]O/H MR = 6 and I_{sp} = 450 s. Descent and ascent velocity changes ΔV_{desc} = 2.115 km/s and ΔV_{asc} = 1.985 km/s assumed.
[c]LLV tanker transports ~25 t of LH_2O to LPO depot; returns to LS with empty 5-t tank.
[d]Total for LLV delivery of PTM from LLO to LS plus PTM return from LS to LLO.

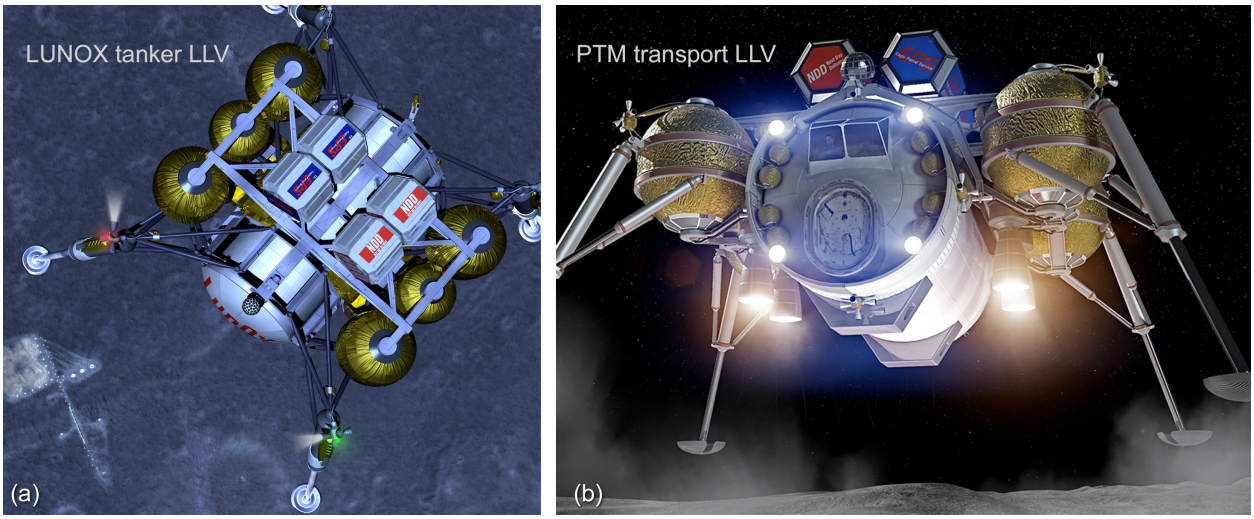

Figure 28.—Tanker and PTM transport LLVs: key elements of LANTR commuter shuttle architecture.

TABLE X.—COMPARISON OF DIFFERENT LUNAR MINING CONCEPTS SHOWING PLANT MASS, REQUIRED OPERATING POWER, AND MINING RATES[a]

Hydrogen reduction of ilmenite (LUNOX production, 1000 t/yr) • Plant mass (mining, beneficiation, processing, and power) ..... 244 t • Power requirements (mining, beneficiation, and processing) ..... 3.0 MW_e • Regolith throughput (assumes soil feedstock at 7.5 wt% ilmenite and mass mining ratio (MMR) of 327 t soil per ton LUNOX) ..... 3.3×10^5 t/yr
Hydrogen reduction of iron-rich volcanic glass (LUNOX production, 1000 t/yr) • Plant mass (mining, processing, and power) ..... 105 t • Power requirements (mining and processing) ..... 1.5 MWe • Regolith throughput (direct feed and processing of "iron-rich" volcanic glass beads, assuming 4% O_2 yield and MMR = 25 to 1) ..... 2.5×10^4 t/yr
Lunar helium-3 extraction (He-3 production, 5 t/yr) • Mobile miners (150 miners required, each weighing 18 t, and each miner producing He-3 at 33 kg/yr) ..... 2700 t • Power requirements (200 kW direct solar power/miner) ..... 30.0 MWe • Regolith throughput (processing and capture of solar-wind-implanted volatiles occurs aboard the miner) ..... 6.0×10^8 t/yr

[a]Acronyms are defined within report and in appendix.

A preliminary assessment of plant mass, power level, feedstock throughput, and required mining area has been made assuming a LUNOX operation employing 12 production plants, each with a capacity of 1000 t/yr. Table X compares the characteristics for two different LUNOX plants: one based on hydrogen reduction of ilmenite (Ref. 31) and the other one "iron rich" volcanic glass (Ref. 27). The advantages of using volcanic glass feedstock are apparent and show mass and power requirements that are 43% and 50%, respectively, lower than that of an ilmenite reduction plant using soil feedstock. Included in the volcanic glass reduction plant mass of ~105.3 t is the mining (~9.6 t) and processing equipment (84.6 t), both of which include a 30% DWC, plus the fission reactor power source (~11.1 t). The plant power requirement of ~1.5 MW_e includes power for the mining and processing equipment and includes a 30% margin. The process power dominates and is a function of the LUNOX production rate and is primarily associated with the electric heaters, electrolysis cell, and oxygen liquefiers.

Using the "low-end" 4% O_2 yield obtained from orange and black volcanic glass beads still translates into more than an order of magnitude reduction in the amount of mined material. The mining equipment used at each 1000-t/yr production plant consists of two front-end loaders and four haulers. To produce

~12,000 t of LUNOX annually will require a glass throughput of ~300,000 t/yr and a soil mining rate at each production plant of ~4 t per hour per loader, assuming the same 35% mining duty cycle used in the ilmenite processing plant results. This duty cycle corresponds to mining operations during ~70% of the available lunar daylight hours (~3067 hours per year).

Although this number is large, it is modest compared to current terrestrial coal and proposed lunar helium-3 (He-3) mining activities. For example, the production rate for coal in the United States in 2017 exceeded 700 million tons, which is understandable when one realizes that a single 1000 MW_e coal-fired power plant consumes about ninety 100-ton train cars of coal per day. In 1986, Wittenberg et al. (Ref. 60) published a paper suggesting that an abundant source of He-3 (estimated at ~1 million metric tons) exists on the Moon implanted in the surface regolith by the solar wind. Since then, an impressive body of scientific and engineering research has been developed (Ref. 61) by the University of Wisconsin's Fusion Technology Institute (FTI) supporting the case for He-3 mining on the Moon (Ref. 62). This lunar resource can play an important role in meeting Earth's future energy demands given the fact that 1 t of He-3 burned with abundant deuterium (D) found in the Earth's oceans can produce ~10 GW_e-yr of electrical energy. Supporting a fusion power economy based on DHe-3 that generates ~250 GWe-yr of electrical energy in the 2035 to 2040 timeframe will require processing ~3 billion tons of regolith to produce the ~25 t of the He-3 needed annually (Ref. 63). The mining requirements for a more modest He-3 production rate of 5 t/yr are shown in Table X.

9.2 Synergy Between Commercial LUNOX Production and a Developing Lunar He-3 Industry

As mentioned above, an estimated million metric tons of solar-wind-implanted (SWI) He-3 is embedded in the near-surface lunar regolith. It is divided roughly equally between the Maria and the Highlands (Ref. 60) although the highest concentrations of He-3 are found in mare regoliths that are rich in titanium-oxide (TiO_2), which is contained in the mineral ilmenite ($FeTiO_3$) (Ref. 64). Approximately 90% of the He-3 is concentrated in small <50-μm-size particles, which constitute ~45% of the lunar regolith. By heating the soil to temperatures of ~700 °C (Ref. 65), ~85% of the He-3 trapped within these fine particles can be extracted via thermal desorption. Cameron (Ref. 66) identified Mare Tranquillitatis and Mare Serenitatis, on the eastern nearside, and Oceanus Procellarum and Mare Imbrium, on the western nearside, as areas rich in titanium and therefore candidate sites for He-3 mining. Hawke et al. (Ref. 23) have pointed out that these regions may be too heterogeneous with sizable impact craters and excavated rock fragments in the upper 2 m of the regolith, making these areas less attractive for mining. As an alternative site, they propose that ilemenite-rich pyroclastic mantling deposits be considered. These deposits are large in their regional extent, tens of meters thick, and numerous on the lunar nearside. The regolith is also uniformly fine grained (~40-μm particles) and relatively rock free making it ideal for lunar mining activities.

The University of Wisconsin's FTI has spent considerable time and effort in designing an automated, multifunction, lunar miner that is self-contained, compact, and lightweight (Refs. 67 and 68). The Mark II lunar miner concept shown in Figure 29 has a mass of 18 t and is capable of producing 33 kg of He-3 per year while operating during the lunar days to take advantage of beamed solar power (~200 kW_e) used for its process energy and operation. Excavation of the regolith is accomplished using a bucket wheel excavator that sweeps out a 120° arc ahead of the miner opening up a trench ~11 m wide and ~3 m deep. A conveyor transports the regolith inside the miner where the larger aggregate material is separated out and regolith beneficiation, down to particles smaller than 50 μm, occurs using a fluidized bed (Ref. 68). These fine-grained particles are then heated to 700 °C to remove the He-3. A recuperator cools the regolith back down to 100 °C, allowing ~85% of the process heat to be recovered. The miner then spreads the cooled regolith back onto the surface filling in the mined area behind it as it moves forward (Fig. 29).

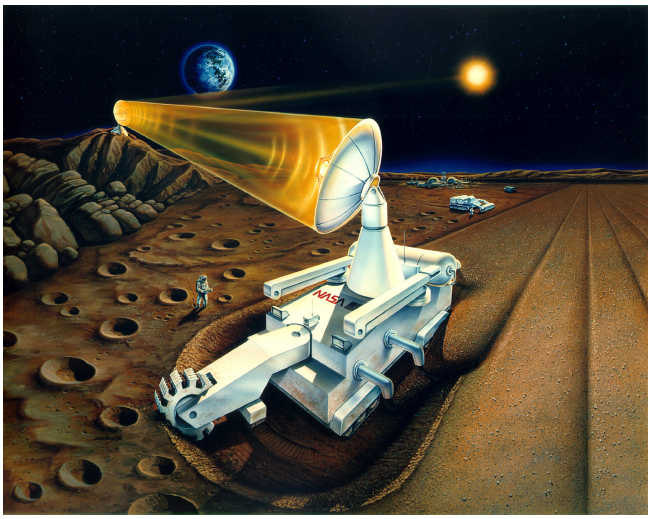

Figure 29.—Automated Mark II lunar miner for extracting He-3 and solar-wind-implanted volatiles from Moon regolith. Courtesy of J. Andrews, Fusion Technology Institute, University of Wisconsin-Madison.

TABLE XI.—VOLATILES RELEASED DURING HEATING LUNAR ILMENITE TO 700 °C
[From Ref. 63.]

Isotope or compound	Amount released per kg He-3, t
H_2	6.1
H_2O	3.3
He-4	3.1
CO	1.9
CO_2	1.7
CH_4	1.6
N_2	0.5
Total volatiles	18.2

During He-3 extraction significant quantities of other volatiles are also produced (see Table XI). Along with the He-3, these volatiles are collected, compressed into cylinders mounted on each of the miners, and later separated out and liquefied at a nearby central processing station. The liquefied He-3 is then shipped back to Earth for use in DHe-3 fusion reactors. A fission power system is used at the lunar processing station, allowing continuous operation. Later, a DHe-3 fusion reactor can be used with deuterium supplied from Earth.

An important fact not to be overlooked is the 6.1 t of LH_2 and 3.3 t of LH_2O produced as "by-products" for each kg of He-3 fuel collected. As the He-3 production rate increases over time, these by-products can eliminate the need for ELH_2 over the full range of LANTR missions discussed above. By electrolyzing the LH_2O, an additional 0.367 t of LH_2 can be produced, providing 6.467 t of LH_2 and 2.933 t of LO_2 for each kilogram of He-3 mined. The 1306 t shortfall in LH_2 shown in Table IX can readily be made up using seven Mark II miners, which produce ~231 kg of He-3 annually.

This production rate is ~22 times lower than the 5 t/yr rate shown in Table X, resulting in a lower mass and power requirement for the miners of ~126 t and ~1.4 MW_e, respectively. The total throughput of regolith is also reduced to ~27.7 million tons with each miner excavating an area of ~1 km^2 each year. For the 5 t/yr example shown in Table X, the excavation area would be ~151.5 km^2.

As mentioned previously, Mare Tranquillitatis is an attractive potential site for He-3 mining. With its titanium-rich regolith and large surface area estimated at ~190,000 km^2, this region could contain ~7100 t of He-3 (Ref. 69). Assuming 50% of this area is minable to a depth of 3 m, and recovery from mining and processing is 60% efficient, ~2130 t of He-3 could be produced from this one area alone. To the northwest is Mare Serenitatis, another potential He-3 mining location and also a candidate site for LUNOX production using iron-rich volcanic glass.

The Taurus-Littrow dark mantle deposit (DMD) (Fig. 30)—located at the southeastern edge of the Mare Serenitatis (~21°N, ~29.5°E), approximately 30 km west of the Apollo 17 landing site—is the author's proposed site for a commercial LUNOX facility. This deposit of largely black crystalline beads covers ~3000 km^2 and is thought to be tens of meters thick. Assuming an area of ~2000 km^2 (equivalent to a square, ~28 miles on each side), a mining depth of ~5 m, a soil density for the volcanic glass of ~1.8 g/cm^3, and a MMR of 25 to 1 (equivalent to a 4% O_2 yield), Figure 31 shows that the Taurus-Littrow DMD could produce ~720 million tons of LUNOX.

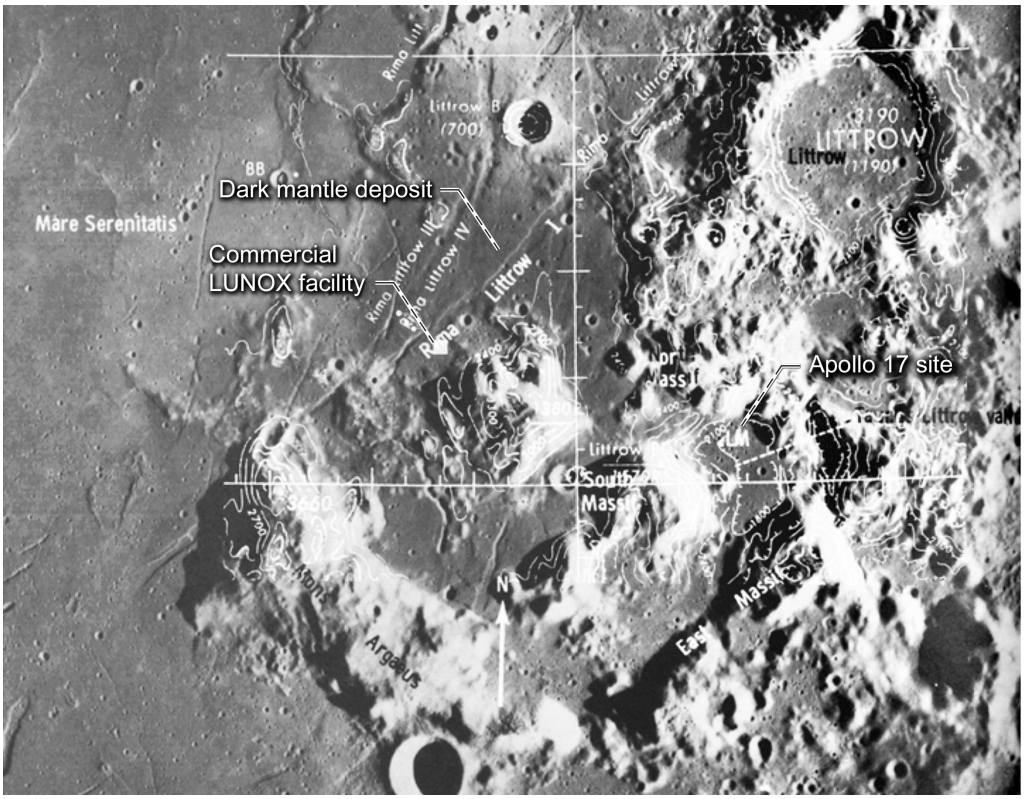

Figure 30.—Apollo 17 landing site and major geographic features of Taurus-Littrow Region.

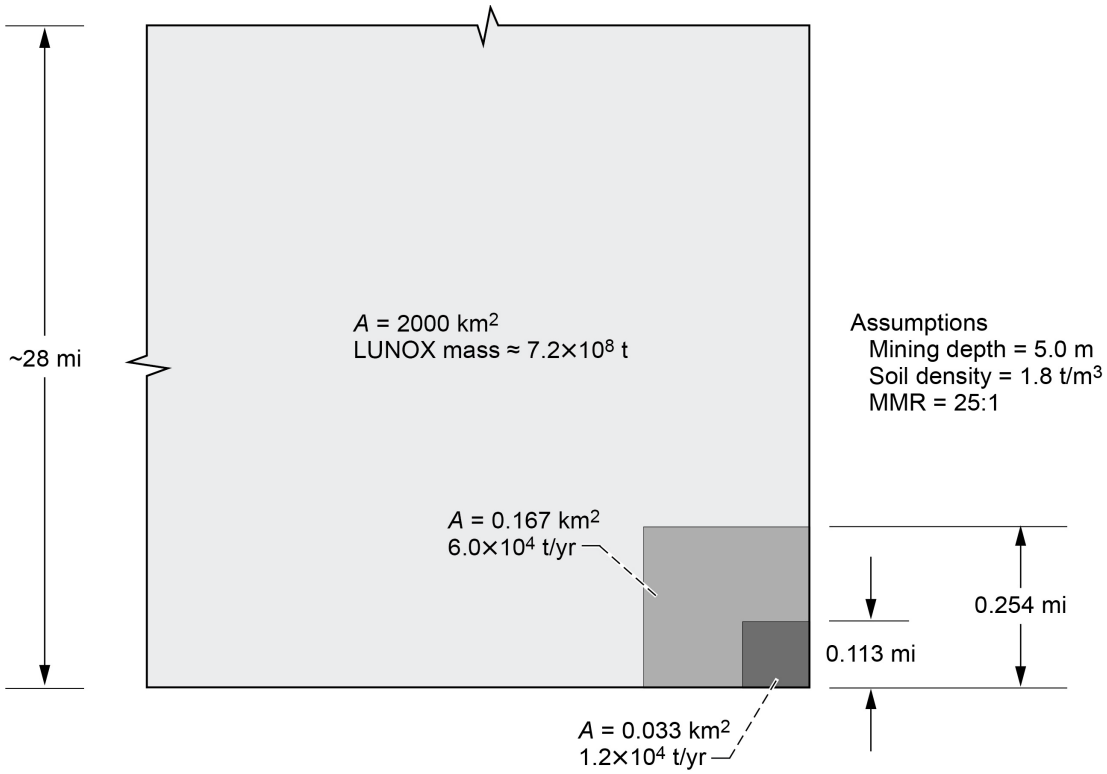

Figure 31.—Required mining areas *A* and LUNOX production rates to support routine commuter flights to Moon.

TABLE XII.—TOTAL LUNOX AND ELH_2 REQUIRED TO SUPPORT CCT He-3 MINER MISSION[a]
[72-hr one-way transits, delivering two 18-t He-3 miners to LLO.]

LANTR CCT	
(52.9 t LUNOX/mission) × (1 mission/year):	52.9 t LUNOX/yr
LLV[b,c]	
(29.9 t LUNOX and 5.0 t ELH_2/flight) × (2 flights/mission) × (1 mission/year):	59.8 t LUNOX/yr
	+ 10.0 t ELH_2/yr
LLV[b,d]	
(33.8 t LUNOX and 5.6 t ELH_2/flight) × (2 flights/mission) × (1 mission/year):	101.4 t LUNOX/yr
	+ 16.8 t ELH_2/yr
Total LUNOX production:	214.1 t/yr
Total ELH_2 required:	26.8 t/yr

[a]Acronyms and symbols are defined within report and in appendix.
[b]O/H MR = 6 and I_{sp} = 450 s. Descent and ascent velocity changes ΔV_{desc} = 2.115 km/s and ΔV_{asc} = 1.985 km/s assumed.
[c]Two LLVs rendezvous with CCT in LLO; each returns to LS with 18-t He-3 miner.
[d]LLV tanker transports ~25 t of LUNOX to LLO; returns to LS with empty 5-t tank.

Figure 31 also shows that the mining areas needed to support commuter flights to the Moon are not unrealistic at ~0.033 km^2 and ~0.167 km^2 for one and five flights/week, respectively. Even at five times the higher rate of ~60,000 t/yr, there are sufficient LUNOX resources at this one site to support ~25 commuter flights carrying 450 passengers each week for the next 2400 years, and more sites containing even larger quantities of iron-rich pyroclastic glass have been identified (Ref. 24). To achieve this high weekly flight rate, ~32,650 t of LLH_2 is needed annually to fuel the supporting LUNOX tanker and PTM transport LLVs. This amount of LLH_2 is consistent with the 5 t/yr He-3 production example in Table X. Although 5 t of He-3 can keep fifty 1000-MW_e DHe-3 fusion power plants operating continuously for a year, this number of plants will not be built and be operational overnight.

In reality, the capabilities of the LANTR LTS and production rates for the commercial LUNOX enterprise and developing He-3 mining industry will evolve over time and in a synergistic manner. As an example, consider the following scenario: A *Conestoga* CCT delivers two 18-t He-3 miners to LLO in 72 hr, then refuels with ~53 t of LUNOX before returning to LEO 3 days later. Two Sikorsky-style LLVs then pick up the miners in LLO and deliver them to a newly built central processing facility used to separate the He-3 from the other lunar volatiles. Here the automated miners are checked out before being deployed to their selected mining site. Three tanker LLVs operating from an established LUNOX facility would deliver 75 t of LUNOX to the depot where it is used to refuel the CCT. The LUNOX and ELH_2 required for this mission scenario is shown in Table XII. The LUNOX requirements for this mission are modest at ~214 t, and the ~27 t of ELH_2 can be supplied by a single NTR tanker. After a year of operation, the miners supply the volatiles to produce 66 kg of He-3 and then after electrolyzing the ~218 t of LH_2O into its constituent elements, ~427 t of LLH_2 and ~194 t of LLO_2. With this amount of LLH_2 now available, and the production rate of LUNOX increasing annually, the CCT flight rate can also be increased in the second year, allowing additional miners and cargo to be delivered to the Moon to support the continued growth of lunar settlements, LUNOX production facilities, and the developing He-3 mining industry.

10.0 A Look Ahead

Whereas others have discussed more conventional space transportation systems supported by strategically located propellant depots (Ref. 70), the performance capability resulting from combining the two "high leverage" technologies, LANTR and LDPs, is quite extraordinary. To illustrate this fact, in order to perform the same 36-hr commuter shuttle mission with the same propellant tanks used in Case 1 of Table V, an all-LH_2 NTP system would require an effective I_{sp} of ~1575 s, which is equivalent to that postulated for an advanced gaseous-fuel-core NTR system.

Besides enabling a robust and versatile LTS, the LANTR concept is expected to dramatically improve space transportation performance wherever extraterrestrial sources of LO_2 and LH_2 can be acquired (Fig. 32) such as the Mars system, main-belt asteroids, and the Jovian satellites Europa, Ganymede, and Callisto. In the future, reusable biconic-shaped LANTR-powered Mars landing vehicles (MLVs), operating from specially prepared landing sites, could be used to transport modular payload elements to the surface and resupply interplanetary transfer vehicles (ITVs) with the propellants (Fig. 33) needed to reach refueling depots in the asteroid belt. From there, LANTR-powered ITVs, carrying cargo and passengers, could continue on to the "water-rich" moons of the Jovian system, providing a reliable foundation for the development and eventual human settlement of the solar system.

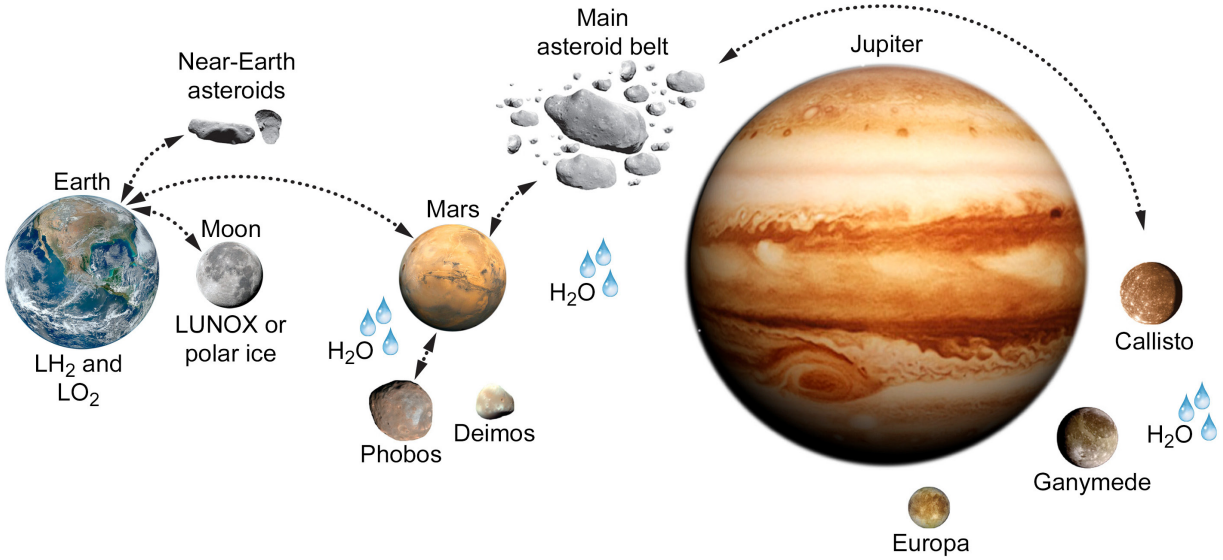

Figure 32.—Human expansion possibilities using LANTR propulsion and extraterrestrial propellant resources.

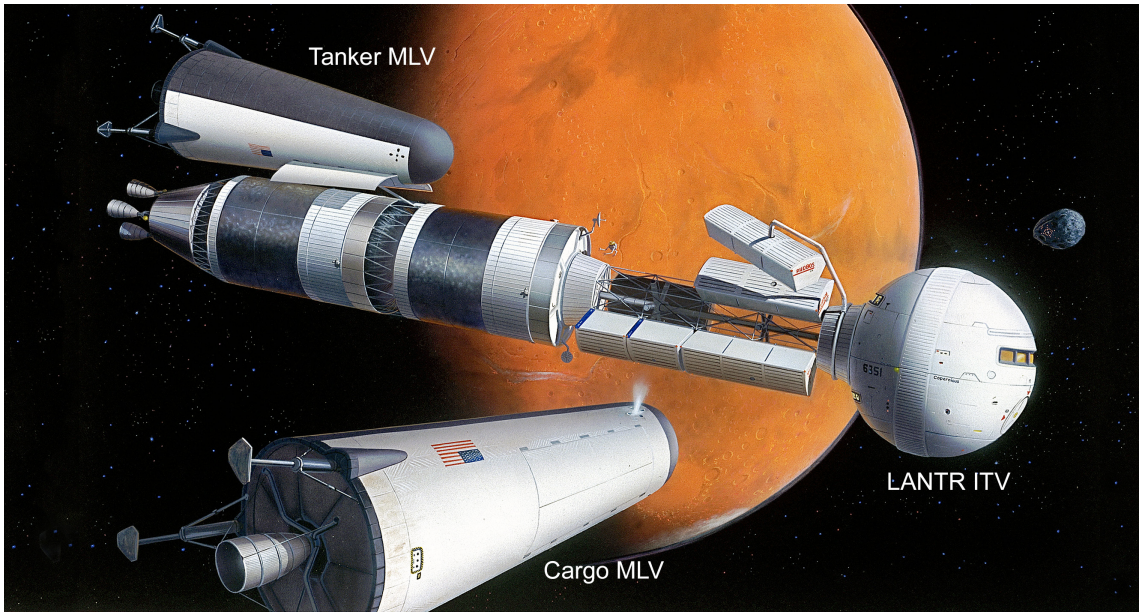

Figure 33.—Conceptual LANTR interplanetary transfer vehicle (ITV) unloading cargo and loading propellant before departing Mars for asteroid belt.

11.0 Concluding Remarks

This report has examined the potential for robust exploration and commercial missions to the Moon brought about by using advanced propulsion and in situ lunar resources. On the propulsion side, the nuclear thermal rocket (NTR) offers significant benefits for lunar missions and can take advantage of the mission leverage provided from using lunar-derived propellants (LDPs) by including liquid oxygen (LO_2) and transitioning to LO_2-augmented NTR (LANTR) propulsion. Using this enhanced version of nuclear thermal propulsion (NTP) has many advantages. It provides a variable thrust and I_{sp} capability, shortens engine burn times, extends engine life and allows bipropellant operation. Its use together with adequate supplies of LDPs extracted from abundant reserves of lunar polar ice (LPI), volcanic glass, and the volatile byproducts from He-3 mining can lead to a robust nuclear lunar transportation system (LTS) that evolves over time and has unique mission capabilities. The examples discussed here include short transit time crewed cargo transports and commuter shuttles operating between transportation nodes and/or propellant depots located in low Earth, low lunar, and lunar polar orbits (LEO, LLO, and LPO, respectively).

The use of LDPs—specifically, lunar liquid oxygen and hydrogen (LLO_2 and LLH_2) from LPI or lunar-derived liquid oxygen (LUNOX) from volcanic glass—offers substantial mission leverage when used with a compatible propulsion system. Although LUNOX is a much more established option, the use of LPI-derived propellant has received considerable attention. In this report, some of the issues that will need to be considered in the mining and processing of LPI for water have been addressed, as well as its subsequent conversion to LO_2 and LH_2 propellant.

For one, the analysis by Spudis and Lavoie had assumed a 10 wt% water concentration in the polar regolith and relatively lightweight mining and processing equipment. However, the extreme environment in which the LPI exists is expected to pose significant engineering challenges to equipment operation. As pointed out by Gertsch et al., at ~10 wt% water ice content ice-cemented regolith could behave like high-strength concrete and require much heavier equipment for its excavation.

Similarly, the design and engineering of systems for mining and processing volcanic glass is expected to be challenging. Since a lunar day is ~29.53 Earth days long, daytime on the Moon lasts ~14.76 days followed by ~14.76 days of lunar darkness. On the lunar nearside near the equator, where the vast deposits of volcanic glass are located, the temperature can vary from a low of ~95 K (~ –178 °C) just before lunar sunrise to a high of ~392 K (~119 °C) at lunar noon. By contrast, in the depths of the permanently dark polar craters where the water ice is located, the temperature is ~2 to 3 times colder than the coldest temperature on the lunar nearside and is unrelenting.

The main problems with mining either volcanic glass or solar-wind-implanted volatiles will be equipment cooling during the lunar day and heating during the lunar night. Illuminating the mine site during the lunar night can also require a large amount of power. In the study by Christiansen et al., ilmenite mining was limited to the lunar daytime and a 35-percent duty cycle was assumed, corresponding to mining operations during ~70% of the available lunar daylight hours (~3067 hours per year). A nuclear fission power source allowed the processing plant to operate both day and night with a 90% duty cycle. The FTI's He-3 miner concept also assumed operation only during the lunar days. A similar detailed study on the mining and processing of LPI will be required to help better define the most viable concepts and systems and to quantify the associated mass and power levels that will be needed for a LPI mining operation.

December 2017 marked the 45th anniversary of the Apollo 17 mission to Taurus-Littrow and unfortunately, the termination of both the Apollo and the Rover/NERVA nuclear rocket programs. In the not-so-distant future, the technological progeny from these two historic programs—LANTR and LDP—could allow the development of a robust, reusable space transportation system that can be adapted to a wide variety of potential lunar missions, using the basic vehicle building blocks discussed in this report.

After developing NTP and the oxygen afterburner nozzle for LANTR, the next biggest challenge to making this vision of a robust LTS a reality will be the production of increasing amounts of LDP and the development of propellant depots for vehicle refueling in LEO, LLO, and/or LPO. An industry-operated, privately financed venture, with NASA as its initial customer, has frequently been mentioned as a possible blueprint for how a commercial lunar propellant production facility and orbital depot might develop. With industry interested in developing cislunar space and commerce, and competitive forces at work, the timeline for developing this capability could well be accelerated beyond anything currently being envisioned. Only time will tell, and it may be quicker than any of us can imagine.

Appendix—Nomenclature

AGS	artificial gravity station
AMBR	Advanced Material Bipropellant Rocket
BA	Bigelow Aerospace
CCT	crewed cargo transport
CPR	circular polarization ratio
DMD	dark mantle deposit
DWC	dry weight contingency
EEO	elliptical Earth orbit
ELH_2	Earth-supplied LH_2
EOC	Earth orbit capture
EVA	extravehicular activity
FE	fuel element
FTI	University of Wisconsin Fusion Technology Institute
GC	graphite composite
HV	hauler vehicle
IMLEO	initial mass in low Earth orbit
ITV	interplanetary transfer vehicle
I_{sp}	specific impulse
L	length
LANTR	LO_2-augmented NTR
LCROSS	Lunar CRater Observation and Sensing Satellite
LDAV	lunar descent and ascent vehicle
LDP	lunar-derived propellant
LEO	low Earth orbit
LH_2	liquid hydrogen
LH_2O	lunar water
LLH_2	lunar liquid hydrogen
LLO	low lunar orbit
LLO_2	lunar liquid oxygen
LLV	lunar landing vehicle
LN_2	liquid nitrogen
LO_2	liquid oxygen
LOC	lunar orbit capture
LPI	lunar polar ice
LPO	lunar polar orbit
LRO	Lunar Reconnaissance Orbiter
LS	lunar surface
LTS	lunar transportation system
LTV	lunar transfer vehicle
LUNOX	lunar-derived liquid oxygen
MAMA	multidisciplinary analysis and mission assessment code
Mini-RF	Miniature Radio Frequency instrument
MLI	multilayer insulation
MLV	Mars landing vehicle
MMR	mass mining ratio
MPCV	multipurpose crew vehicle
MPD	magnetoplasmadynamic
NERVA	Nuclear Engine for Rocket Vehicle Applications
NF–1	Nuclear Furnace 1

NLTV	nuclear-powered LTV
NTP	nuclear thermal propulsion
NTPS	NTP stage
NTR	nuclear thermal rocket
OD	outer diameter
O/H MR	oxygen-to-hydrogen mixture ratio
PL	payload
PPU	power processing unit
PSC	permanently shadowed crater
PTM	passenger transport module
PVA	photovoltaic array
R&D	rendezvous and docking
RCS	reaction control system
REL	ripper-excavator-loader
RMS	remote manipulator system
RP	Resource Prospector (mission)
SAR	synthetic aperture radar
SEC	Shackleton Energy Company
SLS	Space Launch System
SNRE	small nuclear rocket engine
SOFI	spray-on foam insulation
STA	saddle truss assembly
TEI	trans-Earth injection
TLI	translunar injection
TPA	turbopump assembly
TT	tie tube
ULA	United Launch Alliance
ΔV	velocity change
ZBO	zero boil-off

References

1. NASA's Journey to Mars—Pioneering Next Steps in Space Exploration. NASA NP–2015–08–2018–HQ, 2015.
2. Achenbach, Joel: Trump, With NASA, Has a New Rocket and Spaceship. Where's He Going To Go? The Washington Post, Health & Science, 2017. https://www.washingtonpost.com/national/health-science/trump-with-nasa-has-a-new-rocket-and-spaceship-wheres-he-going-to-go/2017/03/11/4193f1be-002d-11e7-8f41-ea6ed597e4ca_story.html?noredirect=on&utm_term=.907de99bcba9 Accessed Aug. 24, 2018.
3. David, Leonard: Lunar Leap: Europe is Reaching for a Moon Base by the 2030s. Space.com, 2015. www.space.com/31488-european-moon-base-2030s.html Accessed Aug. 24, 2018.
4. Aliberti, Marco: When China Goes to the Moon. Springer International Publishing, Switzerland, 2015.
5. Zolfagharifard, Ellie; and Gray, Richard: Russia to Conquer the Moon in 2030: Country Says It's Planning a Permanent Manned Base on the Lunar Surface. Daily Mail, Dec. 3, 2015. www.dailymail.co.uk/sciencetech/article-3344818/Russia Accessed Aug. 24, 2018.
6. Chang, Kenneth: SpaceX Plans to Send 2 Tourists Around the Moon in 2018. The New York Times, Science, 2017. www.nytimes.com/2017/02/27/science/spacex-moon-tourists.html Accessed Aug. 29, 2018.
7. Malik, Tariq: Private Space Stations Could Orbit the Moon by 2020, Robert Bigelow Says. Space.com, 2017. www.space.com/35978-private-moon-refueling-station-by-2020.html Accessed Aug. 29, 2018.
8. Wall, Mike: Mining the Moon's Water: Q&A With Shackleton Energy's Bill Stone. Space.com, 2011. https://www.space.com/10619-mining-moon-water-bill-stone-110114.html Accessed Aug. 29, 2018.
9. David, Leonard: Inside ULA's Plan to Have 1,000 People Working in Space by 2045. Space.com, June 29, 2016. www.space.com/33297-satellite-refueling-business-proposal-ula.html Accessed Aug. 29, 2018.
10. Davenport, Christian: An Exclusive Look at Jeff Bezos's Plan to Set Up Amazon-Like Delivery for 'Future Human Settlement' of the Moon. The Washington Post, The Switch, 2017. www.washingtonpost.com/news/the-switch//wp/2017/03/02/an-exclusive Accessed Aug. 30, 2018.
11. Sullivan, Thomas S.; and McKay, David S.: Using Space Resources. NASA TM–107966, 1991. http://ntrs.nasa.gov
12. Allen, Carlton C.; Morris, Richard V.; and McKay, David S.: Experimental Reduction of Lunar Mare Soil and Volcanic Glass. J. Geophys. Res., vol. 99, no. E11, 1994, pp. 23, 173–23,185.
13. National Aeronautics and Space Administration: Ice on the Moon: A Summary of Clementine and Lunar Prospector Results. 2012. http://nssdc.gsfc.nasa.gov/planetary/ice/ice_moon.html Accessed Sept. 5, 2018.
14. Borowski, Stanley K.: The Rationale/Benefits of Nuclear Thermal Rocket Propulsion for NASA's Lunar Space Transportation System. AIAA 91–2052 (NASA TM–106730), 1991. http://ntrs.nasa.gov
15. Borowski, Stanley K.; and Alexander, Stephen W.: "Fast Track" NTR Systems Assessment for NASA's First Lunar Outpost Scenario. AIAA 92–3812 (NASA TM–106748), 1992. http://ntrs.nasa.gov
16. Borowski, Stanley K.; McCurdy, David R.; and Burke. Laura M.: The Nuclear Thermal Propulsion Stage (NTPS): A Key Space Asset for Human Exploration and Commercial Missions to the Moon. AIAA 2013–5465 (NASA/TM—2014-218105), 2013. http://ntrs.nasa.gov
17. Borowski, Stanley K., et al.: Affordable Development and Demonstration of a Small Nuclear Thermal Rocket (NTR) Engine and Stage: How Small is Big Enough? AIAA 2015–4524 (NASA/TM—2016-219402), 2015. http://ntrs.nasa.gov

18. Borowski, Stanley K.; and Dudzinski. Leonard A.: “2001: A Space Odyssey” Revisited—The Feasibility of 24 Hour Commuter Flights to the Moon Using NTR Propulsion With LUNOX Afterburners. AIAA 97–2956 (NASA/TM—1998-208830/REV2), 1997. http://ntrs.nasa.gov
19. Joyner, C. Russell, et al.: TRITON: A *TRI*modal Capable, Thrust Optimized Nuclear Propulsion and Power System for Advanced Space Missions. AIAA 2004–3863, 2004.
20. Bulman, M.J.; Neill, T.M.; and Borowski, S.K.: LANTR Engine System Integration. AIAA 2004–3864, 2004.
21. Allen, Carlton C.; and McKay, David S.: Lunar Oxygen Production—Ground Truth and Remote Sensing. AIAA 95–2792, 1995.
22. Allen, Carlton C.; Morris, Richard V.; and McKay, David S.: Oxygen Extraction From Lunar Soils and Pyroclastic Glass. J. Geophys. Res., vol. 101, no. E11, 1996, pp. 26085–26095.
23. Hawke, B.R.; Coombs, C.R.; and Clark, B.: Ilmenite-Rich Pyroclastic Deposits: An Ideal Lunar Resource. Proceedings of 20th Lunar and Planetary Science Conference, Houston, TX, 1990, pp. 249–258.
24. Gaddis, Lisa R., et al.: Compositional Analyses of Lunar Pyroclastic Deposits. Icarus, vol. 161, 2003, pp. 262–280.
25. Spudis, Paul D.; and Lavoie, Anthony R.: Using the Resources of the Moon To Create a Permanent, Cislunar Space Faring System. AIAA 2011–7185, 2011.
26. Haruyama, Junichi, et al.: Lack of Exposed Ice Inside Lunar South Pole Shackleton Crater. Science, vol. 322, no. 5903, 2008, pp. 938–939.
27. Borowski, Stanley K., et al.: Robust Exploration and Commercial Missions to the Moon Using Nuclear Thermal Rocket Propulsion and Lunar Liquid Oxygen Derived From FeO-Rich Pyroclastic Deposits. AIAA 2017–4938 (NASA/TM—2018-219725), 2017. http://ntrs.nasa.gov
28. Davis, H.P.: Lunar Oxygen Impact Upon STS Effectiveness. Eagle Engineering Report No. 8363, Eagle Engineering, Inc., Houston, TX, 1983.
29. Frisbee, R.H.; and Jones, R.M.: An Analysis of Propulsion Options for Transport of Lunar Materials to Earth Orbit. AIAA 83–1344, 1983.
30. Taylor, L.A.; and Carrier III, W.D.: Oxygen Production on the Moon: An Overview and Evaluation. Resources of Near Earth Space, J. Lewis, M.S. Matthews, and M.L. Guerrieri, eds., University of Arizona Press, Tuscon, AZ, 1993, pp. 69–108.
31. Christiansen, E.L., et al.: Conceptual Design of a Lunar Oxygen Pilot Plant. EEI Report No. 88–182 (NASA CR–172082), 1988. http://ntrs.nasa.gov
32. Allen, C.C.; Weitz, C.M.; and McKay, D.S.: Prospecting for Lunar Oxygen With Gamma-Ray Spectrometry and Multispectral Imaging. Workshop on New Views of the Moon: Integrated Remotely Sensed, Geophysical, and Sample Datasets, B.L. Jolliff and G. Ryder, eds., LPI Contribution No. 958, 1998, pp. 19–20.
33. Watson, Kenneth; Murray, Bruce C.; and Brown, Harrison: The Behavior of Volatiles on the Lunar Surface. J. Geophys. Res., vol. 66, no. 9, 1961, pp. 3033–3045.
34. Arnold, J.R.: Ice in the Lunar Polar Regions. J. Geophys. Res., vol. 84, 1979, pp. 5659–5668.
35. Nozette, S., et al.: The Clementine Bistatic Radar Experiment. Science, vol. 274, no. 5292, 1996, pp. 1495–1498.
36. Feldman, W.C., et al.: Polar Hydrogen Deposits on the Moon. J. Geophys. Res., vol. 105, no. E2, 2000, pp. 4175–4195.
37. Trinadad, Katherine: NASA Radar Finds Ice Deposits at Moon's North Pole: Additional Evidence of Water Activity on Moon. NASA Press Release 10–055, 2010. https://www.nasa.gov/home/hqnews/2010/mar/HQ_10-055_moon_ice.html Accessed Sept. 10, 2018.
38. Spudis, P.D., et al.: Evidence for Water Ice on the Moon: Results for Anomalous Polar Craters From the LRO Mini-RF Imaging Radar. JGR Planets, vol. 118, 2013, pp. 2016– 2029.
39. Colaprete, Anthony, et al.: Detection of Water in the LCROSS Ejecta Plume. Science, vol. 330, 2010, pp. 463–468.

40. Spudis, P.D., et al.: Initial Results for the North Pole of the Moon From Mini-SAR, Chandrayaan-1 Mission. Geophys. Res. Lett., vol. 37, no. L06204, 2010.
41. The world's 10 coldest mines. Mining Intelligence, 2016. http://www.mining.com/the-worlds-10-coldest-mines/ Accessed Sept. 10, 2018.
42. Amos, Jonathan: 'Coldest Place' Found on the Moon. BBC, 2009. http://news.bbc.co.uk/1/hi/sci/tech/8416749.stm Accessed Sept. 10, 2018.
43. Mining the Lunar Surface. http://www.permanent.com/mining-the-moon-for-lunar-resources.html Accessed Sept. 10, 2018.
44. Gertsch, Leslie Sour; and Gertsch, Richard E.: Surface Mine Design and Planning for Lunar Regolith Production. AIP Conference Proceedings, vol. 654, no. 1, 2003, pp. 1108–1115.
45. Podnieks, Egons R.; and Siekmeier, John A.: Lunar Surface Mining Equipment Study. Proceedings of the 3rd International Conference on Engineering, Construction, and Operations in Space III, Denver, CO, 1992, pp. 1104–1115.
46. Podnieks, E.R.; and Siekmeier, J.A.: Terrestrial Mining Technology Applied to Lunar Mining. Proceedings of the 11th SSI-Princeton Conference, Princeton, NJ, 1993, pp. 301–308. Available from the NASA STI Program.
47. Gustafson, Robert J.; and Rice, Eric E.: Lunar Polar Ice: Methods for Mining the New Resource for Exploration. AIAA 99–0850, 1999.
48. Ethridge, Edwin; and Kaukler, William: Microwave Extraction of Water From Lunar Regolith Simulant. AIP Conference Proceedings, vol. 880, no. 1, 2007, pp. 830–837.
49. Colaprete, A., et al.: Resource Prospector: Evaluating the ISRU Potential of the Lunar Poles. Presented at the Lunar Exploration Analysis Group (LEAG) Annual Meeting, Columbia, MD, 2016.
50. Gertsch, Leslie; Gustafson, Robert; and Gertsch. Richard: Effect of Water Ice Content on Excavatability of Lunar Regolith. AIP Conference Proceedings, vol. 813, no. 1, 2006, pp. 1093–1100.
51. Gertsch, Leslie; Rostami, Jamal; and Gustafson, Robert: Review of Lunar Regolith Properties for Design of Low Power Lunar Excavators. Presented at the 6th International Conference on Case Histories in Geotechnical Engineering, Paper No. 10.02, Arlington, VA, 2008.
52. Koeing, Daniel R.: Experience Gained From the Space Nuclear Rocket Programs (Rover). Los Alamos National Laboratory Report LA–10062–H, 1986.
53. Bulman, M.J.; and Neill, T.M.: Simulated LOX-Augmented Nuclear Thermal Rocket (LANTR) Testing. AIAA 2000–3897, 2000.
54. RL10. Wikipedia: The Free Encyclopedia. Wikimedia Foundation, Inc., 2018. https://en.wikipedia.org/wiki/RL10 Accessed Sept. 10, 2018.
55. Hodge, J., et al.: Space Transfer Vehicle—Lunar Transportation Ground Based LEO Rendezvous & Docking Study. NAS8–37856, Martin Marietta, 1991.
56. Ryan, Stephen W.; and Borowski, Stanley K.: Integrated System Modeling for Nuclear Thermal Propulsion. AIAA 2014–3624, 2014.
57. Conestoga Wagon. A&E Televisions Networks, LLC, 2012. http://www.history.com/topics/conestoga-wagon Accessed Sept. 11, 2018.
58. Kubrick, S.; and Clarke, A.C.: 2001: A Space Odyssey. Metro-Goldwyn-Mayer (MGM), 1968.
59. Clarke, A.C.: 2001: A Space Odyssey. Based on a screenplay by S. Kubrick an A.C. Clarke, SignetBook, The New American Library, Inc., New York, NY, 1968, p. 61.
60. Wittenberg, L.J.; Santarius, J.F.; and Kulcinski, G.L.: Lunar Source of ^{3}He for Commercial Fusion Power. Fusion Technol., vol. 10, no. 2, 1986, pp. 167–178.
61. Lunar Mining of Helium-3. Board of Regents of the University of Wisconsin System, 2014. http://fti.neep.wisc.edu/research/he3 Accessed Sept. 10, 2018.
62. Sviatoslavsky, I.N.: Processes and Energy Costs for Mining Lunar Helium-3. NASA CP–10018, 1988, pp. 129–146. http://ntrs.nasa.gov
63. Kulcinski, G.L.; Sviatoslavsky, I.N.; and Wittenberg, L.J.: Impact of Lunar Volatiles Produced During He-3 Mining Activities. AIAA 96–0490, 1996.

64. Cameron, E.N.: Titanium in Lunar Regolith and Its Use in Mining Site Selection. WCSAR–TR–AR3–8708, 1987.
65. Pepin, R.O., et al.: Rare Gases in Apollo 11 Lunar Material. Proceedings of the Apollo 11 Lunar Science Conference, vol. 2, 1970, pp. 1435–1454.
66. Cameron, Eugene N.: Helium Mining on the Moon: Site Selection and Evaluation. NASA CP–3166, Vol. 1, 1992, pp. 189–197.
67. Sviatoslavsky, I.N.; and Jacobs, M.: Mobile Helium-3 Mining System and Its Benefits Toward Lunar Base Self-Sufficiency. Presented at Space 88 Conference on Engineering, Construction, and Operations in Space, Albuquerque, NM, 1988, pp. 310–321.
68. Sviatoslavsky, Igor N.: Lunar He-3 Mining: Improvements on the Design of the UW Mark II Lunar Miner. Proceedings of the 3rd International Conference on Engineering, Construction, and Operations in Space, vol. I, 1992, pp. 1080–1091.
69. Wittenberg, L.J., et al.: A Review of ^{3}He Resources and Acquisition for Use as Fusion Fuel. Fusion Technol., vol. 21, no. 4, 1992, pp. 2230–2253.
70. Smitherman, David; and Woodcock, Gordon: Space Transportation Infrastructure Supported by Propellant Depots. AIAA 2011–7160, 2011.